

PhD
1939
W

BOSTON UNIVERSITY

GRADUATE SCHOOL

Dissertation

AN INVESTIGATION OF THE SEPARATIONS OF THE COMPONENTS
OF THE H-ALPHA COMPLEX OF HYDROGEN

by

Thomas Homkowycz Wallace

(B.S., Boston University, 1933; A.M., Harvard University, 1936)

submitted in partial fulfilment of the

requirements for the degree of

Doctor of Philosophy

1939

THE UNIVERSITY OF CHICAGO
LIBRARY
1215 EAST 58TH STREET
CHICAGO, ILL. 60637
TEL. 733-4331
FAX 733-4929
WWW.CHICAGO.EDU

1939
w
copy 1

TOPICAL OUTLINE

Page No

APPROVED

by

First Reader.....

PROFESSOR OF PHYSICS

Second Reader.....

ASSISTANT PROFESSOR OF PHYSICS

APPROVED

BY

.....
FIRST READER.....
PROFESSOR OF PHYSICS

.....
SECOND READER.....
ASSISTANT PROFESSOR OF PHYSICS

TOPICAL OUTLINE

Page No.

A- Introduction with historical survey of the work of other investigators.....	1
B- Object of the research.....	7
C- Fine structure of H-alpha.....	10
(a) Development of theory.....	11
(b) Term values and energy states.....	20
(c) Theoretical components.....	24
D- Theory of Lummer plates.....	25
(a) Separation between orders.....	26
(b) Dispersion.....	27
(c) Resolving powers.....	28
(d) Two Lummer plates in tandem.....	31
E- Description of apparatus.....	36
(a) Changes in apparatus.....	37
(b) Radiation source.....	37
(c) Optical system.....	39
(d) Temperature and Vibration effects.....	41
(e) Position of Lummer plates.....	42
(f) Constants of Lummer plates.....	44
F- Experimental procedure.....	49
(a) Optical adjustments.....	50
(b) Discharge conditions.....	51
(c) Photographic procedure.....	52

TOPIGAC CHAPTER

Page No.

A- Introduction with historical survey of the work of	1
other investigators.....	7
B- Object of the research.....	10
C- Fine structure of H-striae.....	11
(a) Development of H-striae.....	12
(b) Form, values and energy states.....	13
(c) Theoretical components.....	14
D- Theory of human distal.....	15
(a) Correlation between orders.....	16
(b) Displacement.....	17
(c) Perceptive powers.....	18
(d) Two lower plates in human.....	19
E- Description of apparatus.....	20
(a) Changes in apparatus.....	21
(b) Radiation source.....	22
(c) Optical system.....	23
(d) Temperature and vibration of set.....	24
(e) Position of human plates.....	25
(f) Constants of human plates.....	26
F- Experimental procedure.....	27
(a) Optical adjustments.....	28
(b) Distance conditions.....	29
(c) Photographic procedure.....	30

	Page No.
G- Spectrograms and data.....	54
(a) List of photographs and data.....	55
(b) Discussions of single plate spectrograms....	61
(c) Discussions of double plate spectrograms....	62
H- Results.....	65
(a) Theoretical calculations of the structure of plate M S-3.....	66
(b) Comparison of calculated and theoretical values.....	73
(c) Microphotometer tracing.....	76
(d) Discussion of results.....	77
I- Conclusions.....	80
J- Bibliography.....	86
K- Autobiography.....	88

LIST OF ILLUSTRATIONS AND TABLES

A- Energy levels.....	19
B- Table I Calculated frequencies in cm^{-1}	23
C- Fig.2 Theoretical fine structure of H-alpha.....	24
D- Fig.3 Formation of fringes.....	26
E- Table II Resolving powers of the Lummer plates.....	30
F- Fig.4 Ray of light through first Lummer plate.....	31
G- Fig.5 Ray of light through second Lummer plate.....	33
H- Fig.6 Position of fringes.....	35
I- Fig.7 Vacuum Tube.....	38
J- Fig.8 Optical system.....	40

Page No.

54	3- Spectrogram and data.....
55	(a) List of photographs and data.....
61	(b) Measurements of single plate spectrograms.....
62	(c) Disposition of double plate spectrograms.....
65	4- Results.....
66	(a) Theoretical calculations of the structure of plate M-8-3.....
73	(b) Comparison of calculated and theoretical values.....
75	(c) Microphotometer tracing.....
77	(d) Discussion of results.....
80	5- Conclusions.....
82	6- Bibliography.....
85	7- Appendix.....

LIST OF ILLUSTRATIONS AND TABLES

12	A- Energy levels.....
23	B- Table I Calculated frequencies in cm ⁻¹
24	C- Fig. 1 Theoretical five structure of H-alpha.....
26	D- Fig. 2 Formation of fringes.....
30	E- Table II Resolving power of the burner plates.....
31	F- Fig. 3 Ray of light through first burner plate.....
32	G- Fig. 4 Ray of light through second burner plate.....
33	H- Fig. 5 Position of fringes.....
35	I- Fig. 6 Vacuum tube.....
40	J- Fig. 7 Optical system.....

	Page No.
K- Optical system within housing.....	43
L- Fig.9 Position of plates and collimator.....	44
M- Table III Variation of index of refraction with wavelengths.....	44
N- Fig.10 Optical arrangement for measuring the angles of Lummer plate prism.....	47
O- Table IV Constants of Lummer plates.....	48
P- Table V Tabulation of plates.....	55
Q- Photographic enlargements.....	56-60
R- Fig.11 Position of Lummer plates for MS-3.....	60
S- Table VI Constants of medium and smallest Lummer plates.....	69
T- Table VII Calculations of ψ_1'	70
U- Table VIII Calculations of ψ_3'	71
V- Table IX Comparison of calculated, and experimental re- sults.....	73
W- Graph 1 Comparison of calculated and experimental po- sitions of lines and group maxima.....	74
X- Graph 2 Variation of intensity with position of com- ponent lines.....	75
Y- Microphotometer tracing.....	76

Page No.

43	Optical system within housing.....
44	Fig. 2 Position of plates and collimator.....
44	Table III Variation of index of refraction with wavelength.....
47	Fig. 10 Optical arrangement for measuring the angles of linear plate gratings.....
48	Table IV Constants of linear gratings.....
50	Table V Relation of angles.....
52-53	Photographic elements.....
53	Fig. 11 Position of linear plates for 10-5.....
53	Table VI Constants of medium and small gratings.....
53	Figures.....
53	Table VII Calculations of λ
51	Table VIII Calculations of λ
51	Table IX Comparison of calculated and experimental results.....
52	Table I Comparison of calculated and experimental positions of lines and group maxima.....
52	Table II Variation of intensity with position of constant lines.....
52	Microphotometer tracing.....

INTRODUCTION WITH HISTORICAL SURVEY OF THE WORK OF OTHER INVESTIGATORS

There are two hydrogen spectra — the molecular and atomic. The latter consists of a number of lines that fall into separate series. These known are the Lyman, Balmer, Paschen, Brackett and Pfund series ranging from the ultra violet to the infra red respectively.

The first four lines of the Balmer series H_α , H_β , H_γ , and H_δ have been investigated the most since they lie in the region of the visible spectrum. Line H_α lies in the red, H_β in the blue-green and H_γ and H_δ in the violet. The wavelengths of the individual lines of the series are governed by a simple mathematical relation discovered first by Balmer in 1885, hence the name of the series. A complete treatment of this series is given by Sommerfeld.¹

INTRODUCTION WITH HISTORICAL SURVEY OF THE WORK OF OTHER INVESTIGATORS

In 1887, Michelson and Morley were the first to discover that the line H_α was of a complex character. From examination of the visibility of the fringes of H_α formed by a Michelson interferometer, they concluded that H_α had a doublet structure. This doublet interval had been of the greatest concern ever to the present day. The magnitude of the interval as determined by many investigators has differed widely and not until the past few years has a fair agreement been reached by workers in this field.

Schr. in 1913, developed a theory for the hydrogen

¹ Sommerfeld, Atomen und Spektrallinien, p. 285.

INTRODUCTION WITH HISTORICAL SURVEY

OF

THE WORK OF OTHER INVESTIGATORS

INTRODUCTION WITH HISTORICAL SURVEY OF THE

WORK OF OTHER INVESTIGATORS

There are two hydrogen spectra — the molecular and atomic. The latter consists of a number of lines that fall into separate series. Those known are the Lyman, Balmer, Paschen, Brackett and Pfund series ranging from the ultra violet to the infra red respectively.

The first four lines of the Balmer series H_{α} , H_{β} , H_{γ} and H_{δ} have been investigated the most since they lie in the region of the visible spectrum. Line H_{α} lies in the red, H_{β} in the blue-green and H_{γ} and H_{δ} in the violet. The wavelengths of the individual lines of the series are governed by a simple numerical relation discovered first by Balmer in 1885 ; hence the name of the series. A complete treatment of this series is given by Sommerfeld.¹

In 1887, Michelson and Morley were the first to discover that the line H_{α} was of a complex character. From examination of the visibility of the fringes of H_{α} formed by a Michelson interferometer, they concluded that H_{α} had a doublet structure. This doublet interval has been of the greatest concern even to the present day. The magnitude of the interval as determined by many investigators has differed widely and not until the past few years has a fair agreement been reached by workers in this field.

Bohr, in 1913, developed a theory for the hydrogen

¹ Sommerfeld, Atombau and Spektrallinien, p. 344.

INTRODUCTION WITH HISTORICAL SURVEY OF THE

WORK OF OTHER INVESTIGATORS

There are two hydrogen spectra — the molecular

and atomic. The latter consists of a number of lines that fall

into separate series. Those known are the Lyman, Balmer, Paschen,

Breckett and Pfund series ranging from the ultra violet to the

infra red respectively.

The first four lines of the Balmer series H_α , H_β ,

H_γ and H_δ have been investigated the most since they lie in the

region of the visible spectrum. Line H_α lies in the red, H_β in

the blue-green and H_γ and H_δ in the violet. The wavelengths of

the individual lines of the series are governed by a simple ma-

thematical relation discovered first by Balmer in 1885; hence the

name of the series. A complete treatment of this series is

given by Sommerfeld.¹

In 1867, Michelson and Morley were the first to

discover that the line H_α was of a complex character. From ex-

amination of the visibility of the fringes of H_α formed by a

Michelson interferometer, they concluded that H_α had a doublet

structure. This doublet interval has been of the greatest con-

cern even to the present day. The magnitude of the interval as

determined by many investigators has differed widely and not

until the past few years has a fair agreement been reached by

workers in this field.

Bohr, in 1913, developed a theory for the hydrogen

¹ Sommerfeld, *Atombau und Spektrallinien*, p. 344.

atom based on quantized circular orbits. Transitions of an electron from one of these orbits of quantum number 3 to another of quantum number 2 resulted in the emission of H_{α} . This simple theory, however, yielded no such structure to H_{α} as was found experimentally. Later with the refinements of the quantum theory and the introduction of relativistic wave mechanics a consistent picture of the complex structure of H_{α} was reached. The relativity correction¹ and the spinning electron correction introduced by Goudsmit and Uhlenbeck² result in five components for H_{α} .

Heisenberg and Jordan³, Darwin⁴, and Dirac⁵ have derived expressions for the separation and relative intensities of these components. The relative intensities have been calculated by Sommerfeld and Unsöld⁶, Saha and Banerji⁷, and Kupper⁸.

Since Michelson and Morley first observed the H_{α} "doublet" in 1887 intensive research had been carried on for the determination of this "doublet" separation. An extensive summary of the results of the numerous investigators in this field from 1887 to 1922 has been given by G. M. Shrum⁹.

¹ Sommerfeld and Unsöld, Zeits. f. Physik, 36, 259 (1926).
38, 237 (1926).

² Goudsmit and Uhlenbeck, Physica, 6, 273 (1926).

³ Heisenberg and Jordan, Zeits. f. Physik, 37, 263 (1926).

⁴ Darwin, Proc. Roy. Soc., A 116, 227 (1927).

⁵ Dirac, Proc. Roy. Soc., A 117, 610 (1928).

⁶ Sommerfeld and Unsöld, Zeits. f. Physik, 38, 237 (1926).

⁷ Saha and Banerji, Zeits. f. Physik, 68, 704 (1931).

⁸ Kupper, Ann. d. Physik, 86, 511 (1928).

⁹ Shrum, G. M., Proc. Roy. Soc., A 105, 262 (1924).

atom based on quantized electron orbits. Transitions of an elec-
tron from one of these orbits of quantum number n to another of
quantum number m resulted in the emission of H α . This simple
theory, however, failed to give structure to H α , as was found
experimentally. Later with the refinements of the quantum
theory and the introduction of relativistic wave mechanics a con-
sistent picture of the complex structure of H α was reached. The
relativistic correction and the spin-orbit interaction intro-
duced by Goudami and Ubbink¹ result in five components for H α .
Weisenberg and Jordan², Darwin³, and Dirac⁴ have
derived expressions for the separation and relative intensities
of these components. The relative intensities have been calcu-
lated by Goudami and Ubbink¹, Seale and Benoit⁵, and Kupper⁶.
Since Michelson and Morley first observed the
H α "doublet" in 1887 intensive research had been carried on for
the determination of this "doublet" separation. An extensive
survey of the results of the numerous investigators in this
field from 1887 to 1937 has been given by G. W. Wiersma⁷.

1. Goudami and Ubbink, Phys. Rev., **55**, 102 (1937).
2. Weisenberg and Jordan, Phys. Rev., **55**, 102 (1937).
3. Darwin, Proc. Roy. Soc. A, **118**, 251 (1927).
4. Dirac, Proc. Roy. Soc. A, **114**, 243 (1926).
5. Seale and Benoit, Phys. Rev., **55**, 102 (1937).
6. Kupper, Ann. d. Physik, **50**, 511 (1933).
7. Wiersma, Phys. Rev., **55**, 102 (1937).

Values of the "doublet" separation differed widely and no evidence was given at this time of the presence of the three minor components as predicted by theory.

In 1925 Janicki and Lau¹ obtained microphotometer curves of the structure of H_{α} as produced by a Lummer plate. Lack of sufficient asymmetry and too high a saddle height failed to reveal other components.

Houston² in 1926 used a Fabry-Perot interferometer instead of the Lummer-Gehrke plate. With the plates used the separation between the two lines of the "doublet" was usually less than one half of the distance between adjacent orders; thus measurements that were made visually with a comparator gave too high a value of separation while, with microphotometer curves, correction had to be made in the opposite direction for the effect of one component on the other. These disadvantages were eliminated with the Fabry-Perot interferometer, the dispersion could be chosen so as to make one component fall halfway between the adjacent orders of the other. Houston's results of the "doublet" interval were in partial agreement with previous investigators.

The most extensive paper up to this time was published by Kent, Taylor, and Pearson³ in 1927. Two crossed Lummer plates and an echelon grating were used as resolving instruments.

¹ Janicki and Lau, Zeits. f. Physik, 35, 1(1925).

² Houston, V. V., Astrophysical Journal, 64, 81 (1926).

³ Kent, Taylor and Pearson, Phys. Rev., 30, 266 (1927).

Values of the "doublet" separation differed slightly and no evidence was given at this time of the presence of the three components as predicted by theory.

In 1935 Latham and I¹ obtained interferometer curves of the structure of λ_{434} produced by a laser plate. Lack of sufficient asymmetry and too high a doublet height failed to reveal other components.

Houston² in 1938 used a Perry-Pot interferometer instead of the Latham-Gentle plate. With the plates used the separation between the two lines of the "doublet" was usually less than one half of the distance between adjacent orders; thus measurements that were made visually with a comparator gave too high a value of separation while, with interferometer curves, correction had to be made in the opposite direction for the effect of one component on the other. These disadvantages were eliminated with the Perry-Pot interferometer, the separation could be chosen so as to make one component fall halfway between the adjacent orders of the other. Houston's results of the "doublet" interval were in general agreement with previous investigators.

The most extensive work up to this time was published by Kent, Taylor, and Pearson³ in 1937. Two crossed laser plates and an echelon grating were used as resolving instruments.

¹ Latham and I, Phys. Rev., 50, 1193 (1942).

² Houston, V. V., Astronomical Journal, 64, 81 (1938).

³ Kent, Taylor and Pearson, Proc. Roy. Soc., B2, 388 (1937).

The resolving powers of the large plate and the echelon were in general about twice that of instruments used by others. The patterns obtained both by the crossed Lummer plates and the echelon were measured visually by the Gaertner comparator and mechanically by a microphotometer. The microphotometer curves of the crossed Lummer plate system revealed a third component which though unresolved was unquestionably present. The curves in general were ragged and irregular for the microphotometer slit had to be very short.

In 1934 Williams and Gibbs¹ discussed the methods employed in applying corrections to an observed "doublet" interval to find the true interval and relating the position of an intensity maximum to that of the components. The fine structure of H_{α} was analyzed by a Zeiss three-prism spectrograph together with a Fabry-Perot etalon. From an analysis of their curves they obtained $\Delta r = 0.308 \text{ cm}^{-1}$ as the separation of the main components. This interval between the main components is about 6% below the expected theoretical value $\Delta r = 0.328 \text{ cm}^{-1}$. Their value, however is in agreement with the results of Houston and Hsieh². The average of the intervals between the intensity peaks of the complex curve given by Kent, Taylor and Pearson from direct measurements of their microphotometer curves, before the "shrinking correction" was erroneously applied, was also found to be in close agreement with their values of this interval.

¹ Williams and Gibbs, Phys. Rev., 45, 475 (1934).

² Houston and Hsieh, Phys. Rev., 45, 132A (1934).

The resolving power of the large plate and the electron were in general about twice that of instruments used by others. The patterns obtained both by the crossed-lamellar plates and the electron were measured directly by the Debye-Scherrer camera and mechanically by a microphotometer. The microphotometer curves of the crossed-lamellar plate system revealed a third component which though unresolved was unquestionably present. The curves in general were ragged and irregular for the microphotometer side had to be very short.

In 1934 Williams and Bragg discussed the methods employed in applying corrections to an observed "doublet" intensity to find the true interval and relating the position of an intensity maximum to that of the components. The line structure of E-Fe was analyzed by a polarized-light spectrograph together with a Fabry-Pérot etalon. From an analysis of their curves they obtained $\Delta\lambda = 0.008 \text{ cm}^{-1}$ as the separation of the main components. This interval between the main components is about 5% below the expected theoretical value $\Delta\lambda = 0.008 \text{ cm}^{-1}$. Their value, however, is in agreement with the results of Houston and Kato². The average of the intervals between the intensity peaks of the component curve given by Kato, Taylor and Pearson from direct measurements of their microphotometer curves, before the "anti-diffraction correction" was mechanically applied, was also found to be in close agreement with their values of this interval.

¹ Williams and Bragg, *Phys. Rev.*, 43, 473 (1934).
² Houston and Kato, *Phys. Rev.*, 40, 1034 (1934).

Spedding, Shane and Grace¹ have also investigated the fine structure of H_{α} with an etalon interferometer together with an auxiliary 30 foot grating spectrograph.

Williams² in 1938 worked with both H_{α} and D_{α} . The microphotometer curves obtained from patterns produced by the same spectroscopic equipment of previous investigation showed component 3 partially resolved for D_{α} . The separation of component 2 and 3 as well as their intensities were thus more accurately determined. These values were then applied to the study of the H_{α} complex on the hypothesis that the interval between components 2 and 3 is the same for both H_{α} and D_{α} . It was found that component 3 is actually considerably removed from its theoretical position and its intensity is far greater than given theoretically. This then would account for the disagreement of the experimental "doublet" separation with the theoretical, since correction to the peak to peak interval of the H_{α} complex, based on the theoretical position and intensity of component 3, will differ from the correction based on its observed position and intensity.

Recently in a personal letter to Prof. Kent, Houston of the California Institute of Technology stated that one of his students had resolved the third component. This was done with an electrodeless discharge. The results of his work have not as yet been published. Without a doubt the outcome of this investigation with the isolation of the third component will yield the best test to date of our theoretical picture of the fine structure of H_{α} .

¹ Spedding, Shane and Grace, Phys. Rev., 38 (1935).

² Williams, Phys. Rev., 54, 558 (1938).

Specimens, X-ray and other have also investigated the line structure of H_{α} with an electron interferometer together with an auxiliary 30 foot grating spectrograph.

Williams in 1933 worked with both H_{α} and H_{β} . The interferometer curves obtained from patterns produced by the same spectroscopic alignment of previous investigation showed component 3 partially resolved for H_{α} . The separation of components 2 and 3 as well as their intensities were then more accurately determined. These values were then applied to the study of the H_{α} complex on the hypothesis that the interval between components 2 and 3 is the same for both H_{α} and H_{β} . It was found that component 3 is actually considerably removed from the theoretical position and its intensity is far greater than given theoretically. This then would account for the displacement of the experimental "doublet" separation with the theoretical, since correction to the peak to peak interval of the H_{α} complex, based on the theoretical position and intensity of component 3, will differ from the correction based on its observed position and intensity.

Recently in a personal letter to Prof. Kent, Houston of the California Institute of Technology stated that one of his students had resolved the third component. This was done with an electron beam discharge. The results of his work have not as yet been published. Without a doubt the outcome of this investigation with the isolation of the third component will yield the best

to date of our theoretical picture of the line structure of H_{α} .
I. Spettig, J. Kent and Kent, Phys. Rev. 57 (1937).
2. Williams, Phys. Rev. 42, 555 (1933).

OBJECT OF THE RESEARCH

CHIEF OF THE RESERVATION

The preliminary investigation of W. H. Robinson¹, in the study of H-alpha of hydrogen with the use of a Lummer plate as an auxiliary spectrograph appeared very promising. This method of using two Lummer plates in tandem with a plane reflection grating located between the two Lummer plates to single out separate lines furnished a new means by which lines of a composite nature could be studied. The whole spectroscopic system had a greater dispersion than instruments used by other investigators and had the advantage that a long and narrow microphotometer slit could be used since the patterns produced were composed of straight lines.

Up to the time of the beginning of this paper no other investigators have completely isolated the third component of the theoretical five component structure of H-alpha. Results of Robinson's work showed the existence of the third component and definitely indicated the presence of the fourth. Recently in a letter to Professor Kent, Houston of the California Institute of Technology, stated that one of his students had resolved the third component, this being done by means of an electrodeless discharge as a source.

The aim of the present research was to extend the ideas advanced by Professor Kent and partially carried out by Robinson. It was hoped that with improved conditions and rearrangement of the spectroscopic system there could be obtained better photographic plates and thus better microphotometer

¹ Robinson, Ph.D. Thesis B.U.Grad.School, 1937

the study of H-alpha of hydrogen with the use of a Lummer plate as an auxiliary spectrograph appeared very promising. This method of using two Lummer plates in tandem with a plane reflection grating located between the two Lummer plates to single out accurate lines furnished a new means by which lines of a complex nature could be studied. The whole spectroscopic system had a greater dispersion than instruments used by other investigators and had the advantage that a long and narrow microphotometer slit could be used since the patterns produced were composed of straight lines.

Up to the time of the beginning of this paper no other investigators have completely isolated the third component of the theoretical five component structure of H-alpha. Results of Robinson's work showed the existence of the third component and definitely indicated the presence of the fourth. Recently in a letter to Professor Kent, Houston of the California Institute of Technology, stated that one of his students had resolved the third component, this being done by means of an electroless discharge as a source.

The aim of the present research was to extend the ideas advanced by Professor Kent and partially carried out by Robinson. It was hoped that with improved conditions and rearrangement of the spectroscopic system there could be obtained better photographic plates and thus better microphotometer

curves which might reveal both the third and fourth components, especially the latter. With this in mind a third Lummer plate was bought for use in this problem.

The spectroscopic system finally decided upon was one in which the two Lummer plates were set directly in tandem with no intervening instruments. From a study of the relative positions of these plates, their constants, and the angles of incidence and emergence of the light rays it was hoped that by means of microphotometer patterns the wavelengths and intensities of the component lines of H-alpha could be obtained.

curves which might reveal both the third and fourth components, especially the latter. With this in mind a third Lummer plate was bought for use in this problem.

The spectroscopic system finally decided upon was one in which the two Lummer plates were set directly in tandem with no intervening instruments. From a study of the relative positions of these plates, their constants, and the angles of incidence and emergence of the light rays it was hoped that by means of microphotometer patterns the wavelengths and intensities of the component lines of H-alpha could be obtained.

DEVELOPMENT OF THEORY

The hydrogen atom consists of a proton and an electron. Due to the Coulombian field of their electrical charges, the nucleus with a charge $+e$ and the electron with a charge $-e$ attract each other.

The wave equation for a conservative Hamiltonian system is

$$\nabla^2 \psi + \frac{2m}{\hbar^2} (E - V) \psi = 0 \quad \text{---(1)}$$

E here represents the energy constant, and V the potential energy expressed as a function of the coordinates.

One FINE STRUCTURE OF this equation is that ψ must be everywhere continuous, H-ALPHA valued, and finite. In a given system there are only certain functions, called "eigenfunctions", that satisfy the above condition and correspondingly, there are only certain characteristic values of E , the energy constant.

If in the Cartesian system we let x_1, y_1, z_1 be the position coordinates for the nucleus and x_2, y_2, z_2 those for the electron---and m_1 and m_2 be the masses, respectively, the above wave equation takes the form

$$\frac{1}{m_1} \left(\frac{\partial^2 \psi}{\partial x_1^2} + \frac{\partial^2 \psi}{\partial y_1^2} + \frac{\partial^2 \psi}{\partial z_1^2} \right) + \frac{1}{m_2} \left(\frac{\partial^2 \psi}{\partial x_2^2} + \frac{\partial^2 \psi}{\partial y_2^2} + \frac{\partial^2 \psi}{\partial z_2^2} \right) + \frac{2m}{\hbar^2} (E - V) \psi = 0 \quad \text{---(2)}$$

V , the potential energy of the system, $= -\frac{Ze^2}{r}$ where r is the distance from the nucleus to the electron.

Thus

$$V = -\frac{Ze^2}{\sqrt{(x_2 - x_1)^2 + (y_2 - y_1)^2 + (z_2 - z_1)^2}}$$

THE STRUCTURE OF
H-ALPHA

DEVELOPMENT OF THEORY

The hydrogen atom consists of a proton and an electron. Due to the Coulombian field of their electrical charges, the nucleus with a charge $+e$ and the electron with a charge $-e$ attract each other.

The wave equation for a conservative Newtonian dynamical system is

$$\nabla^2 \psi + \frac{8\pi^2}{h^2} (W - V) \psi = 0 \quad \text{-----(1)}$$

W here represents the energy constant, and V the potential energy expressed as a function of the coordinates.

One condition imposed on this equation is that ψ must be everywhere continuous, single valued, and finite. In a given system there are only certain functions, called "eigen-functions", that satisfy the above condition and correspondingly, there are only certain characteristic values of W , the energy constant.

If in the Cartesian system we let x_1, y_1, z_1 be the position coordinates for the nucleus and x_2, y_2, z_2 those for the electron---and m_1 and m_2 be the masses, respectively, the above wave equation takes the form

$$\frac{1}{m_1} \left(\frac{\partial^2 \psi_T}{\partial x_1^2} + \frac{\partial^2 \psi_T}{\partial y_1^2} + \frac{\partial^2 \psi_T}{\partial z_1^2} \right) + \frac{1}{m_2} \left(\frac{\partial^2 \psi_T}{\partial x_2^2} + \frac{\partial^2 \psi_T}{\partial y_2^2} + \frac{\partial^2 \psi_T}{\partial z_2^2} \right) + \frac{8\pi^2}{h^2} (W_T - V) \psi_T = 0 \quad \text{-----(2)}$$

V , the potential energy of the system, $= -\frac{Ze^2}{r}$
where r is the distance from the nucleus to the electron.

Thus

$$V = -\frac{Ze^2}{\sqrt{(x_2 - x_1)^2 + (y_2 - y_1)^2 + (z_2 - z_1)^2}}$$

NEWTONIAN MECHANICS

The hydrogen atom consists of a proton and an electron. Due to the Coulombian field of their electrical charges, the nucleus with a charge +e and the electron with a charge -e attract each other.

The wave equation for a conservative Newtonian

dynamical system is

$$\nabla^2 \psi + \frac{2\pi e^2}{h^2} (W - V) \psi = 0 \quad (1)$$

W here represents the energy constant, and V the potential energy expressed as a function of the coordinates.

One condition imposed on this equation is that

ψ must be everywhere continuous, single valued, and finite. In a given system there are only certain functions, called "eigenfunctions", that satisfy the above condition and correspondingly there are only certain characteristic values of W, the energy constant.

If in the Cartesian system we let x_1, y_1, z_1 be the position coordinates for the nucleus and x_2, y_2, z_2 those for the electron---and m_1 and m_2 be the masses, respectively, the

above wave equation takes the form

$$\nabla_1^2 \psi + \frac{2\pi e^2}{h^2} (W - V) \psi = 0 \quad (2)$$

V, the potential energy of the system, is

where r is the distance from the nucleus to the electron.

$$V = -\frac{2\pi e^2}{r} = -\frac{2\pi e^2}{\sqrt{(x_2 - x_1)^2 + (y_2 - y_1)^2 + (z_2 - z_1)^2}}$$

Thus

The subscript T (signifying total) is used with ψ and W to indicate that these quantities refer to the complete system, with six coordinates.

Equation 2 can be transformed into two separate equations, one which represents the translation motion of the atom as a whole and the other the relative motion of the two particles. This transformation may be effected by shifting to polar coordinates.

If $x, y,$ and z are the Cartesian coordinates of the center of mass of the system, and $r, \theta,$ and ϕ the polar coordinates of the second particle relative to the first, the related equations are

$$x_1 = x - \frac{r}{m_1} \sin \theta \cos \phi$$

$$x_2 = x + \frac{r}{m_2} \sin \theta \cos \phi$$

$$y_1 = y - \frac{r}{m_1} \sin \theta \sin \phi$$

$$y_2 = y + \frac{r}{m_2} \sin \theta \sin \phi$$

$$z_1 = z - \frac{r}{m_1} \cos \theta$$

$$z_2 = z + \frac{r}{m_2} \cos \theta$$

Introducing these new variables in equation 2,

we have :-

$$\begin{aligned} & \frac{1}{m_1 + m_2} \left(\frac{\partial^2 \psi_T}{\partial^2 x^2} + \frac{\partial^2 \psi_T}{\partial^2 y^2} + \frac{\partial^2 \psi_T}{\partial^2 z^2} \right) + \frac{1}{\mu} \left\{ \frac{1}{r^2} \frac{\partial}{\partial r} \left(r^2 \frac{\partial \psi_T}{\partial r} \right) \right. \\ & \quad \left. + \frac{1}{r^2 \sin^2 \theta} \frac{\partial^2 \psi_T}{\partial \phi^2} + \frac{1}{r^2 \sin \theta} \frac{\partial}{\partial \theta} \left(\sin \theta \frac{\partial \psi_T}{\partial \theta} \right) \right\} \\ & \quad + \frac{8\pi^2}{h^2} \left\{ W_T - V(r, \theta, \phi) \right\} \psi_T = 0 \end{aligned} \quad \text{----- (3)}$$

The subscript T (signifying total) is used with x and y to indicate that these quantities refer to the complete system, with six coordinates.

Equation 2 can be transformed into two separate equations, one which represents the translation motion of the atom as a whole and the other the relative motion of the two particles. This transformation may be effected by shifting to polar coordinates.

If x , y , and z are the Cartesian coordinates of

the center of mass of the system, and r , θ , and ϕ the polar coordinates of the second particle relative to the first, the related equations are

$$\begin{aligned}x_1 &= x - \frac{y}{m} r \sin \theta \cos \phi \\x_2 &= x + \frac{y}{m} r \sin \theta \cos \phi \\y_1 &= y - \frac{y}{m} r \sin \theta \sin \phi \\y_2 &= y + \frac{y}{m} r \sin \theta \sin \phi \\z_1 &= z - \frac{y}{m} r \cos \theta \\z_2 &= z + \frac{y}{m} r \cos \theta\end{aligned}$$

Introducing these new variables in equation 2,

we have :-

$$\begin{aligned}& \left(\frac{1}{m_1 + m_2} \right) \left(\frac{\partial^2 \psi}{\partial x^2} + \frac{\partial^2 \psi}{\partial y^2} + \frac{\partial^2 \psi}{\partial z^2} \right) + \left(\frac{1}{m} \right) \left(\frac{\partial^2 \psi}{\partial r^2} + \frac{1}{r^2} \left(\frac{\partial^2 \psi}{\partial \theta^2} + \frac{1}{\sin^2 \theta} \frac{\partial^2 \psi}{\partial \phi^2} \right) \right) \\& + \left(\frac{1}{r^2 \sin \theta} \right) \left(\frac{\partial \psi}{\partial \theta} + \frac{1}{\sin \theta} \frac{\partial \psi}{\partial \phi} \right) + \left(\frac{1}{r^2 \sin \theta} \right) \left(\frac{\partial \psi}{\partial \theta} + \frac{1}{\sin \theta} \frac{\partial \psi}{\partial \phi} \right) \\& + \left(\frac{1}{r^2 \sin \theta} \right) \left(\frac{\partial \psi}{\partial \theta} + \frac{1}{\sin \theta} \frac{\partial \psi}{\partial \phi} \right) = 0\end{aligned}$$

If ψ is placed equal to the product of a function of x, y, z and a function of r, θ, ϕ ;

$$\psi(x, y, z, r, \theta, \phi) = F(x, y, z) \psi(r, \theta, \phi)$$

the equation can be separated into two parts, namely

$$\frac{\partial^2 F}{\partial x^2} + \frac{\partial^2 F}{\partial y^2} + \frac{\partial^2 F}{\partial z^2} + \frac{8\pi^2(m_1+m_2)}{h^2} W_{tr} F = 0 \quad \text{----- (4)}$$

$$\text{and } \frac{1}{r^2} \frac{d}{dr} \left(r^2 \frac{\partial \psi}{\partial r} \right) + \frac{1}{r^2 \sin^2 \theta} \frac{\partial^2 \psi}{\partial \phi^2} + \frac{1}{r^2 \sin \theta} \frac{\partial}{\partial \theta} \left(\sin \theta \frac{\partial \psi}{\partial \theta} \right) + \frac{8\pi^2 \mu}{h^2} \{W - V(r, \theta, \phi)\} \psi = 0 \quad \text{----- (5)}$$

in which W_{tr} represents the translational energy of the system and W the residual energy.

If V is now a function of r alone ($V = \frac{-Ze^2}{r}$) and ψ is replaced by the product of a function of r alone, one of θ alone and one of ϕ alone,

$$\psi = R(r) \cdot \Theta(\theta) \cdot \Phi(\phi)$$

then equation 5 can be separated into three distinct total differential equations :

$$\frac{1}{\Phi} \frac{d^2 \Phi}{d\phi^2} = -\alpha = -m^2 \quad \text{----- (6)}$$

$$\frac{1}{\Theta \sin \theta} \frac{d}{d\theta} \left(\sin \theta \frac{d\Theta}{d\theta} \right) - \frac{m^2}{\sin^2 \theta} = -\beta \quad \text{----- (7)}$$

$$\frac{1}{r^2} \frac{d}{dr} \left(r^2 \frac{dR}{dr} \right) - \frac{\beta}{r^2} R + \frac{8\pi^2 \mu}{h^2} \{W - V(r)\} R = 0 \quad \text{----- (8)}$$

If ψ is placed equal to the product of a function of x, y, z

and a function of r, θ, ϕ :

$$\psi(x, y, z, r, \theta, \phi) = F(x, y, z) \psi(r, \theta, \phi)$$

the equation can be separated into two parts, namely

$$(A) \quad \frac{1}{2} \frac{d^2 F}{dx^2} + \frac{1}{2} \frac{d^2 F}{dy^2} + \frac{1}{2} \frac{d^2 F}{dz^2} + \frac{8\pi^2 m E}{h^2} F = 0$$

$$(B) \quad \frac{1}{r^2} \frac{d}{dr} \left(r^2 \frac{d\psi}{dr} \right) + \frac{1}{r^2 \sin^2 \theta} \frac{d}{d\theta} \left(\sin^2 \theta \frac{d\psi}{d\theta} \right) + \frac{1}{r^2 \sin^2 \theta} \frac{d^2 \psi}{d\phi^2} + \frac{8\pi^2 m E}{h^2} \psi = 0$$

in which W_{tr} represents the translational energy of the system and W the residual energy.

If V is now a function of r alone ($V = \frac{K}{r}$) and ψ is replaced by the product of a function of r alone, one of θ alone and one of ϕ alone,

$$\psi = R(r) \cdot \Theta(\theta) \cdot \Phi(\phi)$$

then equation B can be separated into three distinct differential equations :

$$(C) \quad \frac{1}{r^2} \frac{d}{dr} \left(r^2 \frac{dR}{dr} \right) + \frac{8\pi^2 m E}{h^2} R = 0$$

$$(D) \quad \frac{1}{\sin^2 \theta} \frac{d}{d\theta} \left(\sin^2 \theta \frac{d\Theta}{d\theta} \right) - \frac{m^2}{\sin^2 \theta} \Theta = -B$$

$$(E) \quad \frac{1}{r^2 \sin^2 \theta} \frac{d^2 \Phi}{d\phi^2} - \frac{F}{r^2 \sin^2 \theta} \Phi = 0$$

Equation 6 has eigenfunctions¹ only when α is equal to m^2 , with m having any \mp integral value. With these values of the parameter, m , equation 7 has acceptable solutions only when β equals $l(l+1)$ where l has any positive integral value equal to or greater than the absolute value of m . Finally, introducing values of β into equation 8 acceptable solutions are given only for certain values of W , namely --

$$W_n = - \frac{2\pi^2 \mu Z^2 e^4}{n^2 h^2} = - \frac{R_H c Z^2}{n^2} \quad \text{-----} (9)$$

in which n can assume integral values $1, 2, 3, \dots, \infty$ and where

$$R_H = \frac{2\pi^2 \mu e^4}{h^3 c}$$

Solutions of equations 6, 7 and 8 listing the eigenfunctions corresponding to given values of n , l , and m are given in the references¹ at the bottom of the page.

The allowed quantum numbers for the independent wave functions can be written as follows ---

total quantum number $n = 1, 2, 3, \dots,$
 azimuthal quantum number $l = 0, 1, 2, \dots, n-1,$
 magnetic quantum number $m = -l, -l+1, \dots, -1, 0, +1, \dots, +l-1, +l.$

¹

Schrodinger, Ann. d. Phys., 79, 361 (1926).

Pauling and Goudsmit, Structure of Line Spectra, p 27, sec. 6b.

Pauling and Wilson, Introduction to Quantum Mechanics,

pp 117-124.

Equation 6 has eigenfunctions only when λ is equal to m^2 , with m having any integral value. With these values of the parameter m , equation 7 has acceptable solutions only when λ equals $l(l+1)$ where l has any positive integral value equal to or greater than the absolute value of m . Finally, introducing values of λ into equation 8 acceptable solutions are given only for certain values of W , namely --

$$W_n = - \frac{2\pi^2 \mu e^4}{h^2 n^2} = - \frac{R_H}{n^2} \quad (9)$$

in which n can assume integral values $1, 2, 3, \dots$ and where

$$R_H = \frac{2\pi^2 \mu e^4}{h^2}$$

Solutions of equations 6, 7 and 8 listing the eigenfunctions corresponding to given values of n, l , and m are given in the references¹ at the bottom of the page.

The allowed quantum numbers for the independent

wave functions can be written as follows --

- total quantum number $n = 1, 2, 3, \dots$
- azimuthal quantum number $l = 0, 1, 2, \dots, n-1$
- magnetic quantum number $m = -l, -(l-1), \dots, -1, 0, +1, \dots, +l$

¹ Schrodinger, Ann. d. Phys., 78, 361 (1926).
 Pauling and Goudsmith, Structure of Line Spectra, p. 27, sect. 1b.
 Pauling and Wilson, Introduction to Quantum Mechanics, pp. 117-124.

The above expression for the energy levels does not account for the line structure in the lines of the atomic spectrum. For a complete picture two correction terms must be made to the equation 9. The first to be considered is that due to the electron spin.

Consider the electron moving with a velocity (v) in the electric field (F) of the nucleus. The moving electron thus produces according to the electromagnetic theory a magnetic field (H) at the electron.

$$H = \frac{1}{c} F \times v$$

If the effective nuclear charge is Ze the field at the electron is

$$F = \frac{Ze}{r^3} \bar{r} \quad \bar{r} = \text{radius vector}$$

The angular momentum thus is

$$m_0 \bar{r} \times v = \bar{l} \frac{h}{2\pi}$$

$$\therefore H = \bar{l} \times \frac{h}{2\pi m_0 c} \cdot \frac{Ze}{r^3}$$

The magnetic electron in a magnetic field undergoes a precession about the field direction, with an angular velocity equal to the product of the field strength (H) and the ratio of the magnetic ($2\bar{s} \frac{h}{2\pi} \cdot \frac{e}{2m_0 c}$) and the mechanical moment ($\bar{s} \frac{h}{2\pi}$) of the spinning electron

$$\omega_H = \frac{e^2}{m_0 c} \cdot \frac{Z}{r^3} \cdot \frac{\bar{l} h}{2\pi}$$

From the work of L. H. Thomas¹ in the relativ-

¹

L. H. Thomas, Nature, 117, 514 (1926).

From the work of L. H. Thomas¹ in the relative

$$w_H = \frac{e^2}{mc^2} \cdot \frac{h}{2\pi} \cdot \frac{1}{r} \cdot \frac{1}{2\pi}$$

($\frac{h}{2\pi}$) of the spinning electron

ratio of the magnetic ($\frac{e^2}{2mc^2}$) and the mechanical moment

velocity equal to the product of the field strength (H) and the
 goes a precession about the field direction, with an angular

The magnetic electron in a magnetic field under-

$$\therefore H = \frac{h}{2\pi m_e a} \cdot \frac{2e}{r}$$

$$m_e \bar{r} v = \frac{h}{2\pi}$$

The angular momentum thus is

$$p = \frac{2e}{r} \cdot \bar{r} = \text{radius vector}$$

If the effective nuclear charge is Ze the field at the electron

$$E = \frac{1}{c} \times v$$

field (H) at the electron.

thus proceeds according to the electromagnetic theory a magnetic
 in the electric field (E) of the nucleus. The moving electron

Consider the electron moving with a velocity (v)

to the electron again.

made to the equation 2. The first to be considered is that due

spectrum. For a complete picture two correction terms must be

not account for the fine structure in the lines of the atomic

The above expression for the energy levels does

istic treatment of the motion of the spinning electron there exists another precession of the electron axis besides the above magnetic precession. This relativistic precession (ω_r) has one half the value of the magnetic, and has the opposite sign.

The actual angular velocity of the electron axis thus becomes

$$\omega = \omega_H + \omega_r = \frac{1}{2} \frac{e^2}{m_0 c^2} \cdot \frac{Z}{r^3} \cdot \frac{\bar{l} h}{2\pi}$$

The energy of such a precessional motion is equal to the product of the angular velocity and the projection of the mechanical moment ($\bar{s} \frac{h}{2\pi}$) of the precessing system on the axis of precession; i.e., on H or \bar{l} :

$$W_s = \frac{1}{2} \frac{e^2 h^2}{4\pi^2 m_0 c^2} \cdot \frac{Z}{r^3} s l \cos(\bar{s} \bar{l}) \text{ ----- (10)}$$

The factor $1/r^3$ is not constant during the motion of the electron. From quantum mechanics¹

$$\left(\frac{1}{r^3}\right) = \frac{64\pi^6 m_0^3 e^6 Z^4}{h^6 n^3 l(l+\frac{1}{2})(l+1)} \text{ ----- (11)}$$

Thus equation 10 can be written in the form

$$W_s = \frac{R h c \propto Z^4}{n^3 l(l+\frac{1}{2})(l+1)} l s \cos(\bar{l} \bar{s}) \text{ ----- (12)}$$

$$\text{where } R = \frac{2\pi^2 m_0 e^4}{ch^3}$$

$$\text{and } \propto = \frac{2\pi e^2}{hc}$$

The total angular momentum which is given by the quantum vector \bar{j} , is the resultant of the orbital momentum \bar{l}

¹ Pauling and Goudsmit, Structure of Line Spectra, section 7, p 32.

istic treatment of the motion of the spinning electron there exists another precession of the electron axis besides the above magnetic precession. This relativistic precession (ω_r) has one half the value of the magnetic, and has the opposite sign. The actual angular velocity of the electron axis

thus becomes

$$\omega = \omega_H + \omega_r = \frac{1}{2} \frac{e\hbar}{m_0 c} \frac{1}{\hbar} \frac{1}{2} \frac{1}{2} \frac{1}{2} \frac{1}{2}$$

The energy of such a precessional motion is equal to the product of the angular velocity and the projection of the mechanical moment ($\frac{1}{2} \frac{h}{2\pi}$) of the precessing system on the axis of precession; i.e., on H or \bar{L} :

$$W_a = \frac{1}{2} \frac{e\hbar}{m_0 c} \frac{1}{\hbar} \frac{1}{2} \frac{1}{2} \frac{1}{2} \frac{1}{2} \cos(\alpha) \quad (10)$$

The factor $1/2$ is not constant during the motion

of the electron. From quantum mechanics

$$\frac{1}{2} \frac{e\hbar}{m_0 c} \frac{1}{\hbar} \frac{1}{2} \frac{1}{2} \frac{1}{2} \frac{1}{2} \cos(\alpha) \quad (11)$$

Thus equation 10 can be written in the form

$$W_a = \frac{1}{2} \frac{e\hbar}{m_0 c} \frac{1}{\hbar} \frac{1}{2} \frac{1}{2} \frac{1}{2} \frac{1}{2} \cos(\alpha) \quad (12)$$

where $E = \frac{2\pi m_0 c^2}{\hbar}$

and $\omega = \frac{2\pi \nu}{\hbar}$

The total angular momentum which is given by the

quantum vector \bar{J} , is the resultant of the orbital momentum \bar{L}

and the spin moment \vec{s} — where the magnitudes of these vectors in terms of quantum numbers are $\sqrt{j(j+1)}$, $\sqrt{l(l+1)}$, and $\sqrt{s(s+1)}$ respectively.

The following equation follows from a discussion¹ of the resultant quantum vector.

$$sl \cos(\vec{s}\vec{l}) = \frac{j(j+1) - s(s+1) - l(l+1)}{2}$$

Since j can assume only the values $l \pm \frac{1}{2}$

$$sl \cos(\vec{s}\vec{l}) = \frac{l(l + \frac{1}{2}) - \frac{3}{4}}{2}$$

$$W_s = \frac{Rhc\alpha^2 Z^4}{n^3 l(l + \frac{1}{2})} \cdot \frac{l(l + \frac{1}{2}) - \frac{3}{4}}{2} \quad \text{----- (13)}$$

The second correction term to be added to the energy values is that due to the consideration of the relativistic change in mass with the velocity of the electron. This correction splits up the energy levels given by n into n levels (s, p, d, f, \dots etc.). The equation is

$$W_l = \frac{Rhc\alpha^2 Z^4}{n^3} \left(\frac{3}{4n} - \frac{1}{l + \frac{1}{2}} \right) \quad \text{----- (14)}$$

which was first derived by W. Pauli² from quantum mechanics.

Combining equations 13 and 14, we have

$$W' = W_l + W_s = \frac{Rhc\alpha^2 Z^4}{n^3} \left(\frac{3}{4n} - \frac{1}{l + 1} \right) \text{ for } j = l + \frac{1}{2}$$

$$W' = W_l + W_s = \frac{Rhc\alpha^2 Z^4}{n^3} \left(\frac{3}{4n} - \frac{1}{l} \right) \text{ for } j = l - \frac{1}{2}$$

Therefore total energy $W = W_n + W'$ or

¹Pauling and Goudsmit, Structure of Line Spectra, section 14a, p 55.

²Pauli, W., Z. f. Phys., 36 , 336 (1926)

and the spin moment \vec{s} — where the magnitudes of these vectors in terms of quantum numbers are $\sqrt{j(j+1)}$, $\sqrt{l(l+1)}$ and $\sqrt{s(s+1)}$ respectively.

The following equation follows from a discussion of the resultant quantum vector.

$$2l \cos(\vec{s} \vec{l}) = \frac{l(l+1) - s(s+1) - j(j+1)}{2}$$

Since j can assume only the values $l \pm \frac{1}{2}$

$$2l \cos(\vec{s} \vec{l}) = \frac{l(l+1) - s(s+1) - (l \pm \frac{1}{2})(l \pm \frac{1}{2} + 1)}{2}$$

$$W_0 = \frac{K \hbar^2 l(l+1)}{2} \pm \frac{K \hbar^2 l(l+1)}{2} \cos(\vec{s} \vec{l}) \quad (13)$$

The second correction term to be added to the energy values is that due to the consideration of the relativistic change in mass with the velocity of the electron. This correction splits up the energy levels given by a finite n levels (s, p, d, f, ... etc.). The equation is

$$W_1 = \frac{K \hbar^2 l(l+1)}{2} \left(\frac{1}{2l+1} - \frac{1}{2l-1} \right) \quad (14)$$

which was first derived by A. Pauli from quantum mechanics.

Combining equations 13 and 14, we have

$$W = W_0 + W_1 = \frac{K \hbar^2 l(l+1)}{2} \left(\frac{1}{2l+1} - \frac{1}{2l-1} \right) \pm \frac{K \hbar^2 l(l+1)}{2} \cos(\vec{s} \vec{l})$$

Therefore total energy $W = W_0 + W_1$ or

Pauli, W., Zeitschrift für Physik, 1924, 31, 333-382.

$$W = - \frac{R_H c Z^2}{n^2} + \frac{R_H c \alpha^2 Z^4}{n^3} \left(\frac{3}{4n} - A \right)$$

where $A = \frac{1}{l+1}$ for $j = l + \frac{1}{2}$

and $A = \frac{1}{l}$ for $j = l - \frac{1}{2}$

Certain energy levels will be found to coincide; namely, those with the same values of j .

$$R_H = \frac{2\pi^2 m e^4}{ch^3} = 109677.759 \text{ cm}^{-1}, \quad \alpha^2 = 5.305 \times 10^{-5}$$

$$W = - \frac{R_H h c Z^2}{n^2} + \frac{R_H c \alpha^2 Z^4}{n^3} = \frac{109677.759 \times 6.547 \times 10^{-27} \times 2.99796 \times 10^{10}}{n^2} + \frac{109737.42 \times 6.547 \times 10^{-27} \times 2.99796 \times 10^{10} \times 5.305 \times 10^{-5}}{n^3}$$

The equation for the energy levels is thus

$$W = - \frac{2.1527 \times 10^{-11}}{n^2} + \frac{1.1426 \times 10^{-15}}{n^3} \left(\frac{3}{4n} - A \right)$$

Values of A are given above.

The conditions imposed on the three quantum numbers n , l , and j are

$$n = 1, 2, 3, \dots, \infty$$

$$l = 0, 1, 2, \dots, (n-1)$$

$$j = l \pm \frac{1}{2}$$

The main energy levels $n=3$ and $n=2$ for $H\alpha$ are thus split up into 3 l and 2 l levels respectively. These in turn into 2 j levels. It will be found that the energy levels for the same values of j coincide. In the figure 1 those which coincide are slightly separated for clearness. In all we have but five different energy levels. The large letters (S, P, D, F, ---) correspond to values of $l = 0, 1, 2, \dots$ etc.

$$W = - \frac{2\pi^2 e^2}{n^2} + \frac{2\pi^2 e^2}{n^2} \left(\frac{1}{2} - A \right)$$

where $A = \frac{1}{1+1}$ for $j = 1/2 + 1/2$
and $A = \frac{1}{1}$ for $j = 1 - 1/2$

Certain energy levels will be found to coincide,

namely, those with the same values of j .

$$W = - \frac{2\pi^2 e^2}{n^2} = -10887.75 \text{ cm}^{-1} \cdot 2.553 \times 10^{-8}$$

$$W = - \frac{2\pi^2 e^2}{n^2} + \frac{2\pi^2 e^2}{n^2} \left(\frac{1}{2} - A \right) = -10887.75 \text{ cm}^{-1} + \frac{2\pi^2 e^2}{n^2} \left(\frac{1}{2} - A \right) \times 2.553 \times 10^{-8}$$

The equation for the energy levels is then

$$W = - \frac{2.187 \times 10^{-18}}{n^2} + \frac{1.16 \times 10^{-18}}{n^2} \left(\frac{1}{2} - A \right)$$

Values of A are given above.

The conditions imposed on the three quantum

numbers n, l, m are

$$n = 1, 2, 3, \dots$$
$$l = 0, 1, 2, \dots, (n-1)$$
$$m = -l, \dots, +l$$

The main energy levels $n=2$ and $n=3$ for He are

then split up into 3 and 2 levels respectively. These in turn split into 3 levels. It will be found that the energy levels for the same value of j coincide. In the figure 1 those which coincide are slightly separated for convenience. In all we have but five different energy levels. The large letters $2, 3, 4, 5, 6$ correspond to values of $n=2, 3, 4, 5, 6$ respectively.

n	l	j	
3	2	5/2	3, ² D _{5/2}
		3/2	3, ² D _{3/2}
	1	3/2	3, ² P _{3/2}
		1/2	3, ² P _{1/2}
	0	1/2	3, ² S _{1/2}
2	1	3/2	2, ² P _{3/2}
		1/2	2, ² P _{1/2}
	0	1/2	2, ² S _{1/2}

Figure I

ENERGY LEVELS

n	l	l
2	2	2/2
	1	2/2
	1	2/2
	0	1/2
	0	1/2
2	1	2/2
	0	1/2
	0	1/2

Figure 1
ENERGY LEVELS

The frequency of a line emitted by radiation attending a transition from one energy state W_1 to a lower state W_2 is given by

$$\nu = \frac{W_1 - W_2}{h} \text{ sec}^{-1}.$$

ν is the true frequency — not the oscillation frequency $\bar{\nu}$ or $\frac{\nu}{c}$ which is generally used in spectroscopy. The term value, T , becomes $-\frac{W}{hc} \text{ cm}^{-1}$ and

$$\bar{\nu} = T_2 - T_1 \text{ (cm}^{-1}\text{)}$$

The change in sign here is due to the fact that the lowest and most stable state has the largest term value.

Calculations of T and W are as follows:-

$$hc = 1.9628 \times 10^{-16} \text{ erg-cm.}$$

For

$$\begin{array}{l} n = 2 \\ 2, {}^2S_{1/2} \quad \ell = 0 \\ j = \frac{1}{2} \end{array}$$

also

$$\begin{array}{l} n = 2 \\ 2, {}^2P_{1/2} \quad \ell = 1 \\ j = \frac{1}{2} \end{array}$$

$$W = - \frac{2.1527 \times 10^{-11}}{4} + \frac{1.1426 \times 10^{-15}}{8} \left(\frac{3}{8} - 1 \right)$$

$$W = - 5.382 \times 10^{-12} - 0.8927 \times 10^{-16}$$

$$T = - \frac{M - 0.8927 \times 10^{-16}}{hc} = A + .45481 \text{ cm}^{-1}$$

$$\text{where } M = - 5.382 \times 10^{-12}$$

$$A = - \frac{M}{hc}$$

$$\begin{array}{l} n = 2 \\ 2, {}^2P_{3/2} \quad \ell = 1 \\ j = \frac{3}{2} \end{array}$$

$$W = M + \frac{1.1426 \times 10^{-15}}{8} \left(\frac{3}{8} - \frac{1}{2} \right)$$

$$W = M - 0.1785 \times 10^{-16}$$

$$T = - \frac{M - .1785 \times 10^{-16}}{hc} = A + .09094 \text{ cm}^{-1}$$

The frequency of a line emitted by radiation attending a transition from one energy state W_1 to a lower state W_2 is given by

$$\nu = \frac{W_1 - W_2}{h}$$

ν is the true frequency — not the oscillation frequency $\bar{\nu}$ or $\frac{\nu}{c}$ which is generally used in spectroscopy. The term value, T , becomes $-\frac{W}{hc}$ and

$$\bar{\nu} = T_2 - T_1 \quad (\text{cm}^{-1})$$

The change in sign here is due to the fact that the lowest and most stable state has the largest term value.

Calculations of T and W are as follows:-

$$hc = 1.986 \times 10^{-16} \text{ erg-cm.}$$

For	$n = 2$	$2, 2, 1$	$2, 2, 1$
	$l = 0$	$l = 1$	$l = 1$
	$j = \frac{1}{2}$	$j = \frac{3}{2}$	$j = \frac{3}{2}$
also	$n = 2$	$l = 1$	$l = 1$
	$j = \frac{3}{2}$	$j = \frac{1}{2}$	$j = \frac{1}{2}$

$$W = - \frac{2.1887 \times 10^{-18}}{4} \times 1.1432 \times 10^{-18} \left(\frac{1}{2} - \frac{1}{8} \right)$$

$$W = - 5.362 \times 10^{-18} - 0.8327 \times 10^{-18}$$

$$T = - \frac{W}{hc} = \frac{5.362 \times 10^{-18}}{1.986 \times 10^{-16}} = A + .45481 \text{ cm}^{-1}$$

where $W = - 5.362 \times 10^{-18}$

$$A = - \frac{W}{hc}$$

	$n = 2$	$2, 2, 1$	$2, 2, 1$
	$l = 1$	$l = 1$	$l = 1$
	$j = \frac{3}{2}$	$j = \frac{3}{2}$	$j = \frac{3}{2}$

$$W = W + \frac{1.1432 \times 10^{-18}}{8} \left(\frac{1}{2} - \frac{1}{8} \right)$$

$$W = W - 0.1785 \times 10^{-18}$$

$$T = - \frac{W}{hc} = \frac{1.1785 \times 10^{-18}}{1.986 \times 10^{-16}} = A + .05904 \text{ cm}^{-1}$$

$$\begin{array}{l|l}
 n = 3 \\
 3, {}^2S_{1/2} \quad l = 0 \\
 j = \frac{1}{2}
 \end{array}
 \quad
 \begin{aligned}
 W &= - \frac{2.1527 \times 10^{-11}}{9} + \frac{1.1426 \times 10^{-15}}{27} \left(\frac{1}{4} - 1 \right) \\
 &= - 2.3919 \times 10^{-12} - 3.1739 \times 10^{-17} \\
 T &= - \frac{G - 3.1739 \times 10^{-17}}{hc} = B + .16170 \text{ cm}^{-1}
 \end{aligned}$$

also

$$\begin{array}{l|l}
 n = 3 \\
 3, {}^2P_{1/2} \quad l = 1 \\
 j = \frac{1}{2}
 \end{array}
 \quad
 \begin{aligned}
 \text{where } G &= - 2.3919 \times 10^{-12} \\
 B &= - \frac{G}{hc}
 \end{aligned}$$

$$\begin{array}{l|l}
 n = 3 \\
 3, {}^2D_{3/2} \quad l = 1 \\
 j = \frac{3}{2}
 \end{array}
 \quad
 \begin{aligned}
 W &= G + \frac{1.1426 \times 10^{-15}}{27} \left(\frac{1}{4} - \frac{1}{2} \right) \\
 &= G - 1.0580 \times 10^{-17} \\
 T &= - \frac{G - 1.058 \times 10^{-17}}{hc} = B + .053902 \text{ cm}^{-1}
 \end{aligned}$$

also

$$\begin{array}{l|l}
 n = 3 \\
 3, {}^2P_{3/2} \quad l = 2 \\
 j = \frac{3}{2}
 \end{array}
 \quad
 \begin{aligned}
 T &= - \frac{G - 1.058 \times 10^{-17}}{hc} = B + .053902 \text{ cm}^{-1}
 \end{aligned}$$

$$\begin{array}{l|l}
 n = 3 \\
 3, {}^2D_{5/2} \quad l = 2 \\
 j = \frac{5}{2}
 \end{array}
 \quad
 \begin{aligned}
 W &= G + \frac{1.1426 \times 10^{-15}}{27} \left(\frac{1}{4} - \frac{1}{3} \right) \\
 &= G - .35265 \times 10^{-17} \\
 T &= - \frac{G - .35265 \times 10^{-17}}{hc} = B + .017967 \text{ cm}^{-1}
 \end{aligned}$$

These values of T are listed in table I, page 23.

The selection rule governing the possible transitions of an electron from energy state to another is that j can change only by 1 or 0, and any violation of this rule is attributed to the presence of external electric or magnetic fields¹. The total quantum number n can change by any integral value.

¹ White, Introduction to Atomic Spectra, pp149-170; 401-417.

The total quantum number n can change by any integral value. The selection rule governing the possible transitions of an electron from energy state to another is that Δn can change only by 1 or 0, and any violation of this rule is attributed to the presence of external electric or magnetic fields.

The selection rule governing the possible transitions of an electron from energy state to another is that Δn can change only by 1 or 0, and any violation of this rule is attributed to the presence of external electric or magnetic fields.

These values of T are listed in table I, page 170.

$$T = \frac{e - 1.1426 \times 10^{-17}}{hc} = B + .01787 \text{ cm}^{-1}$$

$$= 0 - .7528 \times 10^{-17}$$

$$W = G + \frac{1.1426 \times 10^{-15}}{24} \left(\frac{1}{4} - \frac{1}{2} \right)$$

$$T = \frac{e - 1.058 \times 10^{-17}}{hc} = B + .002902 \text{ cm}^{-1}$$

$$= 0 - 1.058 \times 10^{-17}$$

$$W = G + \frac{1.1426 \times 10^{-15}}{24} \left(\frac{1}{4} - \frac{1}{2} \right)$$

$$T = \frac{e - 3.1732 \times 10^{-17}}{hc} = B + .1619 \text{ cm}^{-1}$$

$$= 0 - 3.3319 \times 10^{-15} - 3.1732 \times 10^{-17}$$

$$W = \frac{2.1527 \times 10^{-17}}{24} + \frac{1.1426 \times 10^{-15}}{24} \left(\frac{1}{4} - \frac{1}{2} \right)$$

The possible transitions arising from the selection rules are represented schematically in figure 2, page 24. It is to be remembered that energy levels ($3,^2D_{3/2}$ and $3,^2P_{3/2}$), ($3,^2P_{1/2}$ and $3,^2S_{1/2}$) and ($2,^2P_{1/2}$ and $2,^2S_{1/2}$) coincide. Thus five lines are given, representing the fine structure of $H\alpha$.

Figure 2, page 24 also gives the separation between the lines and the relative intensities. The components are numbered in order of their descending intensity. The calculated frequencies are listed in table 1, page 23. In this table are also listed the relative intensities¹ of the permitted transitions as predicted by wave mechanics.

Line	Intensity	Freq. cm^{-1}	$\lambda, 10^{-3}\text{cm}^{-1}$
5	8/3	1.0972	183
4	456/75	1.0976	36
3	752/35	1.0980	320
2	35/9	1.2931	186
1	1088/45	1.4007	

¹ Sommerfeld and Unsold, Zeits. f. Phys., 36, 259 (1926).

Schrodinger, E., Ann. d. Phys., 80, 437 (1926).
38, 237 (1926).

Ruark, A. E., and Urey, H. C., Atoms, Molecules and Quanta.

The possible transitions arising from the selection rules are represented schematically in Figure 2, page 24. It is to be remembered that energy levels $(2, 2^2P_{1/2})$ and $(2, 2^2P_{3/2})$ are to be remembered that energy levels $(2, 2^2P_{1/2})$ and $(2, 2^2P_{3/2})$ coincide. Thus five lines are given, representing the fine structure of H α . Figure 3, page 24 also gives the separation between the lines and the relative intensities. The components are numbered in order of their descending intensity. The calculated frequencies are listed in Table I, page 23. In this table are also listed the relative intensities I of the permitted transitions as predicted by wave mechanics.

Mark, A. H., and Gray, H. C., Atomic Spectra and Quantum
 Schroedinger, E., Ann. d. Phys., 60, 407 (1926).
 Sommerfeld and Unsöld, At. Phys., 56, 229 (1926).

Line	Transitions	Freq. Differences cm^{-1}	$\nu \text{ cm}^{-1}$
5	$3, {}^2S_{1/2} - 2, {}^2P_{3/2}$	$A + .09094 - B - .16170(C - 1) + .92924$	
4	$3, {}^2D_{3/2} - 2, {}^2P_{3/2}$	$A + .09094 - B - .05390$	1.03704
1	$3, {}^2D_{5/2} - 2, {}^2P_{3/2}$	$A + .09094 - B - .01797$	1.07297
3	$3, {}^2P_{1/2} - 2, {}^2S_{1/2}$	$A + .45481 - B - .16170$	1.29311
	$3, {}^2S_{1/2} - 2, {}^2P_{1/2}$	" "	"
2	$3, {}^2D_{3/2} - 2, {}^2P_{1/2}$	$A + .45481 - B - .05390$	1.40091
	$3, {}^2P_{3/2} - 2, {}^2S_{1/2}$	" "	"

Line	Intensity	Freq. cm^{-1}	$\Delta\nu \cdot 10^{-3} \text{cm}^{-1}$
5	2/3	.9292	108
4	256/75	1.0370	
1	768/25	1.0730	36
3	35/9	1.2931	220
2	1088/45	1.4009	108

TABLE I

Line	Transitions	Freq. Difference cm ⁻¹	ν cm ⁻¹
5	$3.2_{21}/2-2, 2_{22}/2$	A + .09094 - B - .16170 (E - 1) + .92324	1.03704
4	$3.2_{02}/2-2, 2_{22}/2$	A + .09094 - B - .05330	1.03704
1	$3.2_{02}/2-2, 2_{22}/2$	A + .09094 - B - .01737	1.03704
3	$3.2_{21}/2-2, 2_{21}/2$	A + .45481 - B - .16170	1.40081
	$3.2_{21}/2-2, 2_{21}/2$	"	"
2	$3.2_{22}/2-2, 2_{21}/2$	A + .45481 - B - .05330	1.40081
	$3.2_{22}/2-2, 2_{21}/2$	"	"

Line	Intensity	Freq. cm ⁻¹	$\Delta \nu_{10-3} \text{ cm}^{-1}$
5	2/2	.9232	103
4	222/22	1.0370	30
1	222/22	1.0730	230
3	22/2	1.3231	103
2	1022/22	1.4008	

TABLE I

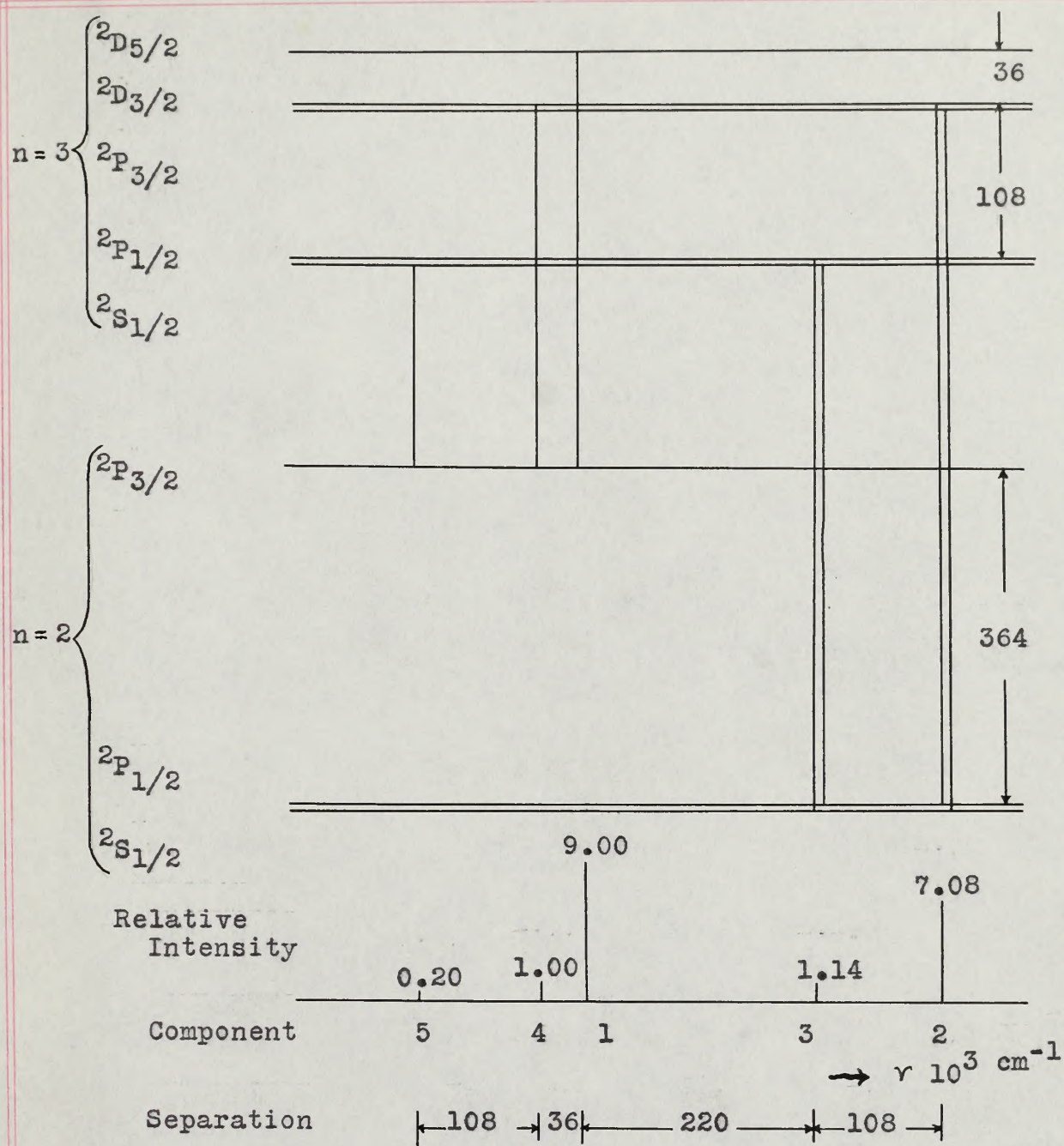


Figure 2

THEORETICAL FINE STRUCTURE OF H-ALPHA

80. V

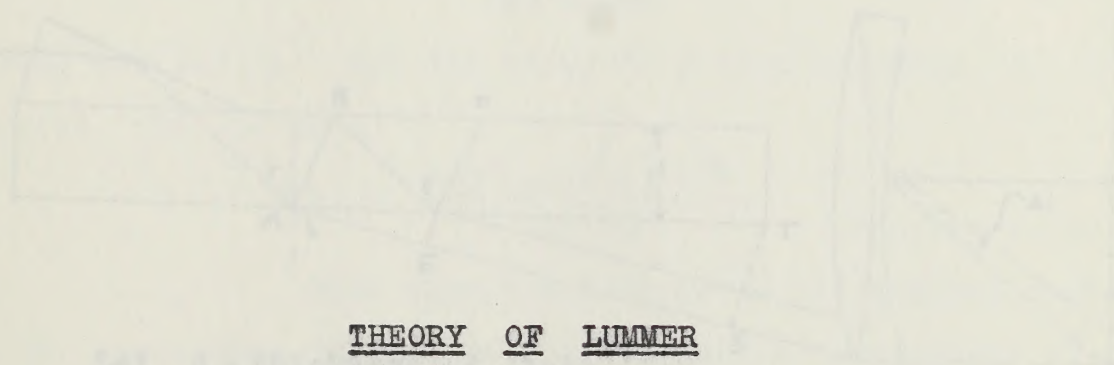
224

SEPARATION BETWEEN CROWN

Consider the following diagram in which a ray of light of wavelength λ passes through a Lummer plate.

FORMATION OF FRINGES

FIG. 3



THEORY OF LUMMER PLATES

λ = wavelength of light

μ = refractive index of the plate

t = thickness of the plate

i = angle between normal to the plate and the incident ray

r = angle between normal to the plate and the reflected ray within the plate

The condition for the reinforcement of the rays is

$$2\mu t \cos r = n\lambda \quad \text{--- (1)}$$

$$\text{or } 2\mu t \cos r = n\lambda \quad \text{--- (2)}$$

From trigonometry $\cos r = \sqrt{1 - \sin^2 r} / \mu$ since $\sin i = \mu \sin r$

$$\text{then } 2\mu t \sqrt{1 - \sin^2 r} = n\lambda \quad \text{--- (3)}$$

Squaring both sides we have

$$4\mu^2 t^2 (1 - \sin^2 r) = n^2 \lambda^2 \quad \text{--- (4)}$$

Differentiating this equation with i and n as variables we have

$$2\mu^2 t^2 (-2\sin r \cos r) di = n^2 \lambda^2 \frac{dn}{n} \quad \text{--- (5)}$$

RECEIVED TO YACHT

RECEIVED

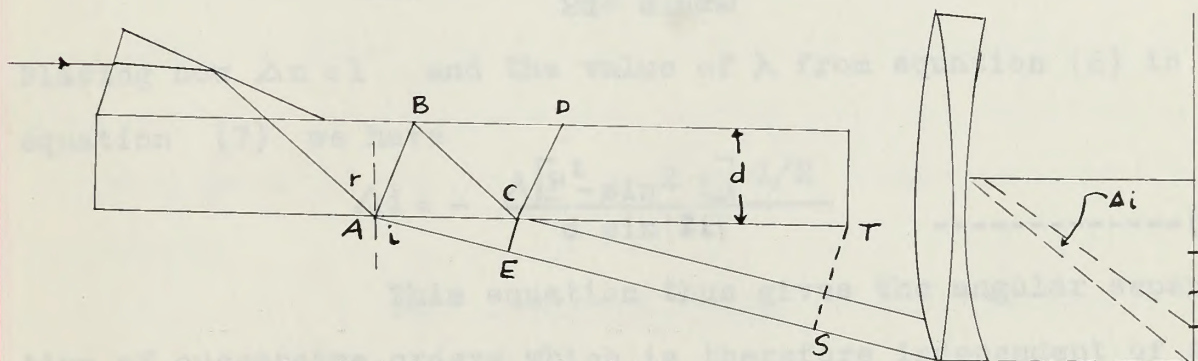
RECEIVED
© 1950-1951
RECEIVED

SEPARATION BETWEEN ORDERS

Consider the following diagram in which a ray of light of wavelength λ passes through a Lummer plate.

FORMATION OF FRINGES

FIG. 3



Let d = thickness of plate

μ = refractive index for wavelength λ

s = path difference = $n\lambda$

n = Order number for wavelength λ

i = angle between normal to the plate and the emergent ray

r = angle between normal to the plate and the ray within the plate

The condition for the reinforcement of the rays is

$$s = n\lambda = \mu (ABC) - AE$$

$$\text{or } n\lambda = 2d\mu \cos r \quad \text{-----(1)}$$

From trigonometry $\cos r = \sqrt{\mu^2 - \sin^2 i} / \mu$ since $\sin i = \mu \sin r$

$$\text{thus } n\lambda = 2d\sqrt{\mu^2 - \sin^2 i} \quad \text{-----(2)}$$

Squaring both sides we have

$$n^2 \lambda^2 = 4d^2 \mu^2 - 4d^2 \sin^2 i \quad \text{-----(3)}$$

Differentiating this equation with i and n as variables we have

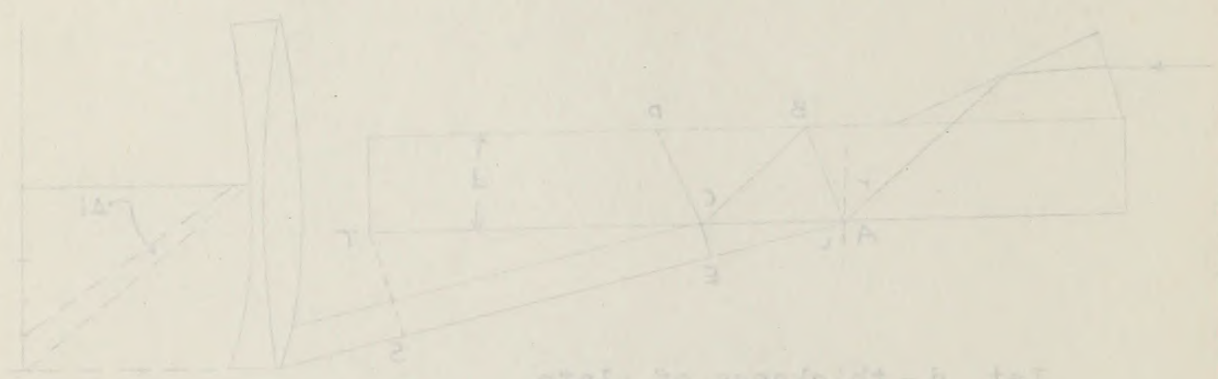
$$2n\lambda^2 \Delta n = -8d^2 \sin i \cos i \Delta i \quad \text{----(4)}$$

SEPARATION BETWEEN ORDERS

Consider the following diagram in which a ray of light of wavelength λ passes through a lamellar plate.

FORMATION OF RAYES

FIG. 2



Let d = thickness of plate

μ = relative index for wavelength λ

s = path difference = $n\lambda$

n = order number for wavelength λ

i = angle between normal to the plate and the

emergent ray

γ = angle between normal to the plate and the ray

within the plate

The condition for the reinforcement of the rays is

$$s = n\lambda = \mu (ABC) - \mu d$$

$$\mu d = \mu d \cos \gamma \quad \text{or} \quad \mu d = \mu d \cos \gamma \quad (1)$$

From trigonometry $\cos \gamma = \sqrt{1 - \sin^2 \gamma} / \mu$ since $\sin^2 \gamma = \mu^2 \sin^2 i$

$$\mu d = \mu d \sqrt{1 - \sin^2 \gamma} / \mu \quad \text{or} \quad \mu d = \mu d \sqrt{1 - \sin^2 \gamma} \quad (2)$$

Squaring both sides we have

$$\mu^2 d^2 = \mu^2 d^2 (1 - \sin^2 \gamma) \quad \text{or} \quad \mu^2 d^2 = \mu^2 d^2 - \mu^2 d^2 \sin^2 \gamma \quad (3)$$

Differentiating this equation with i and n as variables we have

$$2\mu d \sin \gamma = 2\mu d \sin \gamma \cos^2 \gamma \quad \text{or} \quad \sin \gamma = \cos^2 \gamma \quad (4)$$

From trigonometry $\frac{\sin 2i}{2} = \sin i \cos i$ -----(5)

Substituting equation (5) in (4) gives

$$n\lambda^2 \Delta n = -2d^2 \cdot \sin 2i \Delta i \text{ -----(6)}$$

and solving for Δi

$$\Delta i = - \frac{n\lambda^2}{2d^2 \sin(2i)} \cdot \Delta n \text{ -----(7)}$$

Placing now $\Delta n = 1$ and the value of λ from equation (2) in equation (7) we have

$$\Delta i = - \frac{\lambda [\mu^2 - \sin^2 i]^{1/2}}{d \sin(2i)} \text{ -----(8)}$$

This equation thus gives the angular separation of successive orders which is therefore independent of the length of the plate, directly proportional to the wavelength and inversely proportional to the thickness of the plate.

DISPERSION

If the equation (3) above is differentiated with respect to λ considering μ and i as variables, we have

$$n^2 \lambda = 4d^2 \mu \frac{\partial \mu}{\partial \lambda} - 2d^2 \sin 2i \frac{\partial i}{\partial \lambda} \text{ -----(9)}$$

Solving this equation for $\frac{\partial i}{\partial \lambda}$ results:

$$\frac{\partial i}{\partial \lambda} = \frac{4d^2 \mu \frac{\partial \mu}{\partial \lambda} - n^2 \lambda}{2d^2 \sin(2i)} \text{ -----(10)}$$

From trigonometry $\sin \theta = \frac{\Delta z}{\Delta}$ and $\cos \theta = \frac{\Delta x}{\Delta}$ (1)

Substituting equation (1) in (4) gives

$$n\lambda \Delta = 2d \sin \theta \quad \text{and} \quad \Delta x = \Delta \cos \theta \quad (2)$$

and solving for Δ

$$\Delta = \frac{n\lambda \Delta}{2d \sin \theta} \quad \text{and} \quad \Delta x = \Delta \cos \theta \quad (3)$$

Eliminating Δ in (3) and the value of λ from equation (2) is

$$\Delta x = \frac{n\lambda \Delta}{2d \sin \theta} \cos \theta \quad \text{and} \quad \Delta = \frac{2d \sin \theta}{n} \quad (4)$$

$$\Delta x = \frac{n\lambda}{2d \sin \theta} \cos \theta \quad \text{and} \quad \Delta = \frac{2d \sin \theta}{n} \quad (5)$$

This equation gives the angular separation of successive orders which is therefore the angular separation of the

length of the plate, directly proportional to the wavelength

and inversely proportional to the thickness of the plate.

Discussion

If the equation (3) above is differentiated

with respect to λ constant θ and d as variables, we have

$$\Delta x = \frac{n\lambda}{2d \sin \theta} \cos \theta \quad \text{and} \quad \Delta = \frac{2d \sin \theta}{n} \quad (6)$$

Solving this equation for Δ results

$$\Delta x = \frac{n\lambda}{2d \sin \theta} \cos \theta \quad \text{and} \quad \Delta = \frac{2d \sin \theta}{n} \quad (7)$$

$$\Delta x = \frac{n\lambda}{2d \sin \theta} \cos \theta \quad \text{and} \quad \Delta = \frac{2d \sin \theta}{n} \quad (8)$$

Substituting the value of $n^2 \lambda$ from equation (3) in (10)

$$\frac{\partial i}{\partial \lambda} = \frac{4d^2 \mu \frac{\partial \mu}{\partial \lambda} - \frac{4d^2 \mu^2 - 4d^2 \sin^2 i}{\lambda}}{2d^2 \sin 2i}$$

$$\frac{\partial i}{\partial \lambda} = \frac{2 \lambda \mu \frac{\partial \mu}{\partial \lambda} - 2(\mu^2 - \sin^2 i)}{\lambda \sin 2i} \text{ ----- (11)}$$

This equation shows that the dispersion is independent of the size and shape of the plate and depends entirely upon the optical properties of the glass, the angle of emergence, and the wavelength.

RESOLVING POWER

Setting Δi of equation (10) equal to the Δi of equation (8), the resulting value of $\Delta \lambda$ is then the range of the plate without overlap, that is to say $\Delta \lambda$ is the difference of wavelength which a line in any order must have so that it coincides with the image in the next order. We have thus

$$\Delta \lambda = \frac{n \lambda^2}{n^2 \lambda - 4d^2 \mu \frac{\partial \mu}{\partial \lambda}} \text{ ----- (12)}$$

Consider Fig. 3. The width of the beam or wave front ST entering the telescope is $AT \cos i = l \cos i$, l here is the length of the plate. Now the angle ∂i between the central maximum and the first minimum of a beam of this width is

$$\partial i = \frac{\lambda}{l \cos i} \text{ ----- (13)}$$

Substituting the value of $n_2 \Delta$ from equation (5) in (10)

$$\frac{\frac{2\lambda}{\Delta} - \frac{2\lambda}{\Delta} \sin^2 \theta}{\frac{2\lambda}{\Delta} \sin^2 \theta} = \frac{6}{\lambda}$$

$$\frac{2\lambda \left(\frac{1}{\Delta} - \sin^2 \theta \right)}{\lambda \sin^2 \theta} = \frac{6}{\lambda}$$

This equation shows that the dispersion is independent of the size and shape of the plate and depends entirely upon the optical properties of the glass, the angle of emergence, and the wavelength.

RESOLVING POWER

Let Δ be the value of Δ in equation (10) equal to the Δ of equation (5). The resolving power of Δ is then the ratio of the plate without overlap, that is to say Δ is the difference of wavelength which a line in any order may have and still be coincident with the image in the next order. We have then

$$\Delta \lambda = \frac{2\lambda}{\Delta} - \frac{2\lambda}{\Delta} \sin^2 \theta$$

Consider Fig. 2. The width of the beam of rays from the source entering the telescope is $2\lambda \sin \theta$. If λ is the length of the wave, then the angle θ between the central maximum and the first minimum of a beam of this width is

$$\theta = \frac{\lambda}{2\lambda \sin \theta}$$

Rearranging equation (11) we have

$$\delta i = - \frac{1}{\lambda \sin i \cos i} \left\{ \mu^2 - \sin^2 i - \lambda \mu \frac{\partial \mu}{\partial \lambda} \right\} \delta \lambda \text{-----} (14)$$

If we make now $\delta i = \frac{\lambda}{l \cos i}$, the corresponding $\delta \lambda$ will be then the smallest wavelength change resolvable.

Solving for $\frac{\lambda}{\delta \lambda}$ the resolving power, we get

$$\frac{\lambda}{\delta \lambda} = \frac{1}{\lambda \sin i} \left\{ \mu^2 - \sin^2 i - \lambda \mu \frac{\partial \mu}{\partial \lambda} \right\} \text{-----} (15)$$

This value of the resolving power, however, is only strictly correct at grazing emergence since $\delta i = \frac{\lambda}{l \cos i}$ only when the amplitude is uniform over the wavefront ST. To obtain a close approximation to the limit of resolving power we write $\sin i = 1$, whence:-

$\frac{\lambda}{\delta \lambda} \approx \frac{l}{\lambda} (\mu^2 - 1)$ Roughly then the resolving power lies between 1.4 times and twice the metrical length of the plate measured in wavelengths. The dispersion factor term which involves $\frac{\partial \mu}{\partial \lambda}$ only makes a correction of the order of 5 to 10 per cent.

Rearranging equation (11) we have

$$\delta t = - \frac{1}{\lambda \sin i} \left\{ \frac{4b}{\lambda} \sin^2 i - \frac{4b}{\lambda} \sin^2 i - \frac{4b}{\lambda} \sin^2 i \right\} \quad (14)$$

If we make now $\delta t = 0$, the corresponding λ will be then the smallest wavelength change resolvable.

Solving for $\frac{\lambda}{\lambda}$ the resolving power, we get

$$\frac{\lambda}{\lambda} = \frac{1}{\lambda \sin i} \left\{ \frac{4b}{\lambda} \sin^2 i - \frac{4b}{\lambda} \sin^2 i - \frac{4b}{\lambda} \sin^2 i \right\} \quad (15)$$

This value of the resolving power, however, is

$$\frac{\lambda}{\lambda} = \frac{1}{\lambda \sin i} \quad \text{only strictly correct at grazing incidence since } \delta t = 0$$

only when the amplitude is uniform over the aperture. To obtain a close approximation to the limit of resolving power

we write $\sin i = 1$, whence

$$\frac{\lambda}{\lambda} = \frac{2}{\lambda} (1 - 1) \quad \text{Roughly then the re-}$$

solving power lies between 1.4 times and twice the reciprocal length of the plate measured in wavelengths. The dispersion factor term which involves $\frac{4b}{\lambda}$ only makes a correction of the order of 5 to 10 per cent.

THEORY OF TWO LUMMER PLATES IN TANDEM

In Figure 1 a ray of light of wavelength λ enters

TABLE II

RESOLVING POWERS OF THE LUMMER PLATES

Plate	Resolving Power $\lambda/\delta\lambda$
Smallest	254,000
Medium	492,800
Largest	702,000

FIGURE 1

RAY OF LIGHT THROUGH FIRST LUMMER PLATE

Let d = thickness of plate

n = refractive index for wavelength λ

s = path difference = $n\lambda$

m = order number for wavelength λ

The condition for reinforcement of the beams is

$$s = m\lambda = 2d(n-1) \quad (1)$$

TABLE II

RESOLVING POWER OF THE HUMAN EYE

Plate	Resolving Power/λ
Smallest	234,000
Medium	192,800
Largest	102,000

THEORY OF TWO LUMMER PLATES IN TANDEM

In figure 4 a ray of light of wavelength λ upon entering the Lummer plate through the prism will undergo a series of internal reflections within the plate at points A, B, C, D etc. At these points a portion of the light will be refracted giving rise to two groups of parallel beams 1, 2, ---n, one on each side of the Lummer plate. These successive emergent parallel beams can be brought to a focus by an objective and if in phase will reinforce to produce bright fringes.

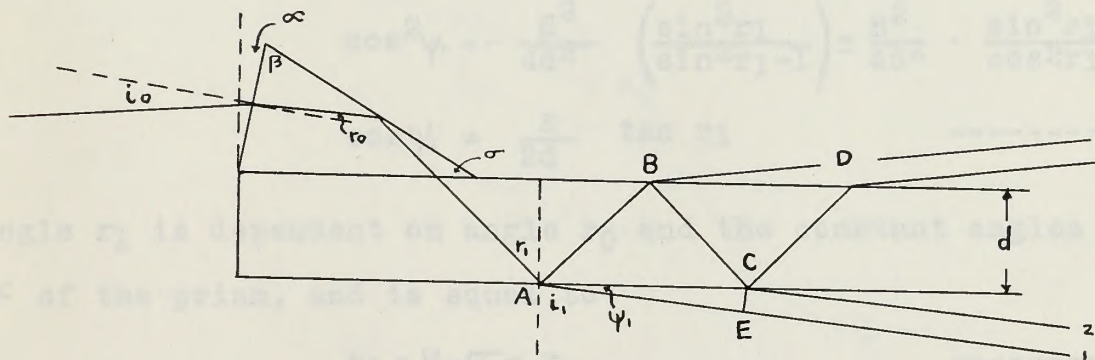


Figure 4

RAY OF LIGHT THROUGH FIRST LUMMER PLATE

Let d = thickness of plate

μ = refractive index for wavelength λ

s = path difference = $n\lambda$

n = order number for wavelength λ

The condition for reinforcement of the beams is

$$S = n\lambda = \mu (ABC) - AE \quad \text{-----(1)}$$

THEORY OF TWO LAMINAR PLATES IN TUNNEL

In figure 1 a ray of light of wavelength λ upon entering the laminar plate through the prism will undergo a series of internal reflections within the plate at points A, B, C, D etc. At these points a portion of the light will be reflected giving rise to two groups of parallel beams I, II, III, etc. on each side of the laminar plate. These successive emergent parallel beams can be brought to a focus by an objective and if in phase will reinforce to produce bright fringes.

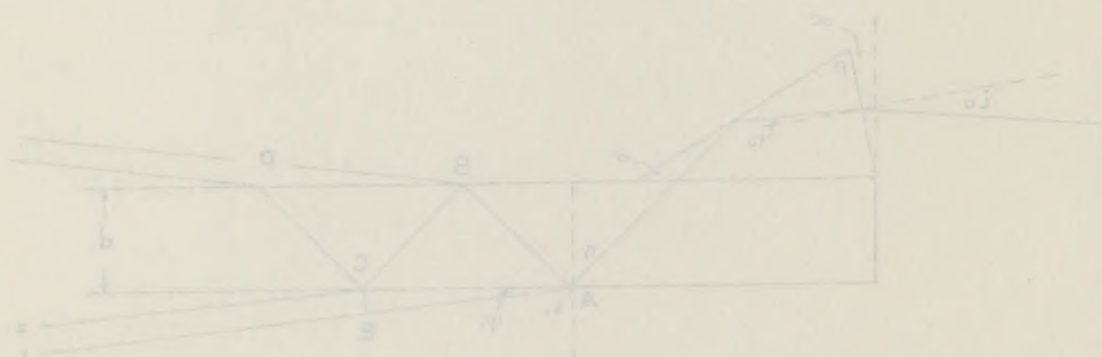


Figure 1

RAY OF LIGHT THROUGH FIRST LAMINAR PLATE

Let d = thickness of plate
 μ = refractive index for wavelength λ
 s = path difference = $n\lambda$
 n = order number for wavelength λ

The condition for reinforcement of the beams is

$$s = n\lambda = \mu(ABD) - AD \quad (1)$$

or

$$S = 2d\mu \cos r_1$$

From trigonometry $\cos r_1 = \sqrt{\mu^2 - \sin^2 i_1} / \mu$ since $\sin i_1 = \mu \sin r_1$

thus

$$S = 2d\sqrt{\mu^2 - \sin^2 i_1}$$

Let ψ_1 be the angle of emergence of the parallel beams, then

$$S = 2d\sqrt{\mu^2 - \cos^2 \psi_1}$$

Squaring both sides and solving for $\cos \psi_1$, we have

$$\cos \psi_1 = \sqrt{\mu^2 - S^2/4d^2}$$

Now

$$\mu^2 = \frac{\sin^2 i_1}{\sin^2 r_1} = \frac{\cos^2 \psi_1}{\sin^2 r_1}$$

hence

$$\cos^2 \psi_1 = -\frac{S^2}{4d^2} + \frac{\cos^2 \psi_1}{\sin^2 r_1}$$

$$\cos^2 \psi_1 = -\frac{S^2}{4d^2} \left(\frac{\sin^2 r_1}{\sin^2 r_1 - 1} \right) = \frac{S^2}{4d^2} \cdot \frac{\sin^2 r_1}{\cos^2 r_1}$$

$$\cos \psi_1 = \frac{S}{2d} \tan r_1 \quad \text{-----(2)}$$

Angle r_1 is dependent on angle r_0 and the constant angles β and σ of the prism, and is equal to

$$r_1 = \beta - \sigma - r_0 \quad \text{-----(3)}$$

thus

$$\cos \psi_1 = \frac{S}{2d} \tan (\beta - \sigma - r_0) \quad \text{-----(4)}$$

In figure 5 let

θ = the angle between the Lummer plates

i_2 = angle of incidence of the parallel rays upon
the prism of the second plate

ψ_3 = angle of emergence of rays from plate

d' = thickness of plate

d' = thickness of plate
 ψ = angle of emergence of ray from plate
 the prism of the second plate
 i_2 = angle of incidence of the parallel rays upon
 θ = the angle between the Lummer plates

In figure 3 let

thus

$$\cos \psi = \frac{2}{2d} \tan (\theta - \alpha)$$

----- (4)

$$r_1 = \theta - \alpha$$

----- (3)

α of the prism, and is equal to

Angle r_1 is dependent on angle r_0 and the constant angles θ and

$$\cos \psi = \frac{2}{2d} \tan r_1$$

----- (2)

$$\cos \psi = -\frac{2}{4d} \left(\frac{\sin^2 r_1}{\sin^2 r_1 - 1} \right) = \frac{2}{4d} \cdot \frac{\sin^2 r_1}{\cos^2 r_1}$$

hence

$$\cos \psi = -\frac{2}{4d} + \frac{2}{4d} \frac{\cos^2 \psi}{\sin^2 r_1}$$

Now

$$4d = \frac{\sin^2 r_1}{\cos^2 \psi} = \frac{\sin^2 r_1}{\cos^2 \psi}$$

$$\cos \psi = \frac{\sqrt{4d^2 - \sin^2 r_1}}{2\sqrt{4d^2 - \sin^2 r_1}}$$

Squaring both sides and solving for $\cos \psi$, we have

$$2 = 2d\sqrt{4d^2 - \cos^2 \psi}$$

Let ψ be the angle of emergence of the parallel beams, then

$$2 = 2d\sqrt{4d^2 - \sin^2 r_1}$$

thus

$$\text{From trigonometry } \cos r_1 = \sqrt{4d^2 - \sin^2 r_1} \text{ since } \sin r_1 = \psi \text{ and}$$

or

$$2 = 2d \cos r_1$$

$\mu' =$ index of refraction of glass for wavelength λ .

The angle of incidence i_2 is dependent on ψ_1 , θ and α' . From the figure below

$$i_2 = \theta + \alpha' - \psi_1 \quad \text{and} \quad \psi_1 = \theta + \alpha' - i_2 \quad \text{-----(5)}$$

Substituting this value of ψ_1 in equation 4, we have

$$\cos(\theta + \alpha' - i_2) = \frac{S}{2d} \tan(\beta\sigma - r_0) \quad \text{-----(6)}$$

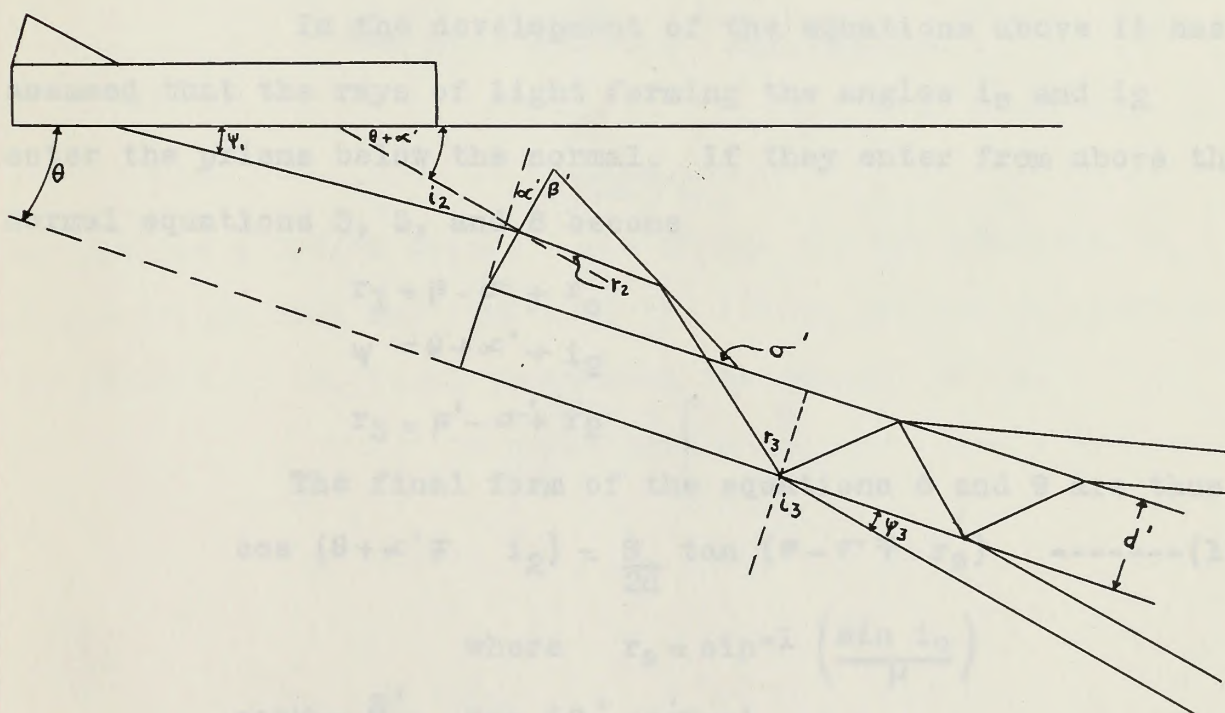


Figure 5

RAY OF LIGHT THROUGH SECOND LUMBER PLATE

A treatment of the second plate as the first leads to equations similar to 2, 3 and 4 namely

$$\cos \psi_3 = \frac{S'}{2d'} \tan r_3 \quad \text{-----(7)}$$

$$r_3 = \beta' - \sigma' - r_2 \quad \text{-----(8)}$$

$$\cos \psi_3 = \frac{S'}{2d'} \tan(\beta' - \sigma' - r_2) \quad \text{-----(9)}$$

$\mu =$ index of refraction of glass for wavelength λ .

The angle of incidence i_2 is dependent only on θ and α . From

the figure below

$$i_2 = \theta + \alpha - \psi_1 \quad \text{and} \quad \psi_1 = \theta + \alpha - i_2 \quad \text{----- (2)}$$

Substituting this value of ψ_1 in equation 4, we have

$$\cos(\theta + \alpha - i_2) = \frac{\mu}{\mu_0} \tan(\theta - i_2) \quad \text{----- (3)}$$

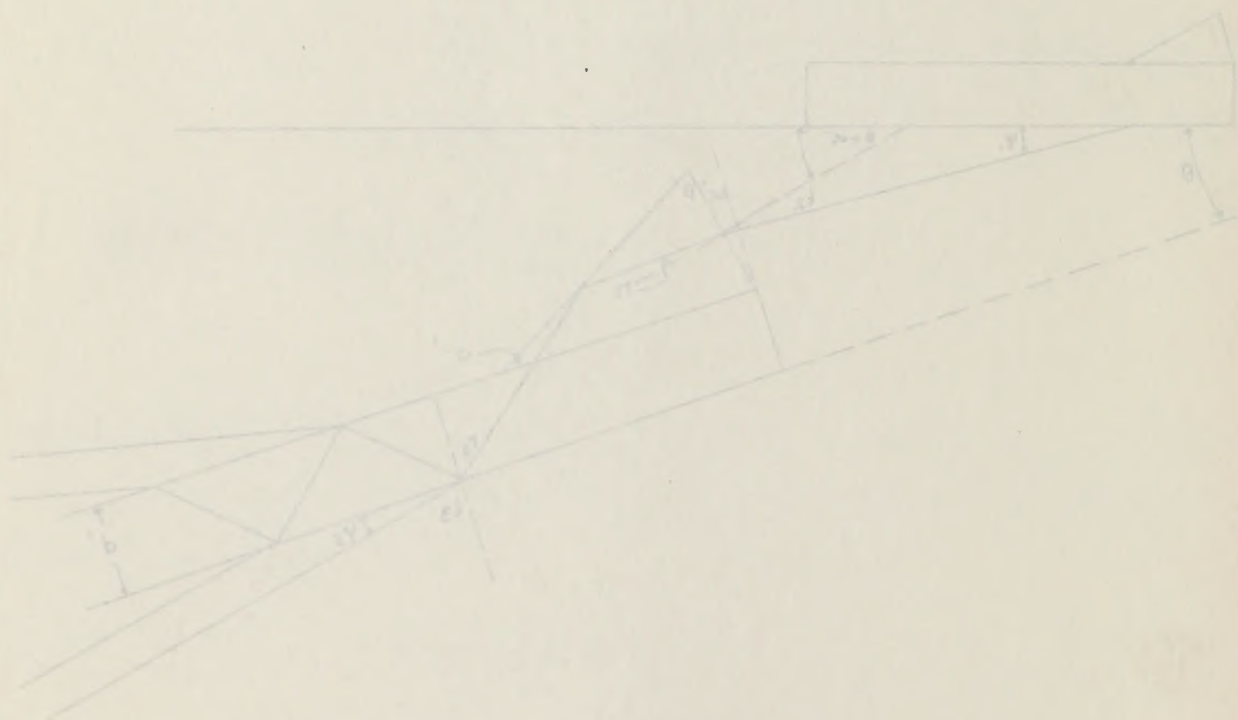


Figure 2

RAY OF LIGHT THROUGH SECOND PLATE

A treatment of the second plate as the first leads

to equations similar to 2, 3 and 4 namely

$$\cos \psi_2 = \frac{\mu_1}{\mu_2} \tan r_2 \quad \text{----- (4)}$$

$$i_2 = \theta - \alpha - i_1 \quad \text{----- (5)}$$

$$\cos \psi_2 = \frac{\mu_1}{\mu_2} \tan(\theta - \alpha - i_1) \quad \text{----- (6)}$$

Given now the angle of incidence i_0 , the angle of refraction r_0 can be found from the relation $\sin r_0 = (\mu - 1) \sin i_0$. Equation 6 will then lead to values of i_2 , angles of incidence on the second plate, for different values of the order number n . From these values of i_2 , the angles of r_2 can be found from the relation $\sin r_2 = (\mu' - 1) \sin i_2$ and finally values of ψ_3 are calculated by equation 9 for the different values of n' .

In the development of the equations above it has been assumed that the rays of light forming the angles i_0 and i_2 enter the prisms below the normal. If they enter from above the normal equations 3, 5, and 8 become

$$r_1 = \beta - \sigma + r_0$$

$$\psi = \theta + \alpha' + i_2$$

$$r_3 = \beta' - \sigma' + r_2$$

The final form of the equations 6 and 9 are thus:-

$$\cos (\theta + \alpha' \mp i_2) = \frac{S}{2d} \tan (\beta - \sigma \mp r_0) \quad \text{-----(10)}$$

$$\text{where } r_0 = \sin^{-1} \left(\frac{\sin i_0}{\mu} \right)$$

$$\cos \psi_3 = \frac{S'}{2d'} \tan (\beta' - \sigma' \mp r_2)$$

$$\text{where } r_2 = \sin^{-1} \left(\frac{\sin i_2}{\mu'} \right) \quad \text{-----(11)}$$

Minus signs are to be taken when the rays of light enter the prisms from below the normal and plus signs when the rays enter from above.

If the successive emergent beams for a given value

Given now the angle of incidence i_0 , the angle of reflection r_0 can be found from the relation $\sin r_0 = (\mu - 1) \sin i_0$. Equation 2 will then lead to values of i_2 , angles of incidence on the second plate, for different values of the order number m . From these values of i_2 , the angles of r_2 can be found from the relation $\sin r_2 = (\mu - 1) \sin i_2$ and finally values of r_2 are related to i_2 by equation 2 for the different values of m .

In the development of the equations above it has been assumed that the rays of light entering the angles i_0 and i_2 enter the prism below the normal. If they enter from above the normal equations 1, 2, and 3 become

$$\begin{aligned} i_1 &= \mu - i_0 + r_0 \\ r_1 &= \mu - i_1 + i_2 \\ i_2 &= \mu - i_2 + r_2 \end{aligned}$$

The final form of the equations 1 and 2 are found

$$\cos (i_0 + r_0) = \frac{1}{\mu} \cos (i_2 + r_2) \quad \text{where } i_2 = \sin^{-1} \left(\frac{\sin i_0}{\mu} \right) \quad (10)$$

$$\cos \mu r_0 = \frac{1}{\mu} \cos \mu r_2 \quad \text{where } i_2 = \sin^{-1} \left(\frac{\sin i_0}{\mu} \right) \quad (11)$$

minus signs are to be used when the rays of light enter the prism above the normal and plus signs when they enter from above.

If the successive emergent beams for a given value

of Ψ_3 , which are parallel, are brought to a common focus by an objective at a point P on the focal plane they will reinforce

POSITION OF FRINGES

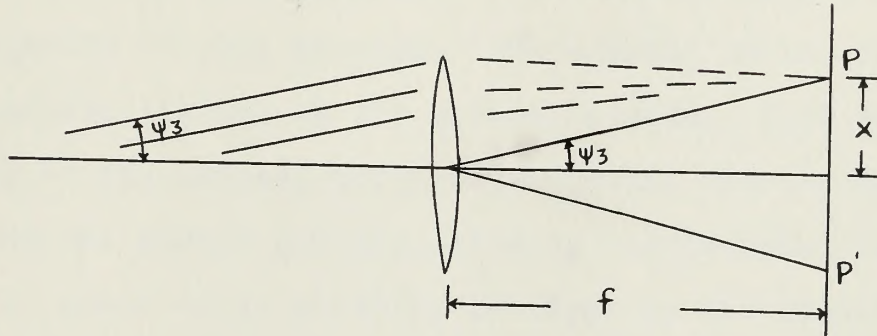


Figure 6

and produce a bright fringe. See figure 6. The distance, x , of the fringe from the center of the fringe pattern is equal to the product of the focal length and the tangent of Ψ_3 .

$$x = f \times \tan \Psi_3$$

of ψ , which are parallel, are brought to a common focus by an objective at a point F on the focal plane they will reinforce

POSITION OF FRINGES

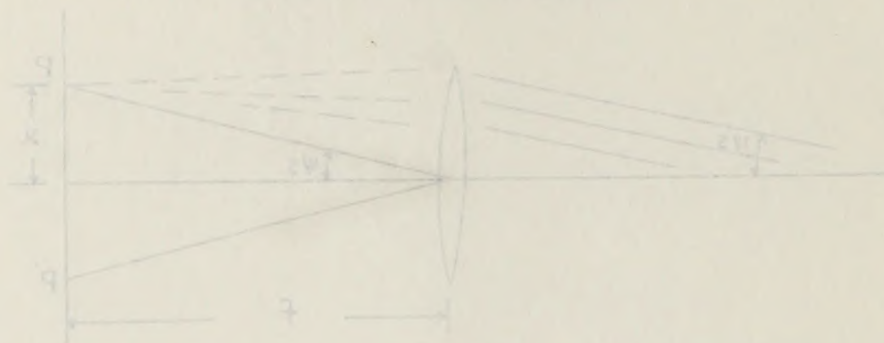


Figure 6

and produce a bright fringe. See Figure 6. The distance, x , of the fringe from the center of the fringe pattern is equal to the product of the focal length and the tangent of ψ .

$$x = f \cdot \tan \psi$$

STATEMENT OF APPARATUS

The apparatus used in this research was essentially the same as that used by Dr. W. H. Rabinowitz¹ in his preliminary investigation of this problem. The changes in the apparatus were centered largely on the optical system. This entailed the removing of the lens, mirror and optical shutter that were between the two burner plates, allowing the emergent light from the first plate to be directly incident on the second plate. With less absorption of the light present, the intensity of the spectrum was increased enough so, that the structure of the pattern system obtained could be studied visually more readily and exposure times were reduced. A complete description of the optical system is given on page 37.

DESCRIPTION OF APPARATUS

RADIATION SOURCE

A discharge tube was connected through a liquid-air trap to a McLeod gauge by means of which the pressure in the tube could be accurately measured. A Lyric pump also connected to the discharge tube served as a means of controlling and maintaining the pressure at any desired value. A milliammeter in series with the tube served to measure the current. With suitable values of pressure and current it was found that the intensity of the secondary spectrum due to the molecular hydrogen could be made to be relatively weak with respect to the Balmer lines produced by the atomic hydrogen. Hydrogen was produced by electrolysis and collected in a reservoir which was connected to the tube through a double stopcock; thus admitting small quan-

¹ Rabinowitz, W. H., Ph.D. Thesis, 1937, Princeton University.

² The present apparatus was designed and constructed by Dr. W. H. Rabinowitz, Princeton University. It is a modification of the apparatus used by Dr. W. H. Rabinowitz in his preliminary investigation of this problem. The changes in the apparatus were centered largely on the optical system. This entailed the removing of the lens, mirror and optical shutter that were between the two burner plates, allowing the emergent light from the first plate to be directly incident on the second plate. With less absorption of the light present, the intensity of the spectrum was increased enough so, that the structure of the pattern system obtained could be studied visually more readily and exposure times were reduced. A complete description of the optical system is given on page 37.

DESCRIPTION OF APPARATUS

CHANGES IN APPARATUS

The apparatus used in this research was essentially the same as that used by Dr. W. H. Robinson¹ in his preliminary investigation of this problem. The changes in the apparatus were centered largely on the optical system. This entailed the removing of the lenses, mirror and special shutter that were between the two Lummer plates, allowing the emergent light from the first plate to be directly incident on the second plate. With less absorption of the light present, the intensity of the spectrum was increased enough so, that the structure of the pattern system obtained could be studied visually more readily and exposure times somewhat reduced. A complete description of the optical system is given on page 39.

RADIATION SOURCE

A discharge tube was connected through a liquid-air trap to a McCleod gauge by means of which the pressures in the tube could be accurately measured. A Hyvac pump also connected to the discharged tube served as a means of controlling and maintaining the pressure at any desired value. A milliammeter in series with the tube served to measure the current. With suitable values of pressure and current it was found that the intensity of the secondary spectrum due to the molecular hydrogen could be made to be relatively weak with respect to the Balmer lines produced by the atomic hydrogen.* Hydrogen was produced by electrolysis and collected in a reservoir which was connected to the tube through a double stopcock; thus admitting small quan-

¹ Robinson, W. H., PhD. Thesis, 1937, Boston Univ. Grad. School

* The atomic spectrum forming the regular atomic series may of course be given by atoms which are still components of the molecule. Only at high temperatures would there exist a preponderance of atomic hydrogen.

CHANGES IN APPARATUS

The apparatus used in this research was essentially the same as that used by Dr. W. H. Robinson in his preliminary investigation of this problem. The changes in the apparatus were centered largely on the optical system. This entailed the removing of the lenses, mirror and special shutter that were between the two Lummer plates, allowing the emergent light from the first plate to be directly incident on the second plate. With less absorption of the light present, the intensity of the spectrum was increased enough so that the structure of the pattern system obtained could be studied visually more readily and exposure times somewhat reduced. A complete description of the optical system is given on page 34.

RADIATION SOURCE

A discharge tube was connected through a lightly air trap to a McLeod gauge by means of which the pressures in the tube could be accurately measured. A Hyvac pump also connected to the discharged tube served as a means of controlling and maintaining the pressure at any desired value. A millimeter in series with the tube served to measure the current. With suitable values of pressure and current it was found that the intensity of the secondary spectrum due to the molecular hydrogen could be made to be relatively weak with respect to the Balmer lines produced by the atomic hydrogen. Hydrogen was produced by electrolysis and collected in a reservoir which was connected to the tube through a double stopcock; thus admitting small quan-

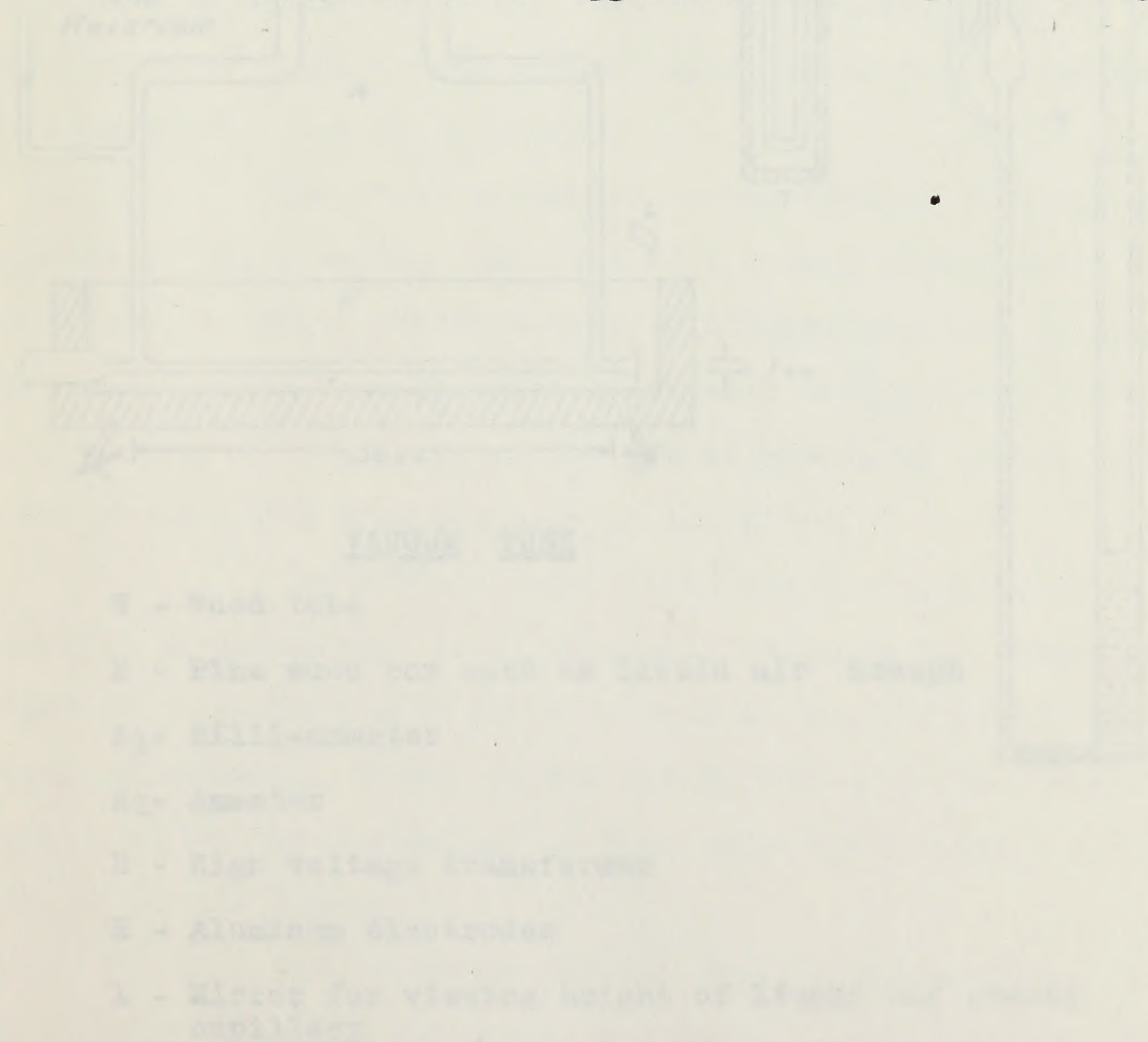
Dr. W. H. Robinson, 1937, Boston Univ. Grad. School
The atomic spectrum forming the regular series may be given by lines which are still components of the series. Only a few lines are visible in the spectrum of atomic hydrogen.

ties of the gas to the tube at will.

The source of radiation was a liquid-air cooled Wood² tube of pyrex glass 36cm long and 0.8 cm internal diameter. A wooden pine box coated with glyptol served as a trough for the liquid-air.

The source of excitation was a 30,000 volt transformer with a variable resistance in series with the primary.

A sketch of the apparatus used is given in Fig. 7.



² Wood, R. W. , Proc. Roy. Soc. London, A 97, 455 (1920)

Effect of the gas to the rate of will.

The source of radiation was a liquid-air cooled

wood tube of pyrex glass 30 cm long and 2 cm internal diameter.

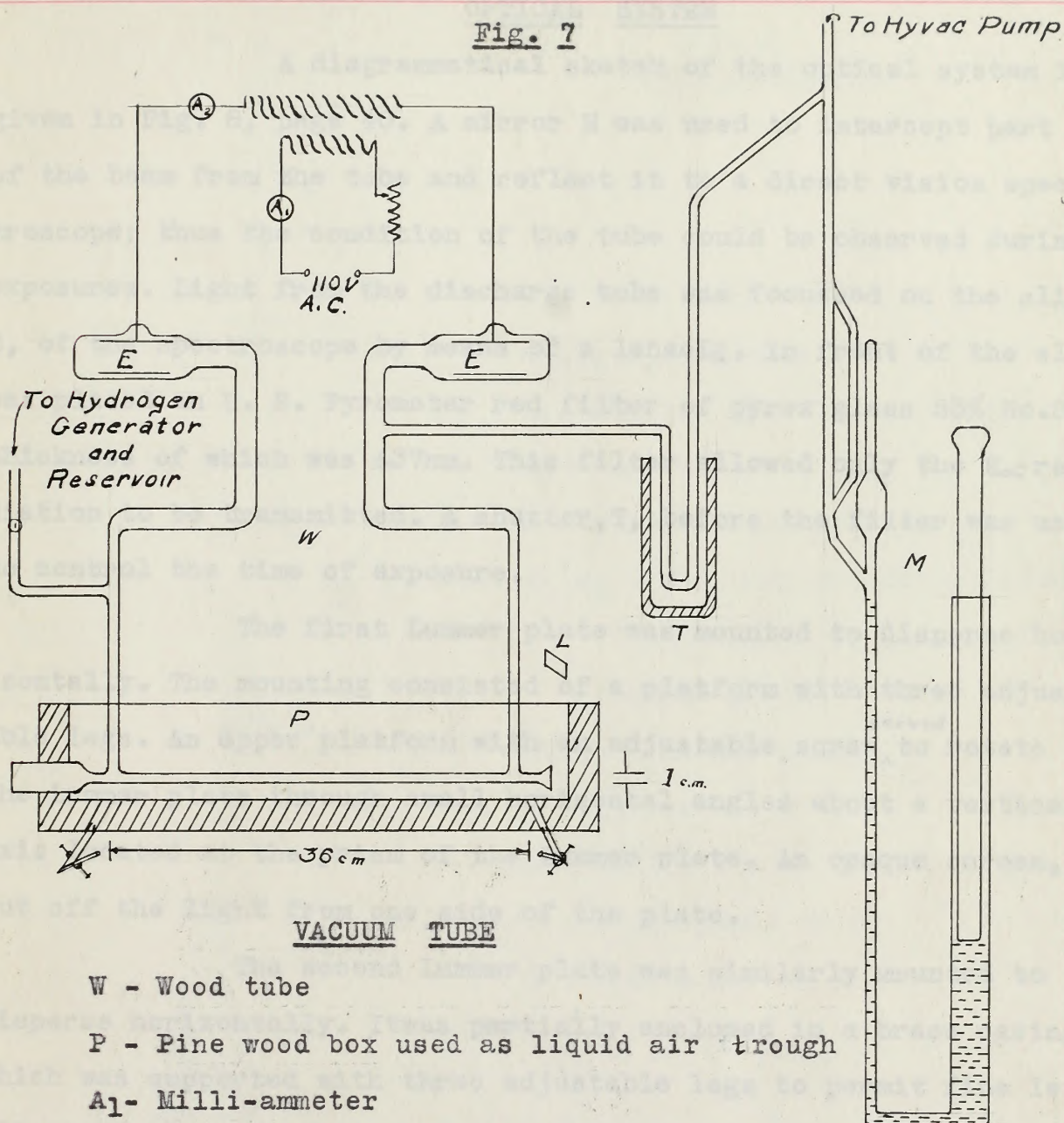
A wooden pine box coated with glycerol served as a trough for the

liquid-air.

The source of excitation was a 30,000 volt trans-

former with a variable resistance in series with the primary.

A sketch of the apparatus used is given in fig. 7.

Fig. 7VACUUM TUBE

W - Wood tube

P - Pine wood box used as liquid air trough

A₁ - Milli-ammeterA₂ - Ammeter

B - High voltage transformer

E - Aluminum electrodes

L - Mirror for viewing height of liquid air around capillary

T - Liquid-air cooled Hg trap

M - McLeod Gauge

OPTICAL SYSTEM

A diagrammatical sketch of the optical system is given in Fig. 8, page 40. A mirror M was used to intercept part of the beam from the tube and reflect it to a direct vision spectroscopy; thus the condition of the tube could be observed during exposures. Light from the discharge tube was focussed on the slit S, of the spectroscopy by means of a lens L_1 . In front of the slit was placed an H. R. Pyrometer red filter of pyrex glass 53% No.241 thickness of which was 4.37mm. This filter allowed only the H_{α} radiation to be transmitted. A shutter, T, before the filter was used to control the time of exposure.

The first Lummer plate was mounted to disperse horizontally. The mounting consisted of a platform with three adjustable legs. An upper platform with an adjustable screw^{served} to rotate the Lummer plate through small horizontal angles about a vertical axis located at the prism of the Lummer plate. An opaque screen, B, cut off the light from one side of the plate.

The second Lummer plate was similarly mounted to disperse horizontally. It was partially enclosed in a brass casing which was supported with three adjustable legs to permit fine leveling adjustments. Motion of the casing itself through small horizontal angles was controlled by four set screws located near the corners of the casing.

The telescope and the second Lummer plate are set on a common platform which can be rotated horizontally about a point between the two plates. Thus rotating this platform changes the angle of incidence of the emergent rays of the light from the first plate upon the prism of the second plate.

OPTICAL SYSTEM

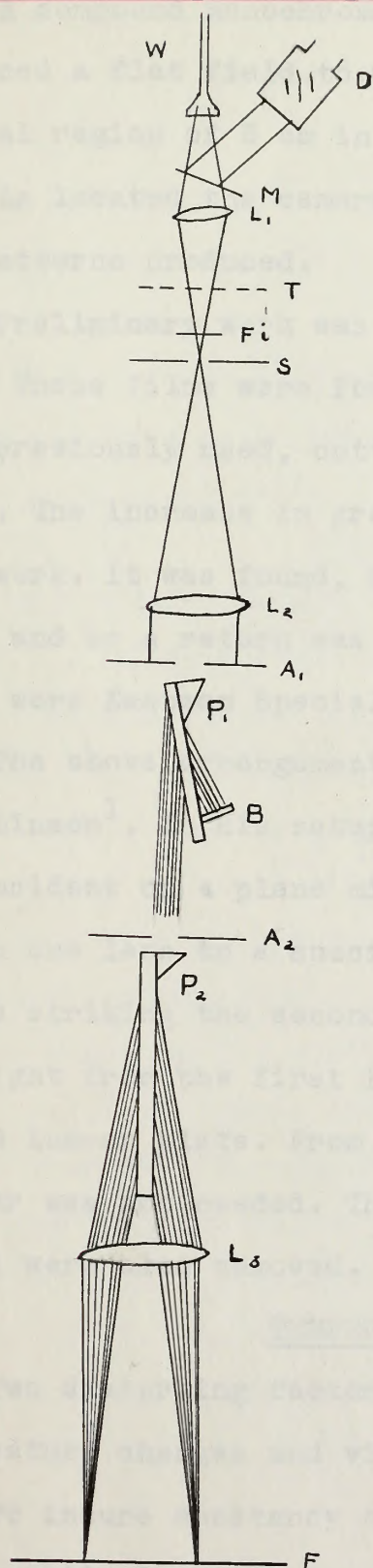
A diagrammatical sketch of the optical system is given in Fig. 8, page 40. A mirror M was used to intercept part of the beam from the tube and reflect it to a direct vision spectroscopy; thus the condition of the tube could be observed during exposures. Light from the discharge tube was focused on the slit of the spectroscopy by means of a lens L. In front of the slit was placed an H. R. Pyrometer red filter of pyrex glass 333 No. 331 thickness of which was 4.5 mm. This filter allowed only the H₂ radiation to be transmitted. A shutter, T, before the filter was used to control the time of exposure.

The first lantern plate was mounted to disperse horizontally. The mounting consisted of a platform with three adjustable legs. An upper platform with an adjustable screw to rotate the lantern plate through small horizontal angles about a vertical axis located at the prism of the lantern plate. An opaque screen, out off the light from one side of the plate.

The second lantern plate was similarly mounted to disperse horizontally. It was partially enclosed in a brass casing which was supported with three adjustable legs to permit fine leveling adjustments. Motion of the casing itself through small horizontal angles was controlled by four set screws located near the corners of the casing.

The spectroscopy and the second lantern plate are set on a common platform which can be rotated horizontally about a point between the two plates. Thus rotating this platform changes the angle of incidence of the emergent rays of the light from the first plate upon the prism of the second plate.

Fig. 8
OPTICAL SYSTEM



W - Wood tube

L_1, L_2, L_3 - Lenses

T - Shutter for time exposure

F_i - Red filter

S - Slit of spectroscope

A_1, A_2 - Shutters for controlling
illumination on prisms of
Lummer plates

P_1, P_2 - Lummer plates

M - Mirror

D - Direct vision spectroscope

F - Focal plane of L_3

B - Opaque screen

A compound monochromat lens, L₃, made by Bausch and Lomb produced a flat field to within a small fraction of a mm over a central region of 5 cm in diameter. At the focal plane of this lens is located the camera box and an ocular for visual study of the patterns produced.

Preliminary work was done with Agfa films, Emulsion No. 487-534. These films were found to be faster than plates that had been previously used, cutting the time of exposure to at least one fifth. The increase in grain size would not affect the results of this work. It was found, however, that halation entered as a difficulty and so a return was made to backed photographic plates. These were Eastman Special Spectroscopic Plates, Type I-C.

The above arrangement of the apparatus differed from that used by Robinson¹. In his setup the light coming from the first plate was incident on a plane mirror; the reflected light then passed through one lens to a special shutter and then through a second lens before striking the second Lummer plate. In the present arrangement the light from the first Lummer plate is directly incident upon the second Lummer plate. From Robinson's² work it was found that the shutter was not needed. The mirror and the lenses between the Lummer plates were also removed.

TEMPERATURE AND VIBRATION EFFECTS

Two disturbing factors causing shifting of the patterns are temperature changes and vibration.

To insure constancy of temperature of the Lummer plates the entire optical system was housed in a triple walled casing of

^{1,2} Robinson, W. H., Ph.D. Thesis, (1937) B.U. Grad. School

A compound monochromatic lens, 10, made by Leuch and Leuch produced a flat field to within a small fraction of a mm over a central region of 5 cm in diameter. At the focal plane of this lens is located the camera box and an ocular for visual study of the patterns produced.

Preliminary work was done with Agfa film, Emulsion No. 48V-533. These films were found to be faster than plates that had been previously used, cutting the time of exposure to at least one fifth. The increase in grain size would not affect the results of this work. It was found, however, that halation entered as a difficulty and so a screen was made to reduce photographic plates.

These were Eastman Special Spectroscopic Plates, Type 1-C. The above arrangement of the apparatus differed from that used by Robinson. In his case the light coming from the first plate was incident on a glass mirror; the reflected light then passed through one lens to a special mirror and then through a second lens before striking the second camera plate. In the present arrangement the light from the first camera plate is directly incident upon the second camera plate. From Robinson's work it was found that the result was not needed. The mirror and the lens between the camera plates were also removed.

TEMPERATURE AND VIBRATION EFFECTS

The disturbing factors causing shifting of the patterns are temperature changes and vibration. To insure constancy of temperature of the camera plates the entire optical system was housed in a triple walled casing of

building paper. The variation in temperature was so small that a further controlled heating circuit within the housing was dispensed with.

The optical system with housing was supported on a concrete table, the concrete and brick legs of which were imbedded in sawdust.

With the above arrangements possible shifts of patterns producing an increase in the spreading of the lines during an exposure were eliminated.

POSITIONS OF LUMMER PLATES

A camera box was set up on a staging above the housing. The top of the housing could easily be removed to expose the Lummer plates, collimator and telescope. The system was photographed using Eastman 50, 5x7 plates. See photograph on page 43.

To aid in this process strips of white paper were accurately pasted along one edge of the upper surfaces of the Lummer plates and a fine line was also scratched along the axis on the blackened surface of the collimator. Thus a permanent record was obtained of the positions of the plates with respect to the collimator for every set of exposures taken of the patterns.

To measure the angle between the collimator and first Lummer plate, and also the angle between the two Lummer plates, a line was scratched with a straight edge on the emulsion side of the photographic plate. See Fig. 9. This then was cut into sections containing a Lummer plate image or collimator with a portion of the scratched line. Two points (A, B) were chosen on the line and that part of the photographic plate mounted on a comparator. With the crosshair of the telescope set parallel to the scratched line, distances were then measured from points

holding paper. The variation in temperature was so small that a further controlled heating circuit within the housing was dispensed with.

The optical system with housing was supported on a concrete table, the concrete and brick legs of which were imbedded in saw dust.

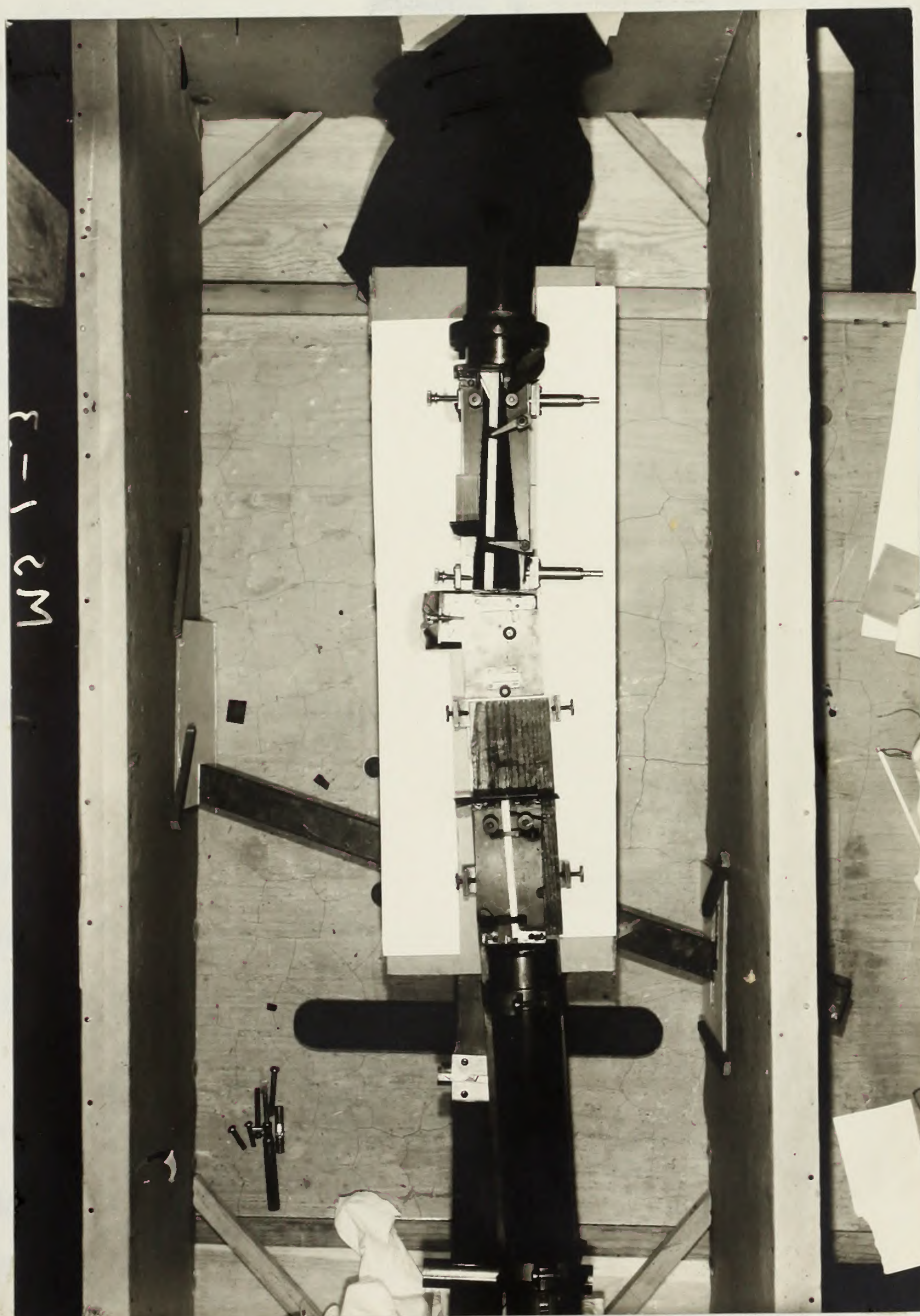
With the above arrangements possible shifts of pattern produced an increase in the spreading of the lines during exposure were eliminated.

POSITIONS OF LUMBER PLATES

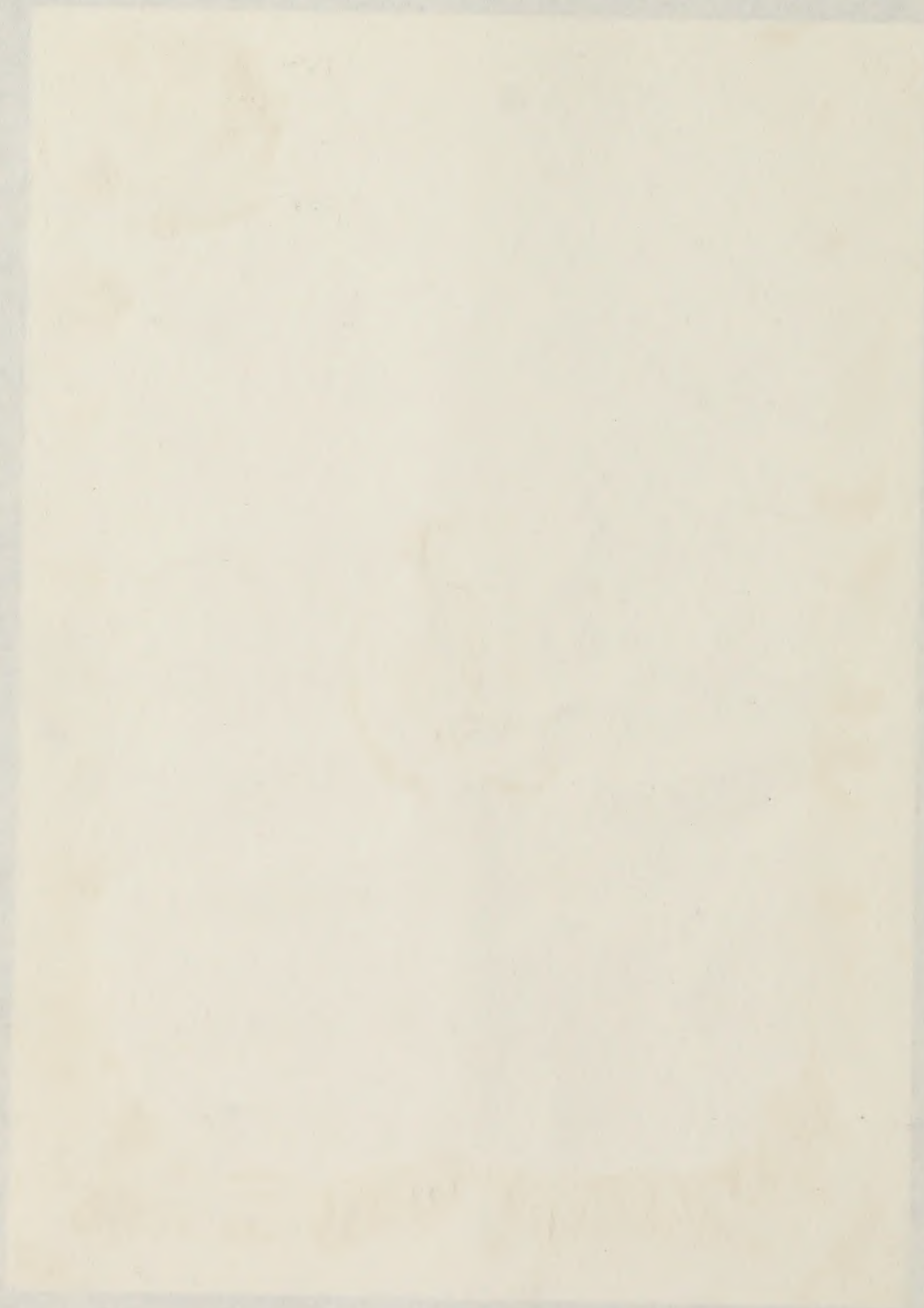
A camera box was set up on a staging above the housing. The top of the housing could easily be removed to expose the lumbar plates, collimator and telescope. The system was photographed using lantern 50, 5x7 plates. See photograph on page 43.

To aid in this process strips of white paper were accurately pasted along the edge of the upper surface of the lumbar plates and a fine line was also scratched along the axis on the back surface of the collimator. Thus a permanent record was obtained of the positions of the plates with respect to the collimator for every set of exposures taken of the pattern.

To measure the angle between the collimator and first lumbar plate, and also the angle between the two lumbar plates, a line was scratched with a straight edge on the surface side of the photographic plate. See Fig. 9. This then was cut into sections containing a lumbar plate image or collimator with a portion of the scratched line. Two points (A, B) were chosen on the line and that part of the photographic plate mounted on a comparator. With the scratches of the telescope set parallel to the scratched line, distances were then measured from points



OPTICAL SYSTEM WITHIN HOUSING



THE END OF THE WORLD

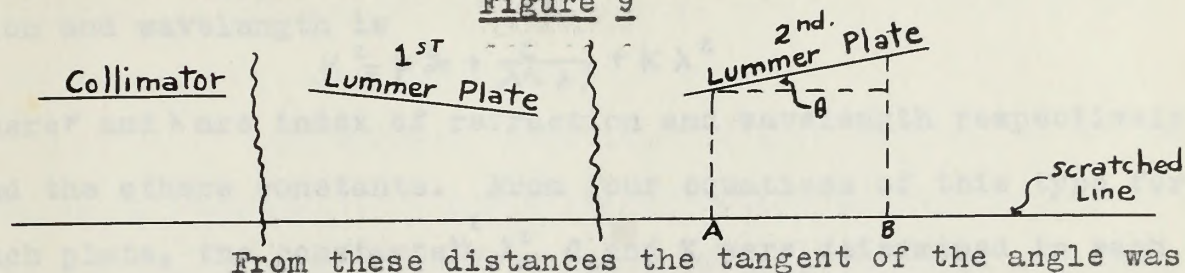
BY J. R. R. TOLKIEN

WITH ILLUSTRATIONS BY J. R. R. TOLKIEN

THE LONDON SCHOOL OF ECONOMICS

A and B to line of the Lummer plate edge. Distance AB was also measured. Position of plates and collimator.

Figure 9



From these distances the tangent of the angle was calculated. Similarly the angles for the other sections were determined and from these the angle between the Lummer plates as well as the angle between the first Lummer plate and the collimator were calculated.

CONSTANTS OF THE LUMMER PLATES

The thicknesses of the Lummer plates as given by the makers are known to within one thousandth of a millimeter. See page 48.

The indices of refractions for the various plates were also given for standard wavelengths of light. See table III. From these were computed the equations connecting the index of refraction with wavelength for the three plates.

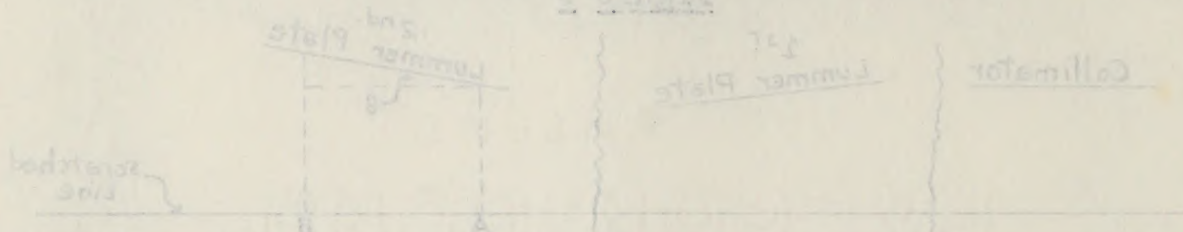
VARIATION OF INDEX OF REFRACTION WITH WAVELENGTH

Table III

Wave Length		Index-----of-----Refraction		
		Smallest Pl.	Medium Pl.	Largest Pl.
λ_c	6562.7845 A	1.50746	1.61772	1.57193
λ_D	5892.9485 A	1.50990	1.62261	1.57590
λ_F	4861.327 A	1.51560	1.63492	1.58581
$\lambda_{G'}$	4340.466 A	1.52025	1.64537	1.59417

A and B to line of the Lummer plate edge. Distance AB was also measured. Position of plates and collimator.

Figure 2



From these distances the tangent of the angle was

calculated. Similarly the angles for the other sections were determined and from these the angle between the Lummer plates as well as the angle between the first Lummer plate and the collimator were calculated.

CONSTANTS OF THE LUMMER PLATES

The thicknesses of the Lummer plates as given by

the makers are known to within one thousandth of a millimeter.

See page 48.

The indices of refraction for the various plates

were also given for standard wavelengths of light. See table II.

From these were computed the equations connecting the index of

refraction with wavelength for the three plates.

VARIATION OF INDEX OF REFRACTION WITH WAVELENGTH

Table III

Wave length	Index of refraction		
	Smallest Pl.	Medium Pl.	Largest Pl.
λ_c 6562.7825 A	1.61772	1.61772	1.61772
λ_c 5892.9485 A	1.62281	1.62281	1.62281
λ_c 4861.327 A	1.63492	1.63492	1.63492
λ_c 4340.466 A	1.65237	1.65237	1.65237

The general equation connecting index of refraction and wavelength is

$$\mu^2 = \mu_\infty^2 + \frac{C}{\lambda^2 - \lambda_1^2} + K\lambda^2$$

where μ and λ are index of refraction and wavelength respectively and the others constants. From four equations of this type for each plate, the constants μ_∞^2 , λ_1^2 , C and K were determined in each case. The resulting equations are as follows:-

$$\text{Smallest plate } \mu^2 = 2.2571775 + \frac{.009042497}{\lambda^2 - .030272729} - .017004441 \lambda^2$$

$$\text{Medium plate } \mu^2 = 2.5620604 + \frac{.023311132}{\lambda^2 - .02932727} - .007245746 \lambda^2$$

$$\text{Largest plate } \mu^2 = 2.4343834 + \frac{.0171249}{\lambda^2 - .032560549} - .015370676 \lambda^2$$

There remains to be found the angles of the attached prisms of the plates.

To achieve this end the plates were placed on the graduated turntable of a spectrometer in front of the collimator. The slit of the collimator was illuminated by focussing the light of a lamp at a right angle prism situated in front of the lower half of the slit. See Fig. 10. With the correct adjustment of the collimator and the level of the turntable the reflected images of the slits from two sides of the Lummer plate prism could be brought successively into the plane of the slit just above the right angle prism.

For aid in the settings a needle was placed in the plane of the slit; thus the needle and its image in the plane of the slit could be viewed with an eye piece and settings made more accurately. The angle through which the plate was turned for settings of the reflected image of the needle from two sides of the prism gives thus a measure of the angle of the prism.

The general equation connecting index of refraction

$$n^2 = 1 + \frac{A}{\lambda^2} + \frac{B}{\lambda^4} + \frac{C}{\lambda^6}$$

where n and λ are index of refraction and wavelength respectively and the other constants A , B and C were determined in each case. The resulting equations are as follows:-

Smallest plate $n^2 = 2.281775 + \frac{0.00000000}{\lambda^2} + \frac{0.00000000}{\lambda^4} - \frac{0.00000000}{\lambda^6}$

Medium plate $n^2 = 2.280000 + \frac{0.00000000}{\lambda^2} + \frac{0.00000000}{\lambda^4} - \frac{0.00000000}{\lambda^6}$

Largest plate $n^2 = 2.431334 + \frac{0.00000000}{\lambda^2} + \frac{0.00000000}{\lambda^4} - \frac{0.00000000}{\lambda^6}$

There remains to be found the angles of the attached prisms of the plates.

To achieve this the plates were placed on the graduated turntable of a spectrometer in front of the collimator. The slit of the collimator was illuminated by focussing the light of a lamp at a right angle prism placed in front of the lower half of the slit. See fig. 10. With the correct adjustment of the collimator and the level of the turntable the reflected image of the slit from two sides of the lower plate prism could be brought successively into the plane of the slit just above the right angle prism.

To aid in the setting a needle was placed in the plane of the slit; thus the needle and its image in the plane of the slit could be viewed with the eyes and settings made more accurately. The angle through which the plate was turned for setting of the reflected image of the needle from two sides of

the prism gives then a measure of the angle of the prism.

The angles as determined in this manner are accurate to within ± 7.5 seconds and are listed on page 48.

Experiments were made to test whether or not the indices of refraction of the attached prisms are the same as that for the plates. It was found that they were the same within experimental error for the smallest and medium plate. For the prism of the largest plate μ for $H_{\alpha} = 1.57531$.

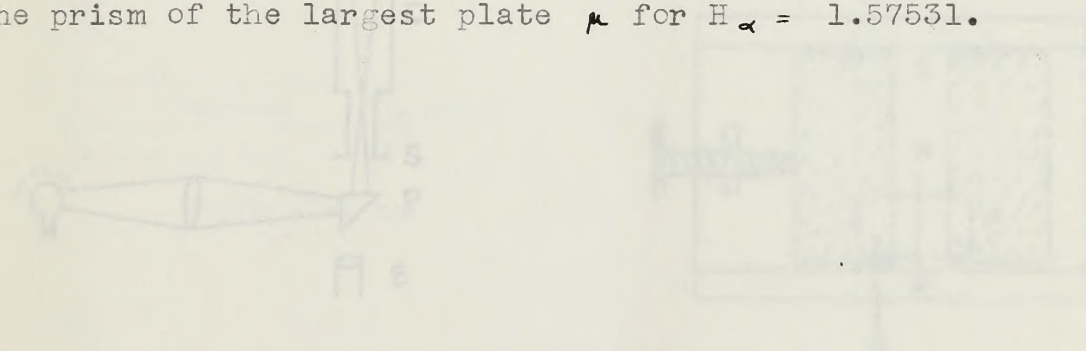


Fig. 10

OPTICAL ARRANGEMENT FOR MEASURING THE INDEX OF REFRACTION OF GLASS PLATES

LEGEND

- 1 - Spectrometer
- 2 - Collimator
- 3 - Lens
- 4 - Glass plate
- 5 - Slit
- 6 - Right angle prism
- 7 - Needle
- 8 - Eye piece

The angles as determined in this manner are accurate to within

7.5 seconds and are listed on page 4.

Experiments were made to test whether or not the

indices of refraction of the attached prisms are the same as

that for the plates. It was found that they were the same with-

in experimental error for the smallest and medium plates. For

the prism of the largest plate $n = 1.57531$.

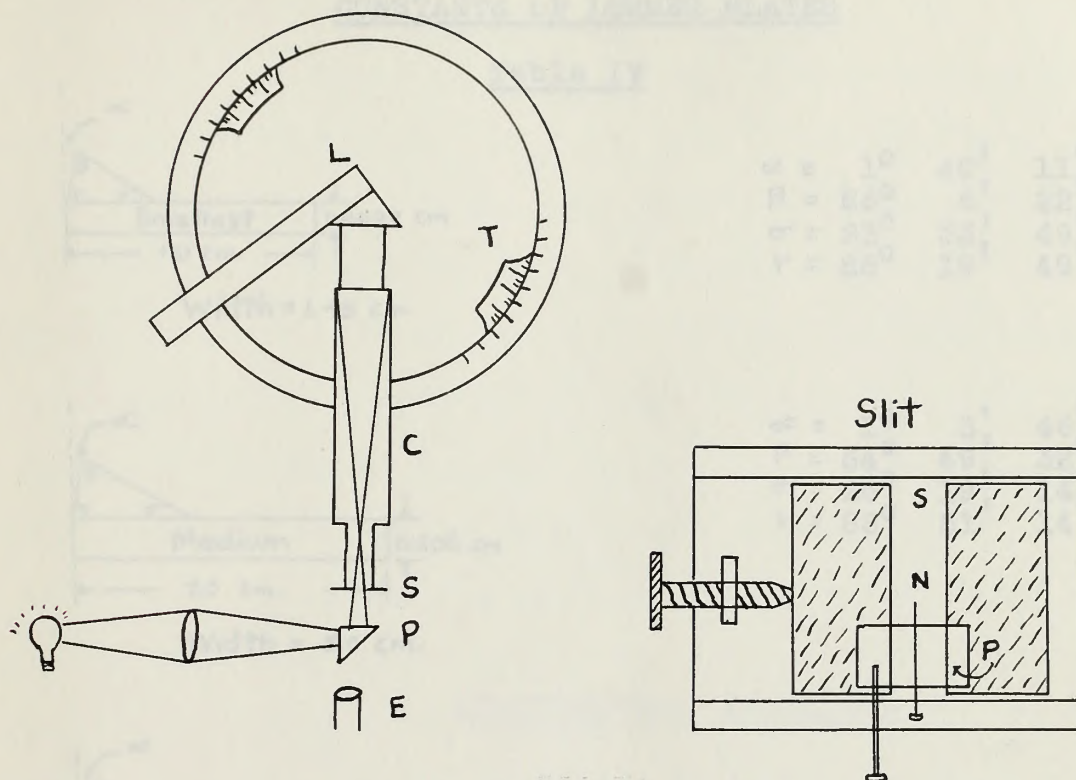


Fig. 10

OPTICAL ARRANGEMENT FOR MEASURING THE ANGLES
OF
LUMMER PLATE PRISM

- T - Spectrometer turntable
- C - Collimator
- L - Lummer plate
- S - Slit
- P - Right angle prism
- N - Needle
- E - Eye piece

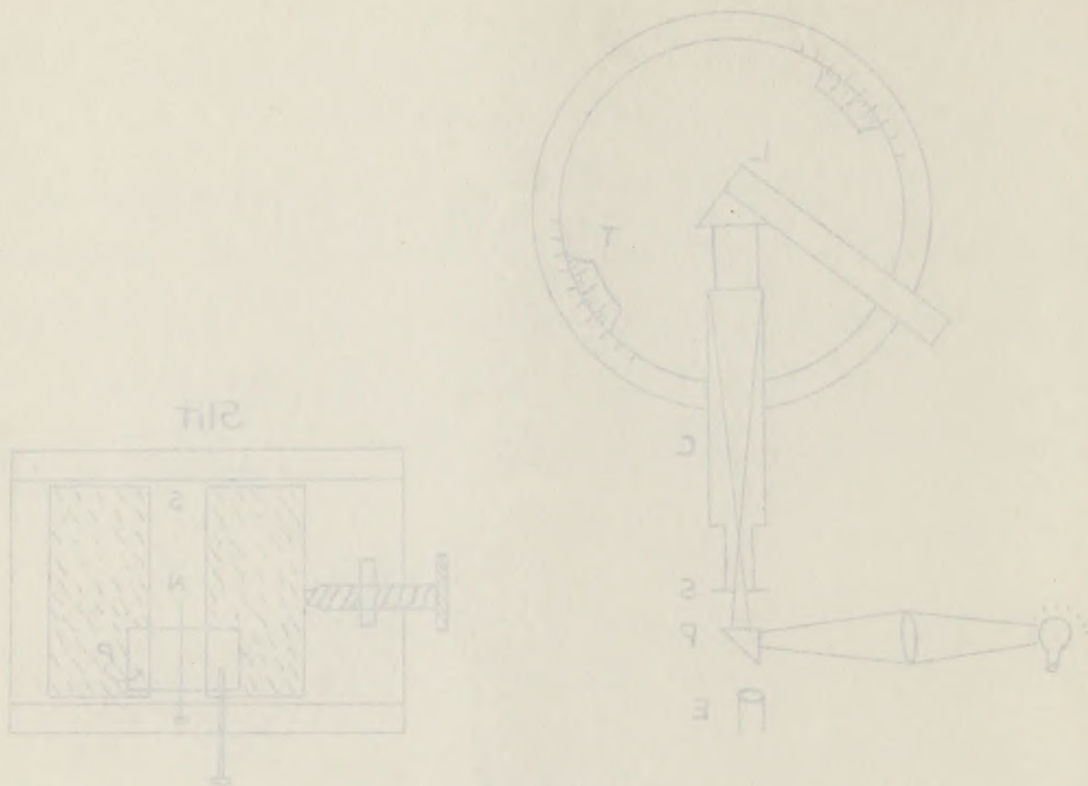


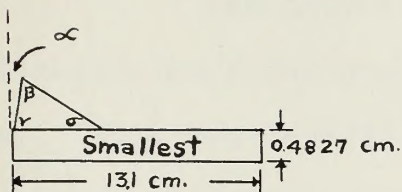
Fig. 10

OPTICAL ARRANGEMENT FOR MEASURING THE ANGLE
OF
LUMINESCENT PLATE PRISM

- T - Spectrometer turntable
- C - Collimator
- L - Luminescent plate
- S - Slit
- P - Right angle prism
- H - Needle
- E - Eye piece

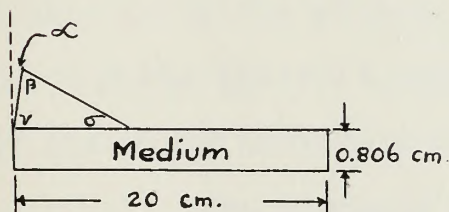
CONSTANTS OF LUMMER PLATES

Table IV



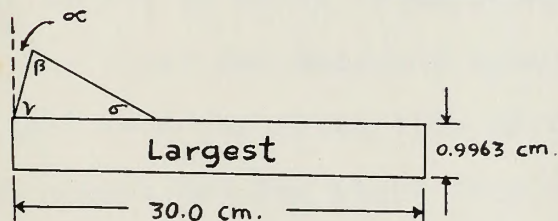
Width = 1.45 cm.

$\alpha =$	1°	$40'$	$11''$
$\beta =$	66°	$6'$	$22''$
$\gamma =$	25°	$33'$	$49''$
$\sigma =$	88°	$19'$	$49''$



Width = 3.0 cm.

$\alpha =$	1°	$8'$	$46''$
$\beta =$	64°	$49'$	$32''$
$\gamma =$	26°	$19'$	$14''$
$\sigma =$	88°	$51'$	$14''$



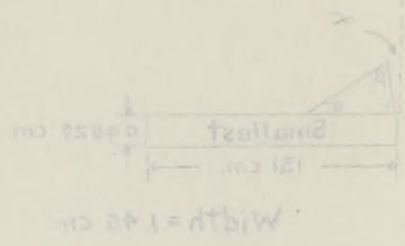
Width = 3.98 cm.

$\alpha =$	1°	$28'$	$25''$
$\beta =$	65°	$19'$	$3''$
$\gamma =$	26°	$9'$	$22''$
$\sigma =$	88°	$31'$	$35''$

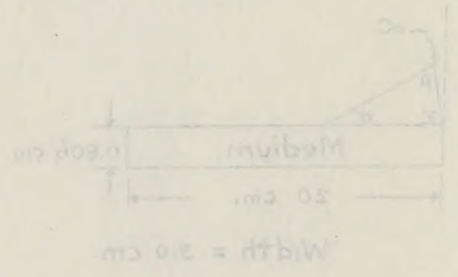
$M_{H\infty}$ for smallest plate and prism =	1.50746	} Hilger Values
$M_{H\infty}$ for medium plate and prism =	1.61772	
$M_{H\infty}$ for largest plate----- =	1.57187	
$M_{H\infty}$ for attached prism of largest plate----- =	1.5753 \mp .001	

CONSTANTS OF LUMBER PLATES

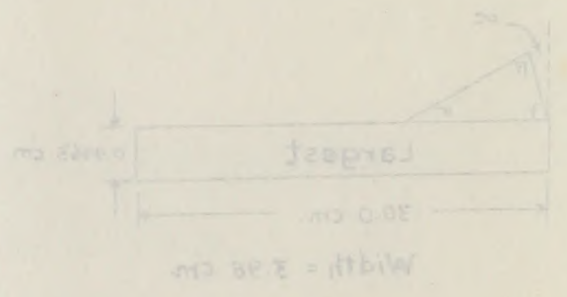
Table IV



$\alpha =$	10	40	11
$\beta =$	60	8	32
$\gamma =$	150	33	43
$\delta =$	88	19	49



$\alpha =$	10	8	40
$\beta =$	60	49	32
$\gamma =$	150	19	14
$\delta =$	88	31	14



$\alpha =$	10	40	33
$\beta =$	60	19	3
$\gamma =$	150	3	32
$\delta =$	88	31	38

μ_{H} for smallest plate and prism = 1.50746
 μ_{H} for medium plate and prism = 1.51372
 μ_{H} for largest plate ----- = 1.5187
 μ_{H} for attached prism of largest plate ----- = 1.5233 \pm .001
 Higher Values

OPTICAL ALIGNMENT

The care of the lumbar plates is extremely important--The surfaces must be very clean and especially free from grease. This was insured by rubbing the surfaces gently with lens paper and a small amount of alcohol. The lumbar plates were then set in their holders and shutters were adjusted so that light would only enter the attached prism. Great care was exercised in clamping the plate in place for any appreciable local pressure on the plate may seriously impair its definition.

The complete optical system was as shown in Fig. 1, page 40. The first lumbar plate was rotated through small horizontal angles by means of the platform until the light was emergent somewhat near the greater angle. The light from the prism side of the plate was cut off by an opaque screen and the light from the other side allowed to fall on the second plate. The intensity of the light emergent from the free side was found to be greater than that from the prism side, apparently due to the one more reflection and corresponding loss of light of the first reflected beam and absorption through glass before finally emerging on the prism side of the plate. The second lumbar plate was set up that its prism was on the opposite side to that of the first prism of the first lumbar plate. This in part, thus corrects for slight curvature of the lines inherent in the prism. With light now filling the prism of second lumbar plate, the platform supporting both the telescope and second lumbar plate was rotated through small horizontal angles until a desired picture was obtained.

EXPERIMENTAL PROCEDURE

OPTICAL ADJUSTMENTS

The care of the Lummer plates is extremely important--the surfaces must be very clean and especially free from grease. This was insured by rubbing the surfaces gently with lens paper and a small amount of alcohol. The Lummer plates were then set in their holders and shutters were adjusted so that light would only enter the attached prisms. Great care was exercised in clamping the plate in place for any appreciable local pressure on the plate may seriously impair its definition.

The complete optical system was as shown in Fig. 8, page 40. The first Lummer plate was rotated through small horizontal angles by means of an adjustable screw on the platform until the light was emergent somewhat near the grazing angle. The light from the prism side of the plate was cut off by an opaque screen and the light from the other side allowed to fall on the second plate. The intensity of the light emergent from the free side was found to be greater than that from the prism side, apparently due to the one more reflection and corresponding loss of light of the first refracted beam and absorption through glass before finally emerging on the prism side of the plate. The second Lummer plate was set so that its prism was on the opposite side to that of the first prism of the first Lummer plate. This in part, thus corrects for slight curvature of the lines inherent in the prism. With light now filling the prism of second Lummer plate, the platform supporting both the telescope and second Lummer plate was rotated through small horizontal angles until a desired pattern system was obtained.

OPTICAL ADJUSTMENTS

The care of the camera plates is extremely im-

portant--the surfaces must be very clean and especially free from

grease. This was insured by rubbing the surfaces gently with

fine paper and a small amount of alcohol. The camera plates were

then set in their holders and shutters were adjusted so that light

would only enter the attached prism. Great care was exercised

in clamping the plate in place for any appreciable local pressure

on the plate may seriously injure its definition.

The complete optical system was as shown in Fig. 1.

page 40. The first camera plate was rotated through small hori-

zontal angles by means of an adjustable screw on the platform

until the light was centered somewhat past the prism angle.

The light from the prism side of the plate was cut off by an

opaque screen and the light from the other side allowed to fall

on the second plate. The intensity of the light emerging from

the first side was found to be greater than that from the prism

side, apparently due to the one more reflection and corresponding

loss of light of the first reflected beam and absorption through

glass before finally emerging on the prism side of the plate.

The second camera plate was set so that the prism was on the

opposite side to that of the first prism of the first camera

plate. This in part, gave correct for slight curvature of the

lines inherent in the prism. With light now falling on the prism

of second camera plate, the platform supporting both the tele-

scope and second camera plate was rotated through small horizon-

tal angles until a desired position was obtained.

Final adjustment in the leveling of the second plate was then made so that the maximum and minimum of the group pattern were parallel to the individual lines. The second plate itself was then rotated until the desired number of groups on either side of the center of the fringe system was obtained. In general the second Lummer plate was set so that more groups were obtained from the plane side of the plate since this was the side of greater intensity. In the process of fixing the position of the second Lummer plate, slight readjustment had to be made in the position of the first plate so that the aperture of the second plate was completely filled with light.

The patterns were studied visually at all times by one observer while another made the adjustments. Any slight changes in either of the two plates themselves, necessitated the rotating of the platform which supported as a whole the telescope, camera box, and second Lummer plate for best conditions of intensity and structure. After a particular pattern was decided upon during this long and tedious adjustment and readjustment, the telescope and plateholder were clamped ⁱⁿ position, and the housing set over the complete optical system.

DISCHARGE CONDITIONS

Before an exposure the mercury trap as well as the pine wood box enclosing the capillary of the discharge tube was filled with liquid air. The tube was then run for about five minutes with the vacuum pump continually exhausting, the tube

Final adjustment in the leveling of the second plate was then made so that the maximum and minimum of the group pattern were parallel to the individual lines. The second plate itself was then rotated until the desired number of groups on either side of the center of the fringe system was obtained. In general the second hammer plate was set so that more groups were obtained from the plane side of the plate since this was the side of greater intensity. In the process of fixing the position of the second hammer plate, slight readjustment had to be made in the position of the first plate so that the positions of the second plate was completely filled with light.

The patterns were studied visually at all times by one observer while another made the adjustments. Any slight changes in either of the two plates themselves, necessitated the rotating of the platform which supported as a whole the telescope, camera box, and second hammer plate for best conditions of intensity and exposure. After a particular pattern was decided upon during this long and tedious adjustment and readjustment, the telescope and plateholder were changed position, and the housing set over the complete optical system.

DISCHARGE TUBE

Before an exposure the mercury trap as well as the pine wood box enclosing the cathode of the discharge tube was filled with liquid air. The tube was then run for about five minutes with the vacuum pump operating continuously, the tube

itself being flushed several times with fresh hydrogen from the reservoir. This procedure removed thoroughly any mercury vapor and set the tube for steady conditions during an exposure. The spectrum was continually observed by a constant deviation spectroscopy. With the secondary spectrum almost absent the desired pressure and secondary current were obtained and kept constant for any one exposure. The pressures and the current densities for the different plates were kept approximately 1.0 mm. of Hg. and 22 ma/cm² respectively. See table V, page 55. In all cases the red filter was used, allowing only the light giving H_α to be transmitted.

PHOTOGRAPHIC PROCEDURE

In general for each setting of the Lummer plates three photographic plates were taken with exposures from 15 to 40 minutes. At the beginning of this research, films which were relatively fast were used; thus saving in exposure time and cost of liquid air. Because of halation, however, a shift was made to Eastman Special Spectroscopic Plates, Type I-C which were properly backed. These plates proved to be not very satisfactory for they were not very clear apparently subject to chemical fog. At a later date Eastman plates, Type 144-F were tried. It was unfortunate that these were not used at the very beginning since they produced very clear spectrograms. All plates were developed by Eastman's D-19 formula, with development time about six minutes.

After the exposure of three photographic plates

itself being flushed several times with fresh hydrogen from the reservoir. This procedure removed thoroughly any mercury vapor and set the tube for steady conditions during an exposure. The spectrum was continually observed by a constant deviation spectrograph. With the secondary spectrum almost absent the desired pressure and secondary current were obtained and kept constant for any one exposure. The pressures and the current densities for the different plates were kept approximately 1.0 mm. of Hg. and 28 mμsec respectively. See table V, page 36. In all cases the red filter was used, allowing only the light giving H_α to be transmitted.

PHOTOGRAPHIC PROCEDURE

In general for each setting of the Lammert plates three photographic plates were taken with exposures from 15 to 40 minutes. At the beginning of this research, films which were relatively fast were used; thus saving in exposure time and cost of liquid air. Because of limitation, however, a shift was made to Eastman Spectroscopic Plates, Type 1-C which were properly backed. These plates proved to be not very satisfactory for they were not very clear apparently subject to chemical fog. At a later date Eastman plates, Type 144-F were tried. It was unfortunate that these were not used at the very beginning since they produced very clear spectrograms. All plates were developed by Eastman's D-19 formula, with development time about six minutes. After the exposure of three photographic plates

for different times for a given pattern the top of the housing was removed and a photograph taken from overhead of the alignment of the collimator, telescope and Lummer plates. Eastman 50, 5 x 7 plates were used here.

SPECTROGRAMS AND DATA

for different times for a given pattern the top of the housing
was removed and a photograph taken from overhead of the align-
ment of the collimator, telescope and camera plates. Between
50, 5 x 7 plates were used here.

TABLE I

Plate No.	Wave Length (m. or μ)	Current (ma./cm ²)	Exposure
1	1.00	18.5	5 sec.
2	0.95	22.5	10 sec.
3	0.90	24.0	20 sec.
41-1	0.85	23.0	27 min.
41-2	1.00	23.5	30 min.
41-3	1.05	24.0	30 min.
41-4	1.10	24.5	30 min.
41-5	1.15	25.0	30 min.
41-6	1.20	25.5	30 min.
41-7	1.25	26.0	30 min.
41-8	1.30	26.5	30 min.
41-9	1.35	27.0	30 min.
41-10	1.40	27.5	30 min.
41-11	1.45	28.0	30 min.
41-12	1.50	28.5	30 min.
41-13	1.55	29.0	30 min.
41-14	1.60	29.5	30 min.
41-15	1.65	30.0	30 min.
41-16	1.70	30.5	30 min.
41-17	1.75	31.0	30 min.
41-18	1.80	31.5	30 min.
41-19	1.85	32.0	30 min.
41-20	1.90	32.5	30 min.
41-21	1.95	33.0	30 min.
41-22	2.00	33.5	30 min.
41-23	2.05	34.0	30 min.
41-24	2.10	34.5	30 min.
41-25	2.15	35.0	30 min.
41-26	2.20	35.5	30 min.
41-27	2.25	36.0	30 min.
41-28	2.30	36.5	30 min.
41-29	2.35	37.0	30 min.
41-30	2.40	37.5	30 min.
41-31	2.45	38.0	30 min.
41-32	2.50	38.5	30 min.
41-33	2.55	39.0	30 min.
41-34	2.60	39.5	30 min.
41-35	2.65	40.0	30 min.
41-36	2.70	40.5	30 min.
41-37	2.75	41.0	30 min.
41-38	2.80	41.5	30 min.
41-39	2.85	42.0	30 min.
41-40	2.90	42.5	30 min.
41-41	2.95	43.0	30 min.
41-42	3.00	43.5	30 min.
41-43	3.05	44.0	30 min.
41-44	3.10	44.5	30 min.
41-45	3.15	45.0	30 min.
41-46	3.20	45.5	30 min.
41-47	3.25	46.0	30 min.
41-48	3.30	46.5	30 min.
41-49	3.35	47.0	30 min.
41-50	3.40	47.5	30 min.
41-51	3.45	48.0	30 min.
41-52	3.50	48.5	30 min.
41-53	3.55	49.0	30 min.
41-54	3.60	49.5	30 min.
41-55	3.65	50.0	30 min.
41-56	3.70	50.5	30 min.
41-57	3.75	51.0	30 min.
41-58	3.80	51.5	30 min.
41-59	3.85	52.0	30 min.
41-60	3.90	52.5	30 min.
41-61	3.95	53.0	30 min.
41-62	4.00	53.5	30 min.
41-63	4.05	54.0	30 min.
41-64	4.10	54.5	30 min.
41-65	4.15	55.0	30 min.
41-66	4.20	55.5	30 min.
41-67	4.25	56.0	30 min.
41-68	4.30	56.5	30 min.
41-69	4.35	57.0	30 min.
41-70	4.40	57.5	30 min.
41-71	4.45	58.0	30 min.
41-72	4.50	58.5	30 min.
41-73	4.55	59.0	30 min.
41-74	4.60	59.5	30 min.
41-75	4.65	60.0	30 min.
41-76	4.70	60.5	30 min.
41-77	4.75	61.0	30 min.
41-78	4.80	61.5	30 min.
41-79	4.85	62.0	30 min.
41-80	4.90	62.5	30 min.
41-81	4.95	63.0	30 min.
41-82	5.00	63.5	30 min.
41-83	5.05	64.0	30 min.
41-84	5.10	64.5	30 min.
41-85	5.15	65.0	30 min.
41-86	5.20	65.5	30 min.
41-87	5.25	66.0	30 min.
41-88	5.30	66.5	30 min.
41-89	5.35	67.0	30 min.
41-90	5.40	67.5	30 min.
41-91	5.45	68.0	30 min.
41-92	5.50	68.5	30 min.
41-93	5.55	69.0	30 min.
41-94	5.60	69.5	30 min.
41-95	5.65	70.0	30 min.
41-96	5.70	70.5	30 min.
41-97	5.75	71.0	30 min.
41-98	5.80	71.5	30 min.
41-99	5.85	72.0	30 min.
41-100	5.90	72.5	30 min.

SPECTROGRAMS AND DATAEXPOSURE OF PLATES

TELEPHONE AND DATA

TABLE V

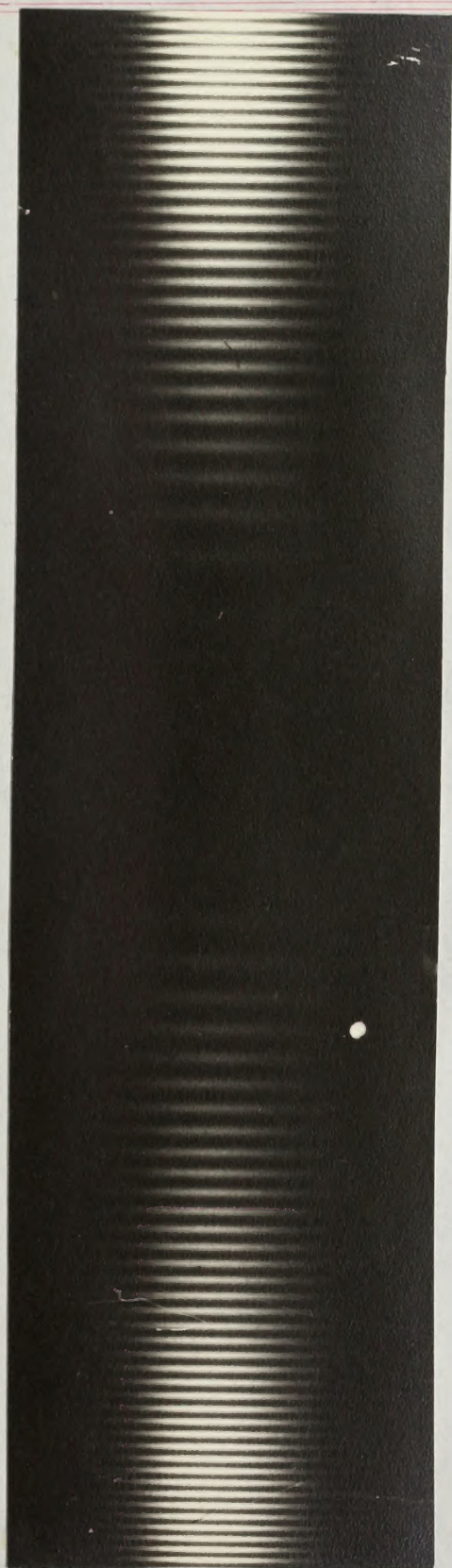
Plate No.	Vacuum (mm of Hg)	Current ma/cm ²	Exposure
L	1.80	18.5	5 sec.
M	0.92	22.0	15 sec.
S	0.92	22.0	30 sec.
SL-9	0.93	22.0	27 min.
SL-2	1.80	20.5	22 min.
ML-3	1.70	18.0	25 min.
(Film) SM-14	2.50	27.0	3 min.
(Film) SM-9	1.50	32.0	1.5 min.
MS-3	0.80	21.0	45 min.

TABULATION OF PLATES

TABLE V

Plate No.	Vacuum (mm of Hg)	Current $\mu\text{a/cm}^2$	Exposure
L	1.80	18.5	5 sec.
M	0.92	22.0	15 sec.
S	0.92	22.0	30 sec.
31-2	0.92	22.0	27 min.
31-2	1.80	20.0	32 min.
31-2	1.70	18.0	32 min.
(111) 31-1a (111)	2.50	17.0	5 min.
31-2	1.80	22.0	1.5 min.
31-2	0.80	22.0	45 min.

EXPOSURE OF FILMS



L



M

PARSONS
FALCON BOND



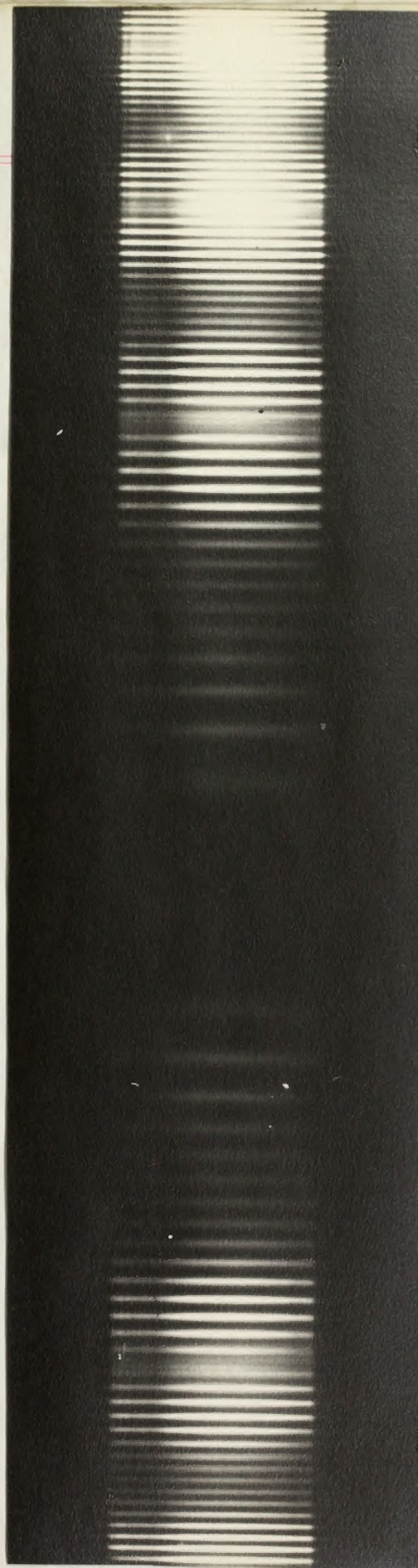
M



L

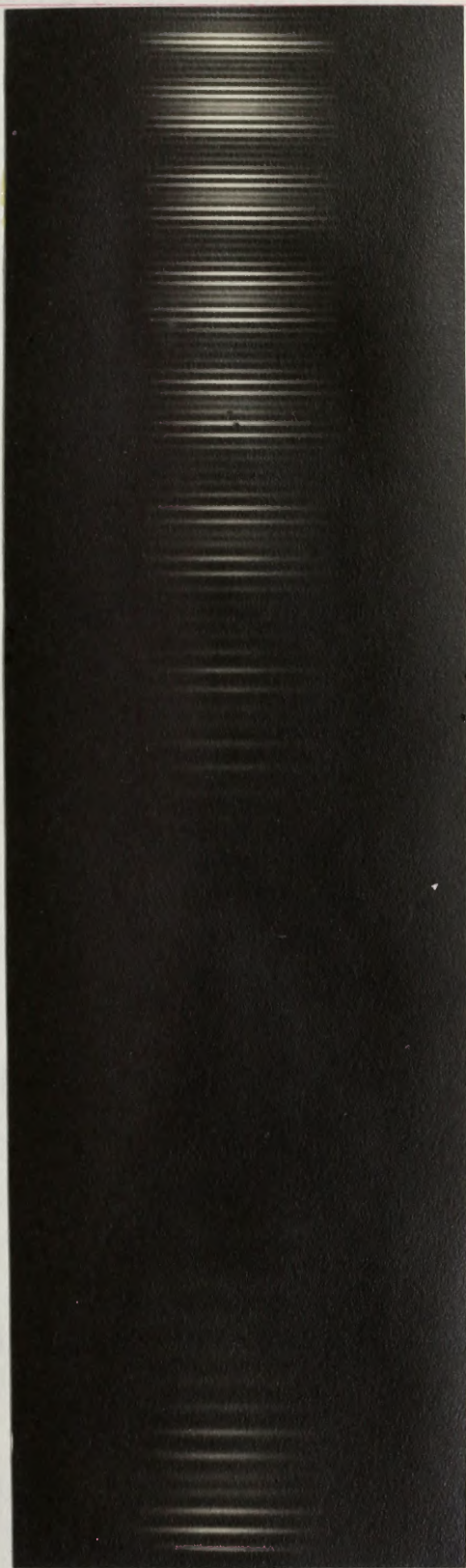


S



SL-9

[Faint, illegible text, possibly bleed-through from the reverse side of the page]



SL-2

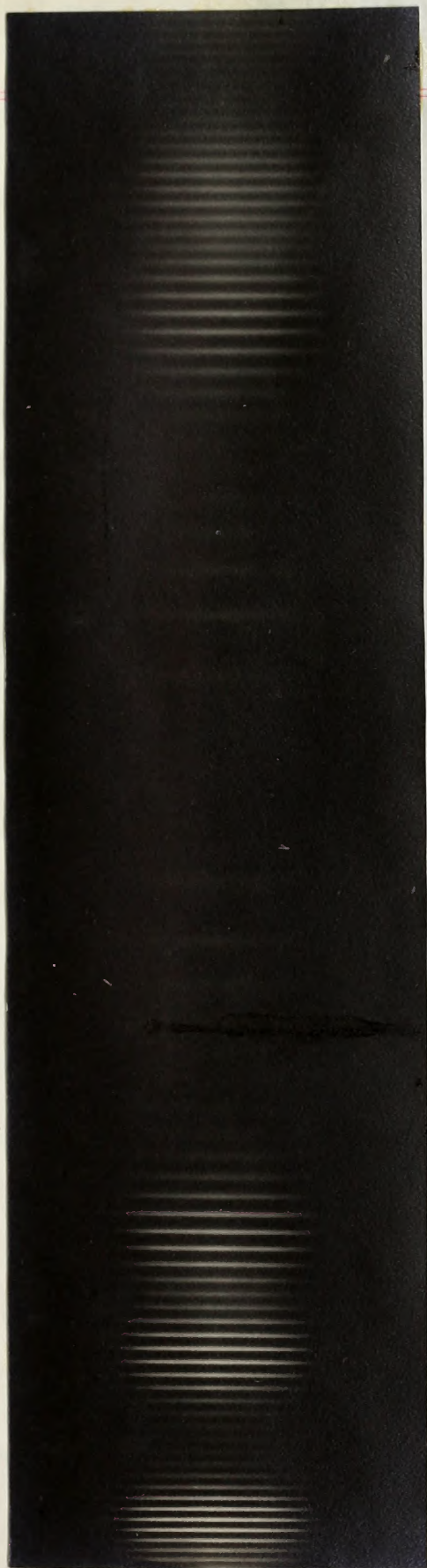


ML-3



HL-3

SL-5



SM-14



SM-9



2M-14



2M-14



MS-3

E-3M

DISCUSSION OF SINGLE PLATE SPECTROGRAMS

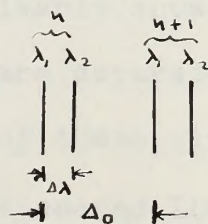
A list of the plates and films that were obtained under different conditions are given in table ^V showing the pressure, current and exposure time. The letters L, M and S used to distinguish the various spectrograms stand for the longest, medium and smallest Lummer plate respectively as described in the section "Constants of the Lummer plates". Where two letters appear, the photographic plate was obtained with two Lummer plates in tandem with the order of the letters L, M and S giving the order of the Lummer plates. Enlarged photographs of the original photographic plates are shown on pages 56-60.

The first three photographs L, M and S are the single Lummer plate patterns. The separation of the two main components of H_{α} and the separation of the successive orders are related in the following way for the 3 Lummer plates.

Δ_0 = order separation

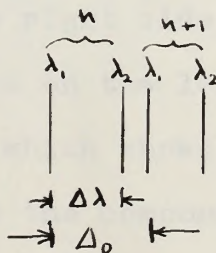
$\Delta\lambda$ = main component separation

Smallest Plate



$$\Delta\lambda = \frac{1}{3} \Delta_0$$

Medium Plate

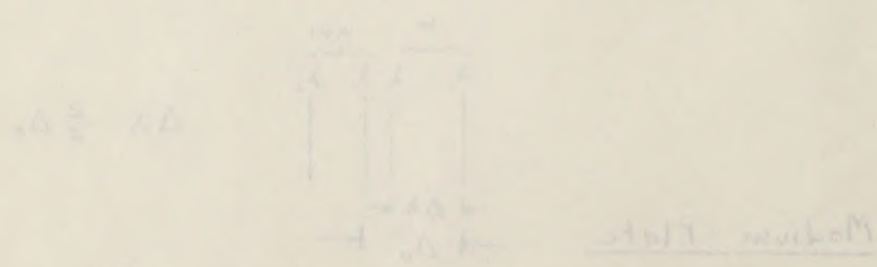


$$\Delta\lambda = \frac{2}{3} \Delta_0$$

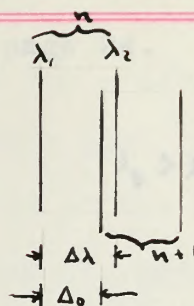
DISCUSSION OF KINEMATIC ANALYSIS

A list of the plates and films that were obtained under different conditions and given in Table I, II and III are current and accurate. The letters I, II and III stand for the location, designating the various experiments stand for the location, position and smallest known plate respectively as described in the section "Description of the known plates". Where two letters appear, the first letter plate was obtained with the known plates in tandem with the order of the letters I, II and III. The order of the letters I, II and III is given in order of the known plates. The plates of the optical spectroscopic plates are shown in Table I, II and III.

The first three experiments I, II and III are the plates of the known plates. The separation of the plates is the order of I, II and III. The separation of the plates is the order of I, II and III. The separation of the plates is the order of I, II and III.



Largest Plate



$$\Delta\lambda \sim 1.2\Delta_0$$

In plate L we see the lines appear very broad due to the fact that $\Delta\lambda \sim 1.2\Delta_0$, i.e., the component of one order overlaps the main component of the next order. The photograph obviously shows that the largest plate cannot be used alone for fine structure work. Passing to plates M and S we find no overlapping of the orders. The components are just separated by plates M and to a ^{larger} degree larger in plate S. The smallest Lummer plate is the best and gives the best definition.

DISCUSSION OF DOUBLE PLATE SPECTROGRAMS

The remaining photographs are those taken with combinations of two Lummer plates in tandem. Using the smallest Lummer plate first and then the largest in tandem, plates SL-9 and SL-2 were obtained. SL-9 clearly shows the group pattern. Both main components λ_1 and λ_2 are separated in the first smallest Lummer plate and each of these gives rise to a distinct series of lines due to the second Lummer plate. There are almost 3 full groups on the right side of the center of the pattern system and $1\frac{1}{2}$ groups on the left. There is present some intergroup structure which shows the existence of a third component. Theoretically the components would be arranged in the following manner with λ_3 to the left of λ_2

$\Delta A \approx 1.5 \Delta$



Largest Plate

In plate 1 we see the lines are very broad due to the fact that $\Delta A \approx 1.5 \Delta$, i.e. the component of the order-overlaps the main component of the next order. The photograph obviously shows that the first plate cannot be used alone for fine structure work. Passing to plates 2 and 3 we find an overlap of the orders. The components are just separated in plates 2 and 3 as before. In plate 3, the smallest human plate is the best and gives the best definition.

DISCUSSION OF ORDER PLATE SPECTROGRAMS

The remaining photographs are those taken with components of two human plates in tandem. Using the smallest human plate first and then the largest in tandem, plates 2B-3 and 2B-2 were obtained. 2B-2 clearly shows the group pattern. Both main components A and B are separated in the first smallest human plate and each of these gives rise to a first order series of lines due to the second human plate. There are about 3 full groups on the right side of the center of the pattern system and 1 group on the left. There is about a half group interval between the components which would be expected. Therefore, the components would be separated in the following manner with A to the left of B.

and λ_4 to the left of λ_1 . See page 24.



Plate SL-2 was taken with the light emergent from the first plate at a greater angle; thus with higher orders the components were closer together and many groups were obtained with but few lines representing each individual component in the final pattern. This plate failed to show any of the minor components, due apparently to loss in resolving power from failure in using the entire length of the first Lummer plate as well as to using higher orders. It is evident then in seeking the fine structure, light must emerge from the first Lummer plate at nearly grazing angle; thus utilizing the full length of the plate. However, it was found that there was an optimum angle for good intensity just beyond grazing emergence. The effective number of reflections at this angle is approximately two-thirds of the maximum possible; thus the resolving power is two-thirds of the theoretical value, or very closely $\frac{2}{3} \frac{d}{\lambda} (\mu^2 - 1)$. The use of the lower orders of the first plate would give greater dispersion of the lines in the final pattern and so aid the study of the fine structure.

and λ_4 to the left of λ_1 . See page 24.



Plate 21-3 was taken with the light source from the first plate at a greater angle; lines with higher orders and components were closer together and many groups were obtained with but few lines represented. Each individual component in the final pattern. This plate failed to show any of the other components. The separation of lines in the final pattern from patterns in which the entire length of the first pattern plate as well as to other higher orders. It is evident that in which the line structure, light that comes from the first plate plate at nearly grazing angle; thus utilizing the full length of the plate. However, it was found that there was an optimum angle for good intensity that beyond grazing distances. The effective number of reflections at this angle is approximately two-thirds of the maximum possible; thus the resolving power is two-thirds of the theoretical value. It is very closely $\frac{2}{3} \lambda (\lambda_1 - \lambda_2)$. The use of the lower orders of the first plate would give greater dispersion of the lines in the final pattern and so aid the study of the line structure.

The following plate ML-3 where the medium Lummer plate was used as the auxiliary spectrograph gave but slight evidence of the third component and none of the fourth. There appears no distinct grouping of lines for main components 1 and 2 as in the other combination of plates.

Films SM-14 and SM-9 gave distinct main component groups. The intergroup structure which was present showed the existence of a third component.

By far, the most interesting of the plates obtained was that obtained with a combination of the medium and smallest Lummer plates where the medium plate was used as the auxiliary spectrograph. The pattern system obtained with this combination is shown in plate MS-3. From direct measurements of the lines with a comparator and a study of the microphotometer tracing made of the plate, the lines fell into four distinct series when the intensities of the lines were plotted against their relative positions on the plate. This then gives complete evidence of the third and fourth components. A detailed discussion of this plate will be given in the next section.

The following plate (M-3) where the medium lower plate was used as the auxiliary spectrograph gave but slight evidence of the third component and none of the fourth. There appears no distinct grouping of lines for main components 1 and 2 as in the other combination of plates.

Plates M-12 and M-13 gave distinct main component groups. The dispersion elements which were present showed the existence of a third component.

By far, the most interesting of the plates obtained was that obtained with a combination of the medium and auxiliary spectrographs. The pattern obtained with this latter plate where the medium plate was used as the auxiliary spectrograph. The pattern obtained with this combination is given in plate M-8. From direct examination of the lines with a comparator and a study of the microphotometer traces and of the plate, the lines fall into four distinct series when the identification of the lines were plotted against their relative positions on the plate. This then gives complete evidence of the third and fourth components. A detailed discussion of this plate will be given in the next section.

THEORETICAL CALCULATIONS OF THE STRUCTURE OF PLATE MS-3

The diagram below gives the positions of the two
lens plates for photographic plate MS-3.

RESULTS

FIG. 11

POSITIONS OF LENS PLATES FOR
MS-3

The angles θ and η were determined by the method
described in the section "Positions of Lens Plates" page 42.
The angle of incidence, i_1 , was then found from the equation
 $i_1 = \alpha - \eta$ and also angle r_1 from the relation $\sin r_1 = \sin i_1 / \mu$.
Angle ψ followed from the equation $\psi = \beta - \theta - r_1$. The position
of ψ was then determined from $\cot \psi = \sin i_1 = \mu \sin r_1$.

With the above values of ψ and r_1 , the integral
order number n was calculated from the equation $n = \frac{2d \sin \psi}{\lambda \sin r_1}$.

RESULTS

THEORETICAL CALCULATIONS OF THE STRUCTURE OF

PLATE MS-3

The diagram below gives the positions of the two Lummer plates for photographic plate M-S 3.

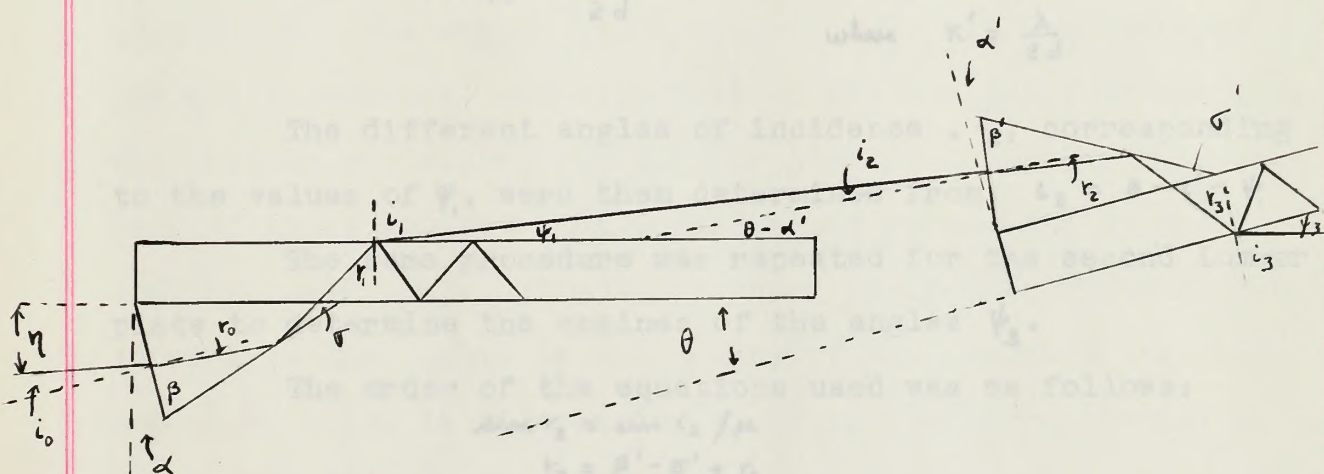


Fig. //

POSITIONS OF LUMMER PLATES FOR MS-3

The angles θ and η were determined by the method described in the section "Positions of Lummer Plates" page 42. The angle of incidence, i_0 , was then found from the equation $i_0 = \alpha - \eta$, and also angle r_0 from the relation $\sin r_0 = \sin i_0 / \mu$. Angle r_1 followed from the equation $r_1 = \beta - \sigma - r_0$. The cosine of ψ_1 was then determined from $\cos \psi_1 = \sin i_1 = \mu \sin r_1$.

With the above values of ψ_1 and r_1 , the integral order number n was calculated from the equation
$$n_M = \frac{2d \cos \psi}{\lambda \tan r_1}.$$

Following this, values of the cosines of the r'_1 and ψ'_1 for values of n above and below n_M from the two equations

$$\cos r_1 = \frac{\lambda}{2d\mu} n = K n \quad \text{where } K = \frac{\lambda}{2d\mu}$$

$$\cos \psi_1 = \frac{\lambda}{2d} n \tan r_1 = K' n \tan r_1 \quad \text{where } K' = \frac{\lambda}{2d}$$

The different angles of incidence, i_2 , corresponding to the values of ψ_1 , were then determined from $i_2 = \theta - \alpha' - \psi_1$.

The same procedure was repeated for the second Lummer plate to determine the cosines of the angles ψ_3 .

The order of the equations used was as follows:

$$\sin r_2 = \sin i_2 / \mu$$

$$r_3 = \beta' - \sigma' + r_2$$

$$\cos \psi_3 = \mu' \sin r_3$$

$$n'_M = \frac{2d' \cos \psi_3}{\lambda \tan r_3}$$

$$\cos r_3 = \frac{\lambda}{2d'\mu'} n' = L n' \quad \text{where } L = \frac{\lambda}{2d'\mu'}$$

$$\cos \psi_3 = \frac{\lambda}{2d'} n' \tan r_3 = L' n' \tan r_3 \quad \text{where } L' = \frac{\lambda}{2d'}$$

The distances, x , of the lines as measured from the center of the pattern system on the microphotometer curve were then calculated from the equation $x = 50 F \tan \psi_3$. F is the focal length of the telescope lens. Since the scale of the microphotometer tracing was 50:1 the values of x had to be multiplied by 50.

All the equations as mentioned above are fully developed and discussed in the section "Theory of two Lummer

Following this, values of the cosines of the r'_2 and ψ'_2 for values of n above and below n_M from the two equations

$$\begin{aligned} \cos r'_2 &= \frac{\lambda}{2b} n = K n \\ \text{where } K &= \frac{\lambda}{2b} \\ \cos \psi'_2 &= \frac{\lambda}{2b} n \tan r'_2 = K n \tan r'_2 \\ \text{where } K' &= \frac{\lambda}{2b} \end{aligned}$$

The different angles of incidence, i'_2 , corresponding to the values of ψ'_2 , were then determined from $i'_2 = \theta - r'_2 - \psi'_2$. The same procedure was repeated for the second layer plate to determine the cosines of the angles ψ'_3 . The order of the equations used was as follows:

$$\begin{aligned} \sin r'_2 &= \sin i'_2 / n \\ r'_2 &= \sin^{-1}(\sin i'_2 / n) \\ \cos \psi'_2 &= n' \sin r'_2 \\ n'_M &= \frac{2b' \cos \psi'_2}{\lambda \tan r'_2} \\ \cos r'_2 &= \frac{\lambda}{2b'} n' = L n' \\ \text{where } L &= \frac{\lambda}{2b'} \\ \cos \psi'_3 &= \frac{\lambda}{2b'} n' \tan r'_2 = L' n' \tan r'_2 \\ \text{where } L' &= \frac{\lambda}{2b'} \end{aligned}$$

The distance, X , of the lines as measured from the center of the pattern system on the microphotometer curve were then calculated from the equation $X = 2b' \tan \psi'_2$. b' is the focal length of the relayed lens. Since the scale of the microphotometer tracing was 50%, the values of X had to be multiplied by 50.

All the equations as mentioned above are fully developed and discussed in the section "Theory of two layer

plates in tandem", page 31.

The constants used as a basis for the above calculations are listed in table **VI**.

In this table are listed the comparative values of the index of refraction for the theoretical wavelengths of the five components. The angles θ and i_0 as used were slightly altered for the theoretical calculations of the positions of the lines. The changes are within the experimental error of the measurement of these angles. The experimental values are $\theta = 6^\circ 34' 55''$ and $i_0 = 32' 57''$. It will be shown later that these angles as well as the angles of the prisms of the Lummer plates are not as critical in determining the final patterns as they at first were thought to be.

The results of the calculations are listed in the following tables.

1. The first part of the report is a general introduction to the subject of the study.

2. The second part of the report is a detailed description of the methods used in the study.

3. The third part of the report is a detailed description of the results of the study.

4. The fourth part of the report is a detailed description of the conclusions of the study.

5. The fifth part of the report is a detailed description of the recommendations of the study.

6. The sixth part of the report is a detailed description of the limitations of the study.

7. The seventh part of the report is a detailed description of the future research.

8. The eighth part of the report is a detailed description of the appendix.

9. The ninth part of the report is a detailed description of the bibliography.

10. The tenth part of the report is a detailed description of the index.

11. The eleventh part of the report is a detailed description of the cover.

12. The twelfth part of the report is a detailed description of the title page.

13. The thirteenth part of the report is a detailed description of the table of contents.

14. The fourteenth part of the report is a detailed description of the list of figures.

15. The fifteenth part of the report is a detailed description of the list of tables.

16. The sixteenth part of the report is a detailed description of the list of references.

17. The seventeenth part of the report is a detailed description of the list of abbreviations.

18. The eighteenth part of the report is a detailed description of the list of symbols.

19. The nineteenth part of the report is a detailed description of the list of units.

20. The twentieth part of the report is a detailed description of the list of definitions.

TABLE VI
MEDIUM LUMMER PLATE

Comp.	λ (A°)	μ	$2d$ (cm)	$\beta - \sigma$
5	6562.8978	1.6177193		
4	6562.8513	1.6177196		
1	6562.8358	1.6177197	1.612	38° 30' 18"
3	6562.7406	1.6177203		
2	6562.6941	1.6177205		

SMALLEST LUMMER PLATE

Comp.	λ A°	μ'	$2d'$ (cm)	$\beta' - \sigma'$
5	6562.8978	1.5074597		
4	6562.8513	1.5074598		
1	6562.8358	1.5074599	.9654	40° 32' 33"
3	6562.7406	1.5074602		
2	6562.6941	1.5074603		

i_0	θ
0° 39' 0"	6° 31' 54"

i_0 = angle of incidence
 θ = angle between plates

TABLE VI
MEDIUM DENSITY FILMS

Comp.	λ (Å)	μ	S_0 (cm)	$\theta - \alpha$
2	6562.8508	1.617193		
4	6562.8513	1.617196		
1	6562.8538	1.617194	1.618	$28^\circ 20' 18''$
3	6562.7408	1.617303		
5	6562.8941	1.617305		

SHALLOW DEPTH FILMS

Comp.	λ (Å)	μ	S_0 (cm)	$\theta - \alpha$
2	6562.8508	1.607457		
4	6562.8513	1.607459		
1	6562.8538	1.607459	1.609	$40^\circ 35' 53''$
3	6562.7408	1.607460		
5	6562.8941	1.607463		

θ	α
$0^\circ 38' 0''$	$8^\circ 31' 54''$

θ - angle between plates
 α - angle of incidence

MEDIUM PLATE

	n	$\cos r_i$	$\cos r_i$	$\cos \psi_i$	ψ_i
(1)	31268	$2.5166523 \times 10^{-5} n$.78690684	.99824916	$3^\circ 23' 27.40''$
(2)	31268	$2.5165968 \times 10^{-5} n$.78688949	.99828543	$3^\circ 23' 20.00''$
(3)	31268	$2.5166149 \times 10^{-5} n$.78689515	.99827361	$3^\circ 22' 2.03''$
(4)	31268	$2.5166584 \times 10^{-5} n$.78690875	.99824514	$3^\circ 23' 41.59''$
	31267	"	.78688358	.99829713	$3^\circ 20' 39.18''$

TABLE VII
CALCULATIONS OF ψ_i

MEDIUM PLATE

	n	cos θ	cos θ'	cos ψ	ψ
(1)	31268	2.51683x10 ⁻² n	.7868084	.9924816	5° 23' 27.40"
(2)	31268	2.51526x10 ⁻² n	.7868849	.9923542	5° 23' 20.00"
(3)	31268	2.51614x10 ⁻² n	.7868615	.9923261	5° 23' 2.02"
(4)	31268	2.51658x10 ⁻² n	.7868375	.9923016	5° 23' 41.22"
	31267	"	.7868358	.99229713	5° 20' 32.13"

TABLE IX

CALCULATIONS OF ψ 's

TABLE VIII
CALCULATIONS OF ψ_3 's

Comp.	λ	$\cos r_3$	n'	$\cos r_3$	$\cos \psi_3$	$\tan \psi_3$
(1)	1° 28' 16.4"	$\cos r_3 = 4.5096046 \times 10^{-5}$	16598	.74850417	.99964180	.026771830
			16599	.74854927	.99956539	.029492480
			16600	.74859436	.99948843	.03199860
			16601	.74863946	.99941177	.03431496
			2	.74868456	.99933500	.03648767
			3	.74872965	.99925824	.03853776
			4	.74877475	.99918138	.04048758
			5	.74881984	.99910460	.04234708
			6	.74886494	.99902776	.04412911
			7	.74891004	.99895106	.04583905
			8	.74895513	.99887411	.04749235
(2)	1° 30' 23.0"	$\cos r_3 = 4.5095060 \times 10^{-5}$	16593	.74822633		
			4	.74830743	.99997700	.0067875
			5	.74835252	.99990020	.01412979
			6	.74839762	.99982188	.01887874
			7	.74844271	.99974718	.02249125
			16598	.74848781	.99967020	.02568868
			9	.74853290	.99959355	.02852000
			16600	.74857800	.99951663	.03110503
			1	.74862309	.99943984	.03348242
			2	.74866819	.99936303	.03571009
			3	.74871328	.99928654	.03779470
			4	.74875838	.99920945	

CALCULATIONS CONTINUED

Comp.	i_2	$\cos r_3$	$\cos nr_3$	$\cos nr_3$	$\cos \psi_3$	$\tan \psi_3$
(u) 31268	1° 29' 40.97"	$\cos r_3 = 4.5095383 \times 10^{-5} n$				
			6	.74840248	.99981421	.01927811
			7	.74844807	.99973771	.02290880
			8	.74849317	.99966098	.02604525
			16599	.74853826	.99958443	.02883950
			16600	.74858336	.99950740	.03140038
			1	.74862845	.99943068	.03375923
			2	.74867355	.99935387	.03596526
			3	.74871864	.99927725	.03863985
			4	.74876374	.99920033	.04001530
(4) 31268	1° 28' 1.41"	$\cos r_3 = 4.5096156 \times 10^{-5} n$				
			0	.74859619	.99950047	.03162137
			1	.74864129	.99940860	.03440681
			2	.74868638	.99933180	.03657406
			3	.74873148	.99925507	.03862130
			16604	.74877657	.99917825	.04056597
			5	.74882168	.99910139	.04242264
			6	.74886677	.99902460	.04419992
			7	.74891186	.99894783	.04590972
			8	.74895696	.99887093	.04755954
(4) 31267	1° 31' 3.82"	$\cos r_3 = 4.5096156 \times 10^{-5} n$				
			1	.74819032		
			2	.74823542		
			3	.74828052		
			4	.74832561	.99994570	.0104239
			16595	.74837071	.99986902	.02038925
			6	.74841580	.99979220	.02385295
			7	.74846090	.99971561	.02688342
			8	.74850600	.99963881	.02959754
			9	.74855109	.99956226	
			16600	.74859619	.99950047	

COMPARISON OF CALCULATED AND EXPERIMENTAL RESULTS

TABLE IX

(1)

n = 31268	
cal.	exp.
73.9	
81.4	
88.3	
94.7	93.1
100.7	99.0
106.3	104.5
111.7	109.7
116.9	114.6
121.8	119.1
126.5	124.2
130.8	

(2)

n = 31268	
cal.	exp.
39.0	43.8
52.1	55.0
62.1	64.2
70.9	72.3
78.7	79.6
85.8	86.3
92.4	92.3
98.6	
104.3	

(3)

n = 31268	
cal.	exp.
53.2	
63.2	67.0
71.9	74.7
79.6	81.0
86.8	87.7
93.2	94.0
99.3	
106.7	
110.4	

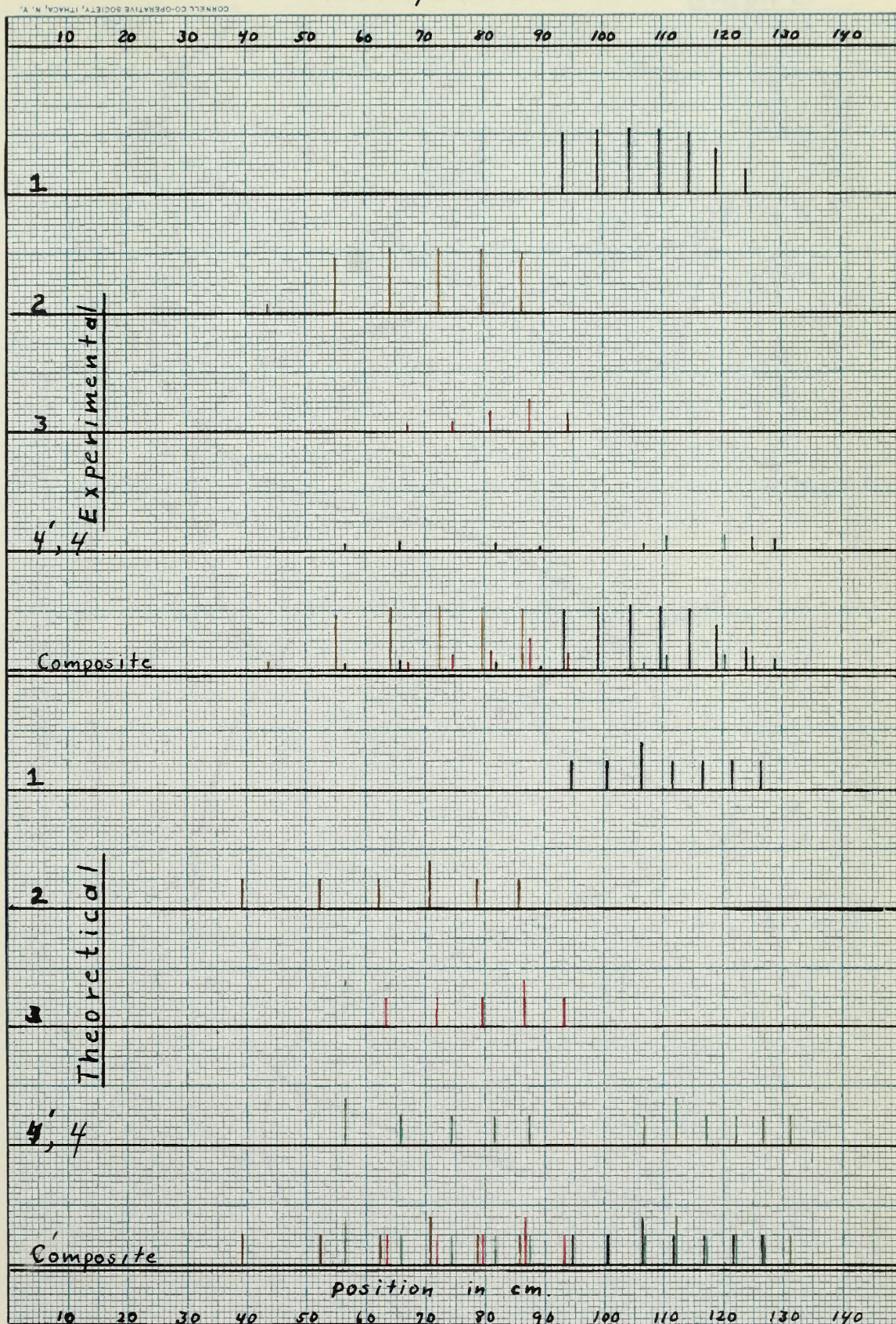
(4)

n = 31268	
cal	exp.
87.3	
95.0	
101.0	
106.6	107.0
112.0	110.8
117.1	
122.0	120.3
126.7	125.0
131.3	128.8

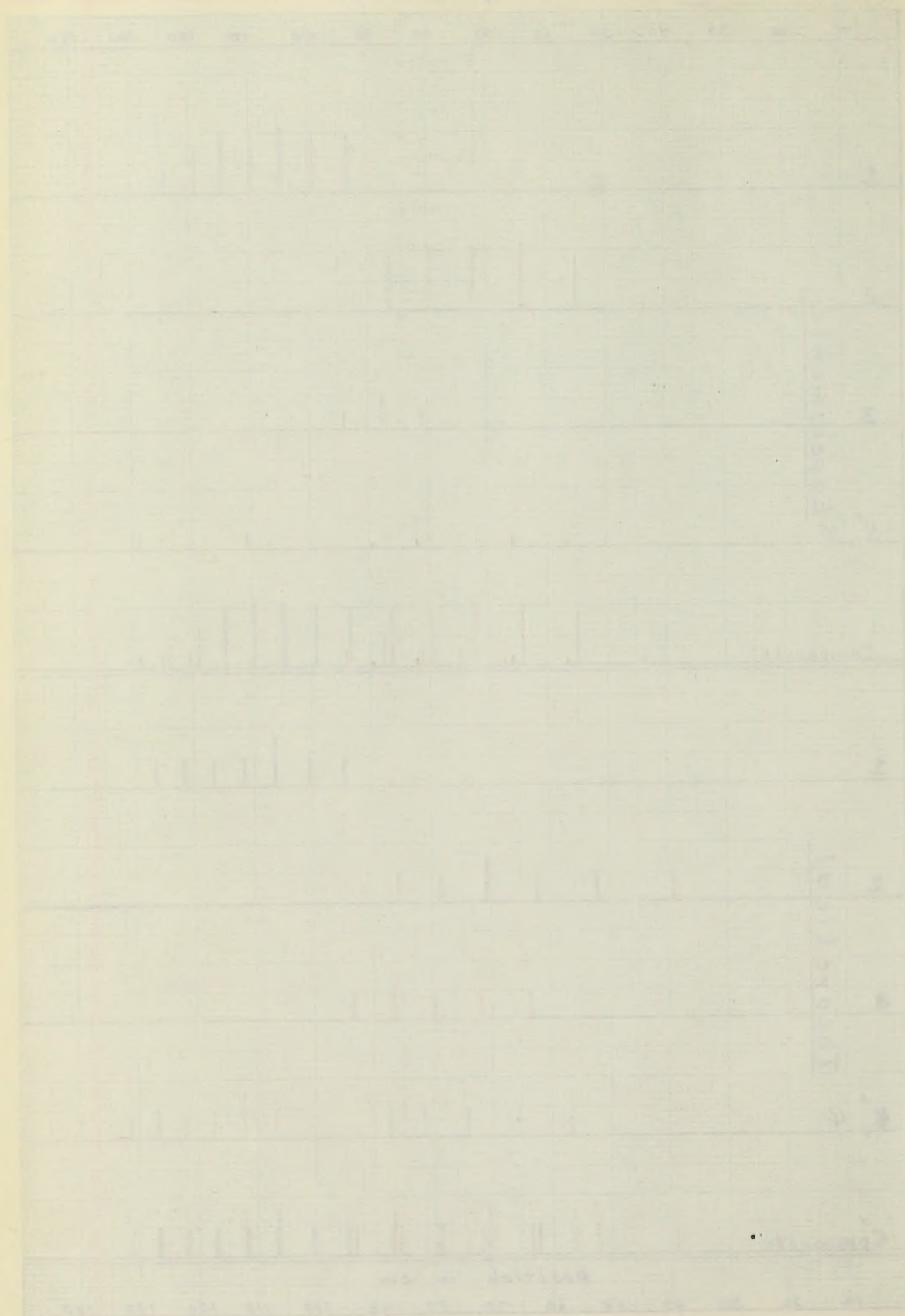
(4')

n = 31267	
cal.	exp.
28.77	
56.31	56.5
65.8	65.7
74.2	
81.7	81.9
87.3	89.2

Graph 1

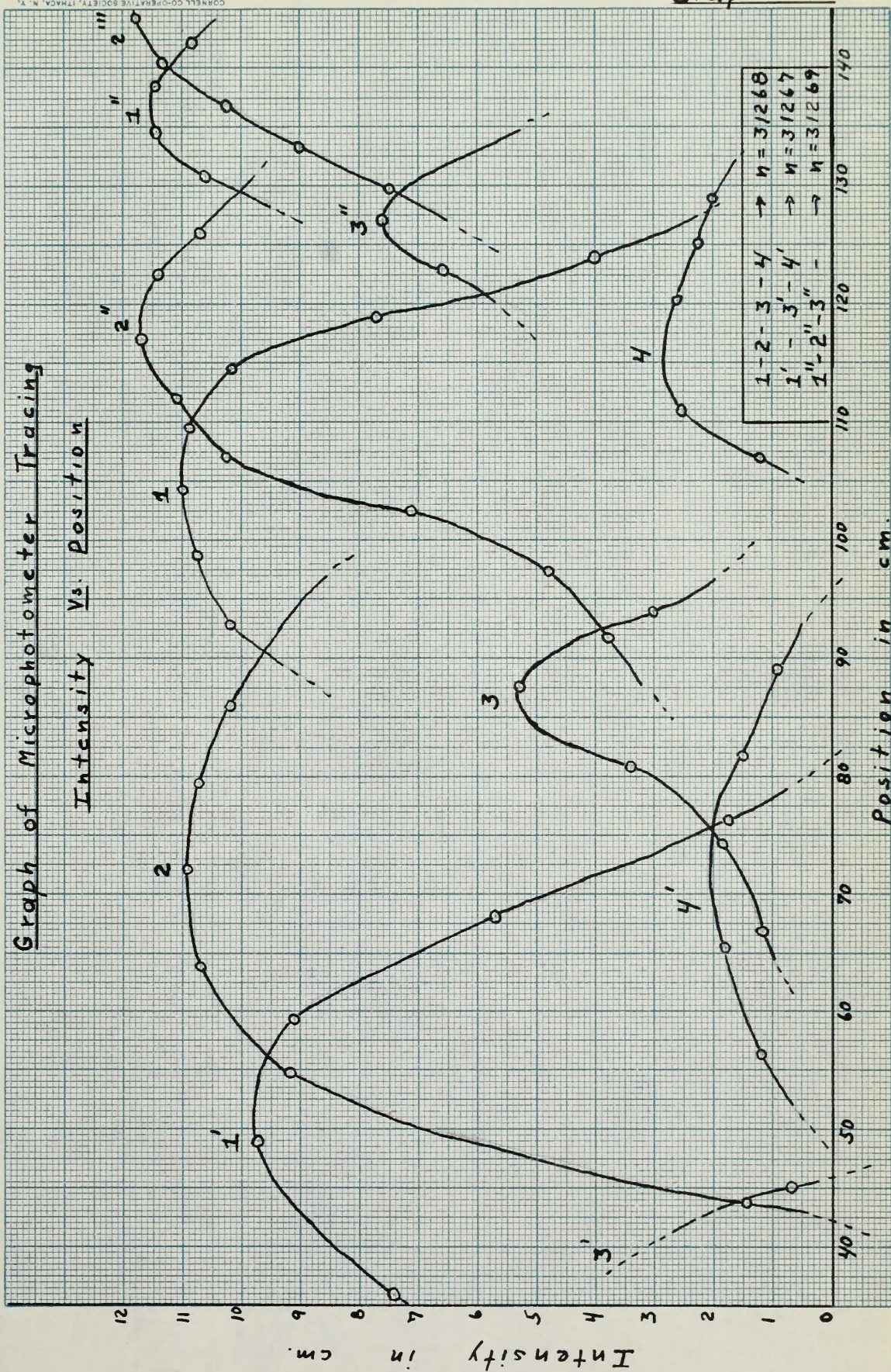


Graph 2

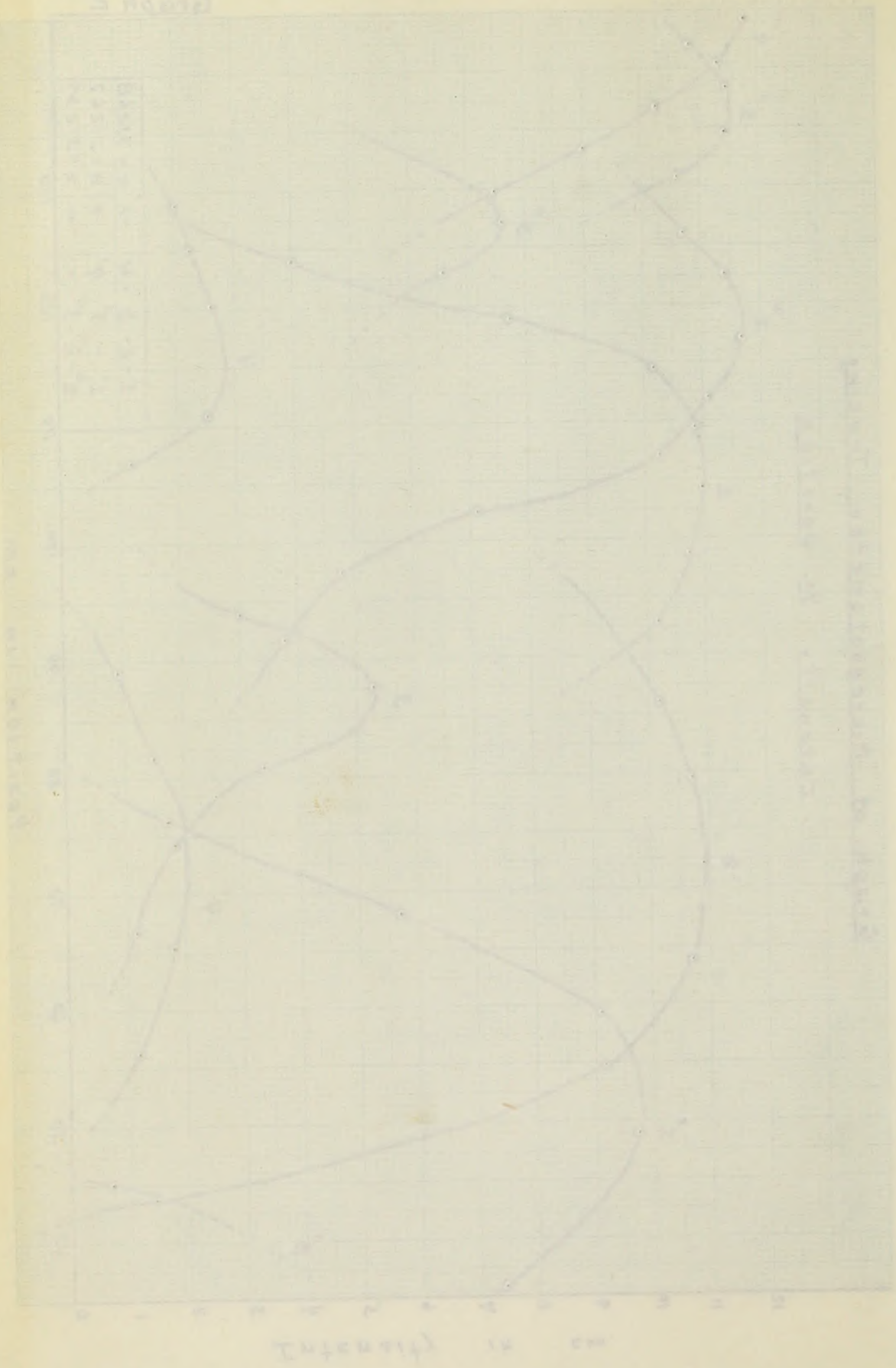


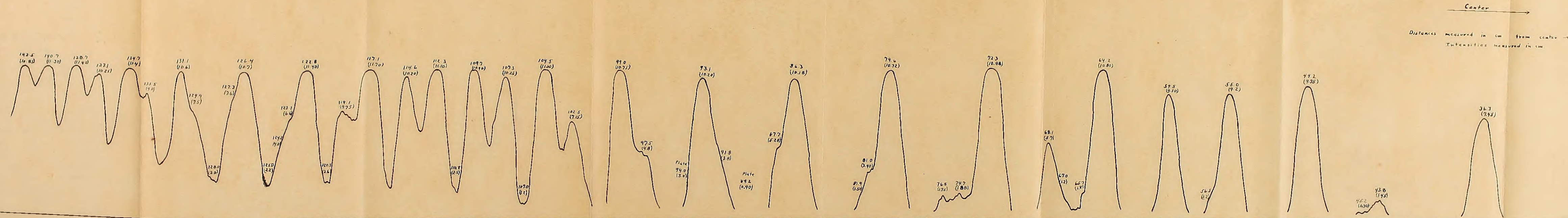
Graph 2

Graph of Microphotometer Tracing
Intensity Vs. Position

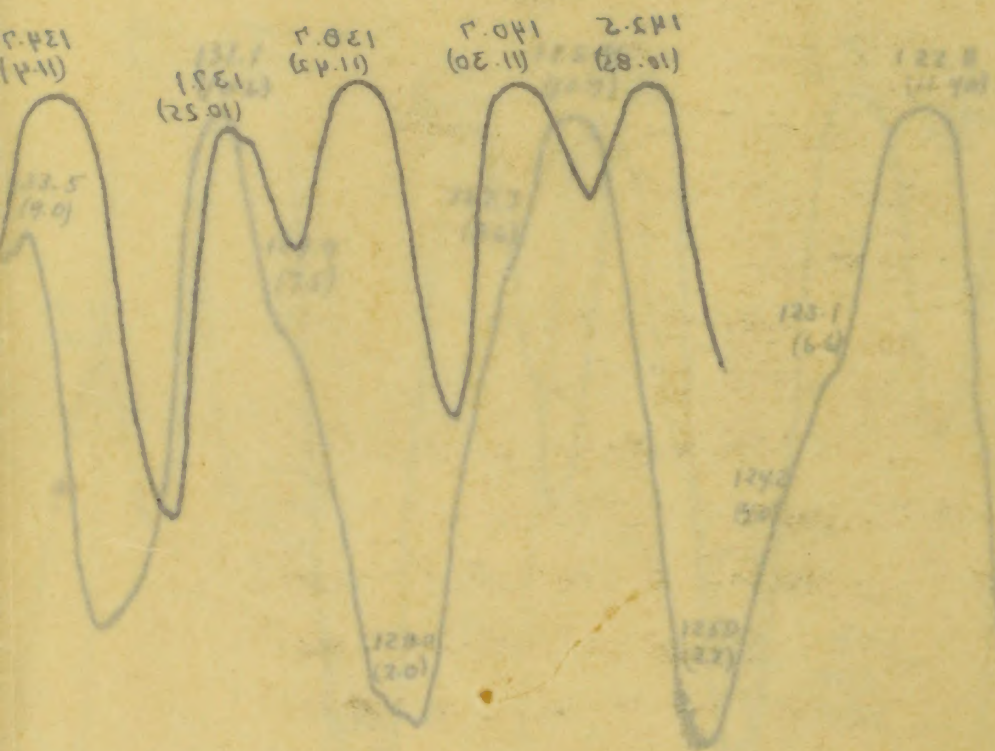


Graph 5





Microphotometer Tracing of
Plate MS-3



DISCUSSION OF RESULTS

The theoretical calculations of the positions of the lines of the H-alpha complex obtained by the combination M S are found to agree closely with the positions of the lines determined experimentally from the microphotometer curve of the photographic plate MS-3.

The graph on page 75 shows the intensity of the various components of the patterns as a function of their distance from the center of the system. These lines fall into four distinct groups clearly indicating four components. Curves (1), (2), (3) and (4) belong to the order number 31268 and (1') & (4') to the order number 31267 of the first plate. Both the component lines and the maxima of the groups agree closely with the theoretical positions resulting from the constants of the Lummer plates, the angles of incidence and the angle between the Lummer plates.

The success achieved in checking so closely (to within 4%) the microphotometer curve by tracing the theoretical components of H_{α} through the two Lummer plates suggests that the problem could be worked backwards to determine the exact wavelengths and corresponding relative intensities. However, before this can be done other important factors must be considered. These will be discussed later.

Let us consider the two fundamental equations for the second Lummer plate.

$$\cos r_3 = \frac{\lambda}{2d'\mu'} n' \quad \text{--- --- A}$$

$$\cos \psi_3 = \frac{\lambda}{2d'} n' \tan r_3 \quad \text{--- --- B}$$

Since n' must be an integral number, then, for a given λ

the angles r_3 and in turn the angles of emergence ψ_3 are fixed.

If now the angle of incidence i_2 is varied slightly, then r_2, r_3

and consequently ψ_3 will change according to the equations -

$$\sin r_2 = \sin i_2 / \mu$$

$$r_3 = \beta' - \alpha' + r_2$$

$$\cos \psi_3 = \mu' \sin r_3$$

Introducing these arbitrarily slightly different values of

ψ_3 & r_3 in the formula

$$n'_{\text{Max}} = \frac{2d' \cos \psi_3}{\lambda \tan r_3} \quad \text{--- --- C}$$

we can determine the value of the order number attending the

direct ray ψ_3 (the most intense one). Thus if i_2 is changed

sufficiently, we shall have a new order number n'_n , which

means that the maximum intensity will shift along the fixed ψ_3

for any given component as determined by equation B. This

was checked experimentally. From a visual study of the pattern

system as the second Lummer plate was rotated the maximum and

minimum regions moved accross the field of view with the com-

ponent lines remaining fixed. This means that the angle between

the plates, the angles of the prisms and the angle of incidence

need not be measured to a high degree of precision as was first

thought necessary. These angles can be altered slightly to

suit the problem at hand. This justifies the slight changes

made in the angles in the theoretical calculation as previous-

ly mentioned.

ly mentioned.

made in the angles in the theoretical calculation as previous-

and the profiles at hand. This justifies the slight changes

thought necessary. These angles can be altered slightly for

need not be measured to a high degree of precision as was first

the angles, the angles of the system and the angle of incidence

present lines remaining fixed. This means that the angle between

distance, which is viewed across the field of view with the con-

system as the second linear plate was rotated the maximum and

was checked experimentally. From a visual study of the pattern

for any given component as determined by equation 2. This

means that the same calculation will apply to the fixed ψ_1

ultimately, we shall have a new order number N' , which

direct ray ψ_3 (the most intense one). Thus if ψ_1 is changed

we can determine the value of the order number attending the

$$N'_{max} = \frac{2 \psi_1 \sin \psi_2}{\lambda \tan \psi_2}$$

$\psi_2 + \psi_3$ in the formula

Introducing these experimentally obtained values of

$$\cos \psi_3 = \frac{1}{\sin \psi_2}$$

$$\psi_3 = 90^\circ - \psi_2$$

and consequently ψ_2 will change according to the equations—

If now the angle of incidence ψ_1 is varied slightly, then ψ_2

the angles ψ_2 and in turn the angles of emergence ψ_3 are fixed.

Since N' must be an integral number, then for a given λ

$$\cos \psi_2 = \frac{\lambda}{2 \psi_1 N}$$

A — — — — —

B — — — — —

The question to be asked is then---Why do not the experimental and theoretical positions of the lines check perfectly? The angles ψ_3 which determine these lines are governed by the equations A and B. Assuming now that the wavelengths and the corresponding μ_1 are accurately known, then d the thickness of the plate must be known to a high degree of precision. Thus, if work is to be continued in this field in getting accurate experimental values of the H_α components, the thicknesses of the Lummer plates must be known more accurately than as given in the section "Constants of the Lummer plates". Furthermore, the focal length of the telescope lens should also be determined more accurately for this controls the order number to be assigned to the most intense line of a component group of the final pattern when the problem is worked backwards.

The results of this research show definitely the existence of the third and the fourth components whose wavelengths are in approximate accord with the theoretical values.

The question to be asked is then---Why do not the
 experimental and theoretical positions of the lines agree
 perfectly? The angles ψ which determine these lines are
 governed by the equations A and B. Assuming now that the
 wavefunctions and the corresponding ψ are accurately known,
 then the thickness of the plate must be known to a high
 degree of precision. Thus, if work is to be continued in
 this field in getting accurate experimental values of the H
 components, the thicknesses of the lamina plates must be known
 more accurately than as given in the section "Constants of the
 lamina plates". Furthermore, the focal length of the plate-
 second lens should also be determined more accurately for this
 control the order number to be assigned to the spot in the
 line of a component group of the final pattern when the
 problem is worked backward.
 The results of this research show definitely the
 existence of the third and the fourth components whose wave-
 lengths are in approximate accord with the theoretical values.

To obtain better photographed plates of the H_α pattern given by two Lamm plates in tandem and thus obtain better microphotometer curves which might reveal the third and fourth theoretical components, a new optical arrangement was devised, as is described in the section "Optical System". In this arrangement the light from the first Lamm plate was directly incident on the second. With three Lamm plates of different dispersions and resolving power, six combinations of two plates each were possible. The patterns obtained by these combinations were photographed and studied. A detailed discussion of each pattern is given in the section "Spectrograms and Data". Many of these failed to yield the expected complex structure of H_α . The best result by far was obtained in which the medium

C O N C L U S I O N S

plate was not first and the smallest plate last. A study of the microphotometer tracing obtained from this combination clearly indicated the presence of four components of the theoretical five component structure of H_α . The combination of the smallest plate and the largest also gave some structure indicating the presence of the third component but failed to show the existence of the fourth. This particular combination which was used by Robinson with a different spectroscopic system did, however, reveal the presence of the fourth component. It was apparent then that the present optical system showed lesser resolving power than Robinson's, although the intensity of the transmitted light was increased sufficiently so that the visual study of the pattern was made easier. This reduction in resolving power was

COLEMAN

To obtain better photographic plates of the H_α patterns given by two Lummer plates in tandem and thus obtain better microphotometer curves which might reveal the third and fourth theoretical components, a new optical arrangement was decided upon, as is described in the section "Optical System". In this arrangement the light from the first Lummer plate was directly incident on the second. With three Lummer plates of different dispersion and resolving power, six combinations of two plates each were possible. The patterns obtained by these combinations were photographed and studied. A detailed discussion of each pattern is given in the section "Spectrograms and Data". Many of these failed to yield the expected complex structure of H_α . The best result by far was the combination in which the medium plate was set first and the smallest plate last. A study of the microphotometer tracing obtained from this combination clearly indicated the presence of four components of the theoretical five component structure of H_α . The combination of the smallest plate and the largest also gave some structure indicating the presence of the third component but failed to show the existence of the fourth. This particular combination which was used by Robinson with a different spectroscopic system did, however, reveal the presence of the fourth component. It was apparent then that the present optical system showed lower resolving power than Robinson's, although the intensity of the transmitted light was increased sufficiently so that the visual study of the patterns was made easier. This reduction in resolving power was

To obtain better photographs of plates of the H patterns
given by two burner plates in tandem and thus obtain better
microphotometer curves which might reveal the third and fourth
theoretical components, a new optical arrangement was decided
upon, as is described in the section "Optical System". In this
arrangement the light from the first burner plate was directly
incident on the second. With three burner plates of different
separations and receiving power, six combinations of two plates
each were possible. The patterns obtained by these combinations
were photographed and studied. A detailed discussion of each
pattern is given in the section "Patterns and Data". Many
of these failed to yield the expected complex structure of 4.
The best result by far was the combination in which the medium
plate was not first and the smallest plate last. A study of the
microphotometer tracing obtained from this combination clearly
indicated the presence of four components of the theoretical
five component structure of H. The combination of the smallest
plate and the largest also gave some structure indicating the
presence of the third component but failed to show the existence
of the fourth. This particular combination which was used by
Robinson with a different spectroscopic system did, however, re-
veal the presence of the fourth component. It was apparent then
that the present optical system showed lower resolving power
than Robinson's, although the intensity of the transmitted light
was increased sufficiently so that the visual study of the
patterns was made easier. This reduction in resolving power was

due to the fact that some of the light coming from the first plate near grazing emergence did not fall upon the prism of the second plate. This diminished the effective length of the first plate and therefore its resolving power. Moreover, the combination (medium-smallest) which yielded the most interesting patterns in the present optical system is characterized by the least resolving power because of the small aperture of the smallest plate which was last in the train. The results suggest then that this combination should be tried with Robinson's spectroscopic system in which the full effective length of the first Lummer plate is utilized.

A study of the three Lummer plates separately, showed that the new medium plate, bought purposely for this investigation, gave the poorest definition while the smallest gave the best. If, then, the medium plate is to be used at all, it would be best to use it as the first plate of the combination where the light coming from it acts as a source for the second plate.

It was found experimentally during the middle of the research that the light emerging from the plain side of a Lummer plate was more intense than that coming from the prism side due to the greater number of reflections of the beam before emerging. Accordingly the last group of photographs taken were made with this arrangement. This saved time in exposure. The plates were also placed such that their prisms were on opposite sides, thus partially compensating for the slight curvature imposed upon the line patterns which is inherent in a prism.

due to the fact that some of the light coming from the first plate was grazing emergence did not fall upon the prism of the second plate. This diminished the effective length of the first plate and therefore its resolving power. Moreover, the combination (medium-amplified) which yielded the most interesting patterns in the present optical system is characterized by the least resolving power because of the small aperture of the first plate which was used in the train. The results suggest that this combination should be tried with Robinson's spectroscopic system in which the full effective length of the first luminescent plate is utilized.

A study of the three luminescent plates separately showed that the new medium plate, though supposedly for this investigation, gave the poorest definition while the smallest gave the best. If, then, the medium plate is to be used at all, it would be best to use it as the first plate of the combination where the light coming from it acts as a source for the second plate.

It was found experimentally during the study of the research that the light emerging from the plate side of a luminescent plate was more intense than that coming from the prism side due to the greater number of reflections of the beam before emerging. Accordingly the last group of photographs taken were made with this arrangement. This saved time in exposure. The plates were also placed so that their prisms were on opposite sides, thus partially compensating for the slight curvature imposed upon the line pattern which is inherent in a prism.

This pattern composed of perfectly straight lines gives better microphotometer curves because a finer and longer microphotometer^{slit} can be used. The use of this type of slit gives smooth microphotometer curves eliminating plate grain effects and resulting in better resolution of the fine structure.

Neither of the microphotometers available, one at the Crufts Laboratory and one at the Harvard Observatory were suitable for the present problem. Besides the many mechanical difficulties which came up in preventing the running of the microphotometers, a great deal of time had to be spent in adapting a special lamp with a long filament, and additional lenses, to give a long, well defined image of the microphotometer slit on the photographic plate.

From the many photographs taken it was learned that for the best definition of the patterns the pressure and the current in the hydrogen tube had to be low. This reduced to a minimum the broadening of lines due to the Doppler effect. For best conditions it was found that the pressure should be about 0.9 - 1.2 mm of Hg with a current in the neighborhood of 20 milliamperes or a current density of 40 ma/cm^2 .

Great difficulty has been experienced in this research in getting good photographic plates. At first films were used. These proved relatively fast, saving time in exposure and thus in cost of liquid air. However, they showed halation. Subsequently, plates were used and these were properly backed. Of the several types that were tried the majority of photographs

This pattern composed of perfectly straight lines gives better microphotometer curves because a finer and longer microphotometer can be used. The use of this type of slit gives smooth microphotometer curves eliminating plate grain effects and resulting in better resolution of the fine structure. Better of the microphotometers available, one at the Griggs Laboratory and one at the Harvard Observatory were suitable for the present problem. Besides the many mechanical difficulties which came up in preventing the turning of the microphotometers, a great deal of time had to be spent in waiting a special lamp with a long filament, and additional lenses, to give a long, well defined image of the microphotometer slit on the photographic plate.

From the many photographs taken it was learned that for the best definition of the patterns the pressure and the current in the hydrogen tube had to be low. This reduced to a minimum the broadening of lines due to the Doppler effect. For best conditions it was found that the pressure should be about 0.5 - 1.2 mm of Hg with a current in the cell of about 20 milliamperes or a current density of 40 amp/cm².

Great difficulty has been experienced in this research in getting good photographic plates. At first films were used. These proved relatively fast, saving time in exposure and time in cost of liquid air. However, they showed distortion. Subsequently, plates were used and these were properly treated. Of the several types that were tried the majority of photographs

were taken with Eastman 4 l-C plates. These were none too satisfactory for they were never very clear, possibly due to chemical fog. The last few photographs taken were with the Eastman 144-F plates. These gave by far the best results.

Although the present research has fallen somewhat short of its objective, the presence of the fourth component of H_{α} has been indubitably proven. The constants of the Lummer plates have been determined and a means for obtaining the relative positions of these plates as well as the angles of incidence and emergence of the light rays. From a study of these angles and constants a method has been developed for the theoretical calculation of the positions of lines of the pattern system as obtained by two Lummer plates. This method has been applied successfully for one plate giving an agreement with experimental results, to within a maximum of 4%, establishing the existence of four components of the theoretical five component structure of H_{α} . With the suggestions as given in the section "Discussion of Results", the way appears clear for determining the exact wavelengths of these components.

In conclusion, the writer suggests a return to the spectroscopic system used by Robinson minus the "mirror" between the Lummer plates. His arrangement of the spectroscopic system should give greater resolving power. The best combination of plates is the medium plate first, followed by the smallest. The exclusive use of Eastman plates Type 144-F is advised. The overhead structure for photographing the optical

*This was necessary because of cramped conditions in the research room.

were taken with Eastman 1-1-C plates. These were none too satisfactory for they were never very clear, possibly due to chemical fog. The last few photographs taken were with the Eastman 144-B plates. These gave by far the best results. Although the present research has failed somewhat short of its objective, the presence of the fourth component of λ_K has been indirectly proven. The constants of the Lamer plates have been determined and a means for obtaining the relative positions of these plates as well as the angles of incidence and emergence of the light rays. From a study of these angles and constants a method has been developed for the theoretical calculation of the positions of lines of the pattern system as obtained by two Lamer plates. This method has been applied successfully for one plate giving an agreement with experimental results. It yields a maximum of 22, establishing the existence of four components of the theoretical λ_K component structure of λ_K . This the one section as given in the section "Discussion of Results", the key element clear for determining the exact wavelengths of these components.

In conclusion, the writer suggests a return to the spectroscopic system used by Robinson minus the "mirror" between the Lamer plates. His arrangement of the spectroscopic system should give greater resolving power. The best combination of plates is the medium blue line, followed by the violet. The exclusive use of Lamer plates Type 144-B is advised. The overcast atmosphere for photographing the optical

This was necessary because of special conditions in the research.

system has already been built---anticipating the continuation of this investigation. Lastly, besides obtaining good photographic plates which reveal the fine structure components of H_{α} , a suitable microphotometer is absolutely essential.

ACKNOWLEDGEMENTS

The writer is grateful to Dr. Kent for having suggested this research problem, and for his invaluable assistance and time so generously given in all the investigations of ^{an} experimental nature. A like debt of gratitude is due Dr. Frye for his aid in the theoretical approach to this problem.

The writer also wishes to express his indebtedness to Dr. Shapley and Dr. Dimitroff of the Harvard Observatory for placing the microphotometer at his disposal, and to Mr. Albee for making the tracings.

system has already been built--anticipating the completion
of this investigation. Lastly, besides obtaining good photo-
graphic plates which reveal the fine structural components of the
a suitable microprojector is absolutely essential.

ACKNOWLEDGMENTS

The writer is grateful to Dr. Reed for having sug-
gested this research problem, and for the invaluable assistance
and time so generously given in all the investigations of the
experimental nature. A like debt of gratitude is due Dr. Reed
for his aid in the (revisions) approach to this problem.
The writer also wishes to express his indebtedness to Dr.
Shapley and Dr. Gilmartin of the Bureau of Entomology for placing the
microprojector at his disposal, and to Dr. Albee for making the facilities.

BOSTON UNIVERSITY

GRADUATE SCHOOL

Dissertation

AN INVESTIGATION OF THE SEPARATIONS OF THE COMPONENTS
OF THE H-ALPHA COMPLEX OF HYDROGEN

by

Thomas Homkowycz Wallace

(B.S., Boston University, 1933; A.M., Harvard University, 1936)

submitted in partial fulfilment of the

requirements for the degree of

Doctor of Philosophy

1939

(ABSTRACT)

1 Robinson, E. A. Ph.D. Thesis, B.U. Graduate School, 1937

* This was necessary because of limited space in the original paper.

BOSTON UNIVERSITY

GRADUATE SCHOOL

Dissertation

AN INVESTIGATION OF THE SEPARATIONS OF THE COMPONENTS
OF THE K-LENA COMPLEX OF HYDROGEN

by

Thomas H. K. Wallace

(B.S., Boston University, 1957; A.M., Harvard University, 1958)

Submitted in partial fulfillment of the

requirements for the degree of

Doctor of Philosophy

1959

(ABSTRACT)

The preliminary investigation of W. H. Robinson¹ in the study of H-alpha of hydrogen with the use of a Lummer plate as an auxiliary spectrograph appeared very promising. The source of radiation was a liquid -air cooled Wood's tube. Light from the tube passed through a filter which allowed only the H-alpha radiation to be transmitted. This radiation was brought to a focus on the slit of the first spectroscope that contained the first Lummer plate. The light emerging from this plate was reflected by a mirror* and then brought to a focus at the slit of the second Lummer plate spectroscop. Both plates were set to disperse horizontally. This method of using two Lummer plates in tandem furnished a new method for the study of fine structure. The results of Robinson's work showed the existence of a third component and indicated the presence of a fourth—— of the theoretical five component structure of H-alpha.

The aim of the present research was to extend Robinson's work in this field. It was hoped that with improved conditions and rearrangement of the spectroscopic system there could be obtained better photographic plates and thus better microphotometer curves which might more clearly reveal both the third and fourth components, especially the latter. With this in mind a third Lummer plate was bought for use in this problem.

1 Robinson, W. H. PhD. Thesis, B.U. Grad.School, 1937

* This was necessary because of limited space in the research room.

The preliminary investigation of W. S. Robinson in

the study of α -alpha of hydrogen with the use of a luminescent plate as an extremely sensitive apparatus and very promising. The source of radiation was a flooded air-cooled radio tube. Light from the tube passed through a filter which allowed only the α -alpha radiation to be transmitted. This radiation was focused to a focus on the left of the first spectroscopic slit and the first luminescent plate. The light emerging from this plate was reflected by a mirror and then brought to a focus at the left of the second luminescent plate spectroscopic. Both plates were set to different wavelengths. This method of using two luminescent plates in tandem furnished a way worked for the study of the spectrum. The results of Robinson's work showed the existence of a third component and indicated the presence of a fourth of the theoretical five elements α -alpha of hydrogen.

The aim of the present investigation was to extend Robinson's work in this field. It was hoped that with improved conditions and a more accurate spectroscopic system there would be observed better spectroscopic plates and that better spectroscopic curves might be obtained. Several other points were found and fourth component, especially the latter. With this in mind a third luminescent plate was added for use in this system.

The spectroscopic system finally decided upon was one in which the two Lummer plates were set directly in tandem with no intervening lenses. This allowed the emergent light from the first plate to be directly incident on the second plate. With less absorption of the light present, the intensity of the spectrum was increased enough so that the structure of the pattern could be studied visually more readily and exposure time somewhat reduced. From a study of the relative positions of these plates, their constants, and the angles of incidence and emergence of the light rays it was hoped that microphotometer curves might be obtained which would make possible a quantitative determination of both the wavelengths and intensities of the component lines of H-alpha.

The microphotometer tracing of one of the combinations of Lummer plates definitely showed the existence of four distinct groups of lines corresponding to four components of H-alpha. The constants of the Lummer plates have been determined and a means for obtaining the relative positions of these plates as well as the angles of incidence and emergence of the light rays. From a study of these angles and constants a method has been developed for the theoretical calculation of the positions of the lines of the pattern system as obtained by two Lummer plates. This method has been applied successfully for one Lummer plate combination. Both the component lines and the maxima of the groups were in agreement with experimental results to within a

The experimental results are shown in Table I.

One of the main points of the present study is to determine the effect of the concentration of the reactants on the rate of the reaction.

The results of the experiments are shown in Table I. It is seen that the rate of the reaction increases with increasing concentration of the reactants.

From the data in Table I, it is found that the rate of the reaction is proportional to the concentration of the reactants.

Thus, the rate of the reaction is directly proportional to the concentration of the reactants.

The results of the experiments are shown in Table I. It is seen that the rate of the reaction increases with increasing concentration of the reactants.

From the data in Table I, it is found that the rate of the reaction is proportional to the concentration of the reactants.

Thus, the rate of the reaction is directly proportional to the concentration of the reactants.

The results of the experiments are shown in Table I. It is seen that the rate of the reaction increases with increasing concentration of the reactants.

From the data in Table I, it is found that the rate of the reaction is proportional to the concentration of the reactants.

Thus, the rate of the reaction is directly proportional to the concentration of the reactants.

The results of the experiments are shown in Table I. It is seen that the rate of the reaction increases with increasing concentration of the reactants.

From the data in Table I, it is found that the rate of the reaction is proportional to the concentration of the reactants.

Thus, the rate of the reaction is directly proportional to the concentration of the reactants.

The results of the experiments are shown in Table I. It is seen that the rate of the reaction increases with increasing concentration of the reactants.

From the data in Table I, it is found that the rate of the reaction is proportional to the concentration of the reactants.

Thus, the rate of the reaction is directly proportional to the concentration of the reactants.

The results of the experiments are shown in Table I. It is seen that the rate of the reaction increases with increasing concentration of the reactants.

From the data in Table I, it is found that the rate of the reaction is proportional to the concentration of the reactants.

Thus, the rate of the reaction is directly proportional to the concentration of the reactants.

The results of the experiments are shown in Table I. It is seen that the rate of the reaction increases with increasing concentration of the reactants.

From the data in Table I, it is found that the rate of the reaction is proportional to the concentration of the reactants.

Thus, the rate of the reaction is directly proportional to the concentration of the reactants.

The results of the experiments are shown in Table I. It is seen that the rate of the reaction increases with increasing concentration of the reactants.

From the data in Table I, it is found that the rate of the reaction is proportional to the concentration of the reactants.

maximum of 4% definitely establishing the existence of four components.

The success achieved in checking so closely the microphotometer curve by tracing the theoretical components of H-alpha through the two Lummer plates suggests that the problem could be worked backwards to determine the exact wavelengths and the corresponding relative intensities. Before this can be done, however, it will be necessary to obtain the thicknesses of the Lummer plates to a greater degree of precision, as well as to know more accurately the focal length of the telescope lens. A suitable microphotometer is also absolutely essential.

Comparison of the present spectroscopic system with Robinson's indicates that his should give greater resolving power. The combination of Lummer plates that has yielded the most structure of H_{α} in the present optical system is characterized by the least resolving power because of the small apertures of the smallest plate which was last in the train. The results suggest then that this combination should be tried with Robinson's spectroscopic system in which the full effective length of the first Lummer plate is utilized. The methods determined for the theoretical calculations of the final pattern can be easily adapted to this system.

Although, in this research, the wavelengths and the intensities of the components have not been determined, the presence of the fourth component ~~component~~ of H-alpha has been indubitably proven. It appears from the results of the present

...of the

...

The

... ..

... ..

... ..

... ..

... ..

... ..

... ..

... ..

... ..

... ..

... ..

... ..

... ..

... ..

... ..

... ..

... ..

... ..

... ..

... ..

... ..

... ..

... ..

investigation that the path is clear for determining the exact wavelengths and intensities. The present combination of the two Lummer plates (medium and small) has shown, by far, to be the best for revealing the fourth component and the possible detection of the fifth component if it exists.

Investigation that the past is about the determination of the
as scientific and industrial. The present condition of the
two main places (the film and the) has shown, by far, to be
the best for testing the film component and the possible
detection of the film component it is easier.

B I B L I O G R A P H Y

- Darwin, Proc. Roy. Soc., A116, 227 (1927).
- Dirac, Proc. Roy. Soc., A117, 610 (1928).
- Goudsmit and Uhlenbeck, Physica, 6, 273 (1926).
- Heisenberg and Jordan, Zeits. F. Physik, 37, 263 (1926).
- Houston, V.V., Astrophysical Journal, 64, 81 (1926).
- Houston and Hsieh, Phys. Rev., 45, 132A (1934).
- Janecki and Lau, Zeits. F. Physik, 35, 1 (1925).
- Kent, Tayler and Pearson, Phys. Rev., 30, 266 (1927).
- Kupper, Ann. D. Physik, 86, 511 (1928).
- Pauli, W., Zeits F. Physik, 36, 336 (1926).
- Pauling and Goudsmit, Structure of Line Spectra, sections 6b, and 14a.
- Pauling and Wilson, Introduction to Quantum Mechanics, pp 117-124, McGraw Hill, N.Y. (1935).
- Robinson, W.H., Ph.D. Thesis, B.U. Grad. School (1937).
- Ruark, A.E., and Urey, H.C., Atoms, Molecules and Quanta McGraw Hill, N. Y. (1930)
- Saha and Banerji, Zeits. F. Physik, 68, 704 (1931).
- Schrodinger, Ann. D. Phys., 80, 437 (1926).
- Shrum, G.M., Proc. Roy. Soc., A 105, 262 (1924).
- Sommerfeld, Atombau und Spektrallinen, Druck und Verlag Von Frieder Vieweg und Sohn Art., Ges. Braunschweig (1924)
- Sommerfeld and Unsold, Zeits.F.Physik, 36, 259 (1926).
38, 237 (1926)
- Spedding, Shane and Grace, Phys. Rev., 47, 38 (1935)
- Thomas, L. H., Nature, 117, 514 (1926).
- White, Introduction to Atomic Spectra, McGraw Hill, N. Y. (1934)

Williams, W.I., Applications of Interferometry, pp.94-103,
Dutton and Co., N.Y. (1930).

Williams, Phys. Rev., 54, 558 (1938).

Williams and Gibbs, Phys. Rev., 45, 475 (1934).



Thomas Montgomery Wallace
 Wallace was born in 1901 in
 and was educated at the High School,
 where he graduated. Graduated from
 Boston University, College of Liberal
 Arts in 1923 with the degree of B.S.
 in Mathematics. Served as an under-
 graduate assistant in the Physics
 Department during 1921-22. Entered the Harvard Graduate School
 in 1923 and received officially the degree of A.B. in Physics
 in 1924. Attended the Boston University Graduate School in 1925
 with appointment as a graduate assistant. Appointed to the
 Williams College faculty in 1926 where the position of Assistant
 in Physics was held the first semester of that year. Was re-
 appointed to this position during 1927-1928. Member of the
 American Physical Society.

Williams, W.I., Applications of Interferometry, pp. 94-103,
Gordon and Breach, S.A. (1960).

Williams, Faye, Rev., 54, 552 (1958).

Williams and Gibbs, Faye, Rev., 55, 475 (1959).

AUTOBIOGRAPHY



Thomas Homkowycz Wallace

Born August 27, 1912 in Brighton, Boston, Massachusetts. Son of Anna Powlick and Wallace Homkowycz. Attended the Thomas Gardner Grammar School in Allston and the Mechanic Arts High School, both in Boston. Graduated from Boston University, College of Liberal Arts in 1933 with the degree of B.S. in Mathematics. Acted as an undergraduate assistant in the Physics

Department during 1931-33. Entered the Harvard Graduate School in 1933 and received officially, the degree of A.M. in Physics in 1936. Attended the Boston University Graduate School in 1934 with appointment as a graduate assistant. Appointed to the Williams College Faculty in 1935 where the position of Assistant in Physics was held the first semester of that year. Was re-appointed to this position during 1936-1938. Member of the American Physical Society.

BIOGRAPHY

Born August 27, 1912 in

Belmont, Boston, Massachusetts.

Son of Anna Powell and Wallace

Honoway. Attended the Thomas

Wentworth Grammar School in Allston

and the Massachusetts Arts High School.

Left in Boston. Graduated from

Boston University, College of Liberal

Arts in 1933 with the degree of B.S.

in Mathematics. Served as an under-

graduate assistant in the Physics

Department during 1931-32. Entered the Harvard Graduate School

in 1932 and received officially the degree of A.M. in Physics

in 1933. Attended the Boston University Graduate School in 1934

with appointment as a graduate assistant. Appointed to the

William College faculty in 1935 where the position of Assistant

in Physics was held the first semester of that year. Was re-

appointed to this position during 1935-1936. Member of the



Thomas Honoway Wallace

Department during 1931-32.

in 1932 and received officially the degree of A.M. in Physics

in 1933. Attended the Boston University Graduate School in 1934

with appointment as a graduate assistant. Appointed to the

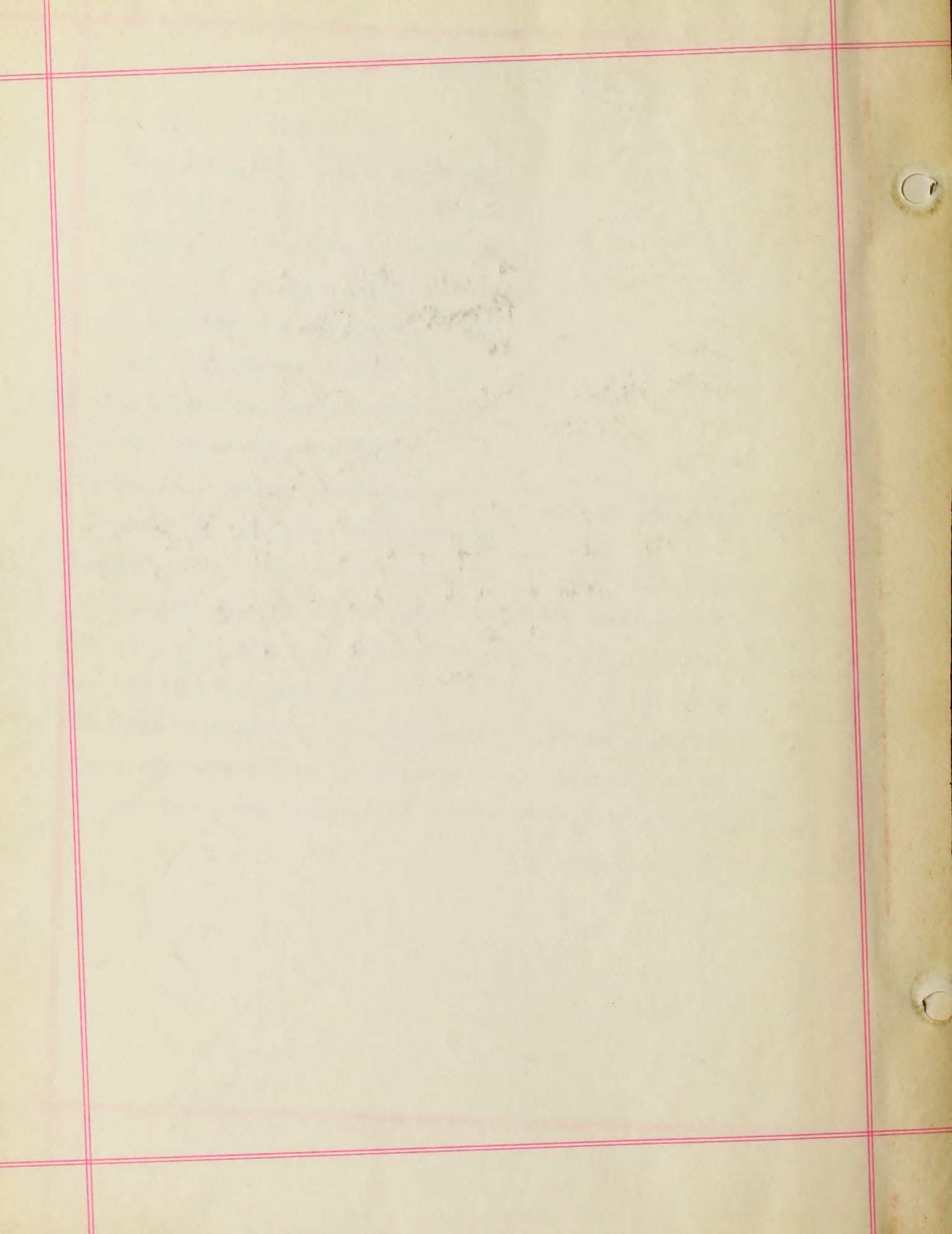
William College faculty in 1935 where the position of Assistant

in Physics was held the first semester of that year. Was re-

appointed to this position during 1935-1936. Member of the

American Physical Society.

PARSONS
FALCON FORD
RIS CONSENT



BOSTON UNIVERSITY



1 1719 02480 5006

